



FACULTAD DE CIENCIAS BIOLÓGICAS
PONTIFICIA UNIVERSIDAD CATÓLICA DE CHILE

EXO70 INVOLVEMENT ON NMDAR DYNAMICS IN TRAUMATIC BRAIN INJURY

Thesis submitted to the Pontificia Universidad Católica de Chile in partial compliance with the requirements for the Ph.D. in Biological Sciences with a mention in Cellular and Molecular Biology

MATÍAS SEBASTIÁN LIRA MENDIETA

Thesis Advisor

Waldo Cerpa

November 2021

TABLE OF CONTENTS

1.-Introducción.....	1
1.1.- Glutamatergic transmisión.....	1
1.1.1.- Glutamate receptors.....	2
1.1.2.- Iontropic glutamate receptor trafficking.....	4
1.1.3.- Iontropic glutamate receptor in long term potentiation (LTP).....	8
1.1.4.- Iontropic glutamate receptors in learning and memory.....	9
1.2.- Traumatic brain injury.....	11
1.2.1.- Pathophysiology of TBI.....	13
1.2.2.- Cellular and molecular mechanisms of TBI.....	15
1.2.3.- Iontropic glutamate receptors in TBI.....	16
1.3.- The exocyst complex.....	18
1.3.1.- Exocyst in ionotropic glutamate receptor trafficking and delivery.....	20
1.3.2.- The exocyst complex in brain pathologies.....	23
2.- Hypothesis and objectives.....	25
2.1.- Hypothesis.....	24
2.2.- General objective.....	24
2.3.- Specific objektivies.....	25
3.- Materials and methods.....	26
3.1.- Animals.....	26
3.2.- Traumatic brain injury procedure.....	26
3.3.- Biochemical analyses.....	28
3.3.1.- Inmunoblot.....	28
3.3.2.- Subcellular fractionation.....	30
3.3.3.- Co-immunoprecipitation.....	31
3.3.4.- Cell Surface biotinylation.....	32
3.4.- Imunohistochemistry.....	33
3.5.- Intrahippocampla lentiviral injection.....	34
3.6.- Behavioral tests.....	34
3.6.1.- Spatial memory.....	34
3.6.2.- Memory flexibility.....	35
3.7.- Electrophysiology.....	35
3.8.- Dorsal hippocampus isolation	36
3.9.- Statistical analysis.....	37
4.- Results.....	38
4.1.- Objective 1: To determine if mTBI changes Exo70 expression.....	38
4.1.1.- Evaluation of Exo70 expression.....	38
4.1.2.- Evaluation of Exo70 expression after mTBI.....	40
4.2.- Objective 2: To evaluate Exo70 subcellular localization after mTBI.....	41
4.2.1.- Exo70 compartmentalization following mTBI.....	41
4.2.2.- Exo70 membrane proximity following mTBI.....	46
4.2.3.- Exocyst assembly following mTBI.....	48

4.3.- Objective 3: To determine if Exo70 gain of function rescues learning/memory and NMDAR synaptic availability after mTBI induction.....	51
4.3.1.- Intrahippocampal lentiviral injection.....	51
4.3.2.- Learning and memory.....	53
4.3.3.- Synaptic transmission.....	56
4.3.4.- NMDAR synaptic availability.....	59
5.- Discussion.....	63
5.1.- First part: Objectives 1 and 2.....	63
5.2.- Second part: Objective 3.....	72
6.- Conclusion.....	81
7.- References.....	82
8.- Appendices.....	96

TABLE OF FIGURES

Figure 1.- Tripartite excitatory synapse structure.....	2
Figure 2.- Ionotropic glutamate receptor trafficking.....	7
Figure 3.- Scheme depicting cellular and pathophysiological outcomes after TBI induction...	14
Figure 4.- Dysregulation of NMDARs performance in TBI.....	17
Figure 5.- The exocyst complex.....	19
Figure 6.- Exocyst in glutamatergic receptor trafficking.....	22
Figure 7.- Frontal impact device.....	27
Figure 8.- Protocol for repeated mTBI induction.....	28
Figure 9.- Schematic representation of the steps followed in the subcellular fractionation.....	31
Figure 10.- Map of the bicistronic lentiviral construct.....	34
Figure 11.- Evaluation of Exo70 expression in the forebrain, cortex and hippocampus.....	39
Figure 12.- Exo70 protein levels are not altered after mTBI induction.....	40
Figure 13.- Exo70 localization is increased in forebrain synapses upon mTBI induction.....	42
Figure 14.- Hippocampal subcellular fractionation.....	44
Figure 15.- Exo70 is redistributed into PSD in the hippocampus of mTBI mice.....	45
Figure 16.- Exo70 proximity to the plasma membrane decreases after mTBI induction.....	47
Figure 17.- mTBI increases exocyst complex assembly in the PSD fraction.....	49
Figure 18.- mTBI increases Exo70-GluN2B interaction in the PSD fraction.....	50
Figure 19.- Schematic representation of proteins expressed by the lentiviral system.....	52
Figure 20.- Characterization of the lentiviral system expressing Exo70.....	53
Figure 21.- Learning and memory impairment is prevented by Exo70 overexpression.....	55
Figure 22.- Memory flexibility test.....	56
Figure 23.- Basal synaptic transmission in hippocampus from mTBI mice.....	57
Figure 24.- NMDAR-related synaptic transmission in hippocampus from mTBI mice.....	58
Figure 25.- Characterization of the lentiviral expression in all experimental groups.....	60
Figure 26.- NMDAR synaptic localization after mTBI in Exo70-overexpressing mice.....	61
Figure 27.- NMDAR synaptic signaling after mTBI in Exo70-overexpressing mice.....	62
Figure 28.- Scheme depicting Exo70 redistribution after traumatic brain injury.....	71
Figure 29.- Schematic representation of synaptic NMDAR signaling following traumatic brain injury.....	75
Figure 30.- Schematic summary of Exo70 overexpression effects in our mTBI model.....	80

RESUMEN

El correcto funcionamiento de la sinapsis es fundamental para mantener la estabilidad neuronal. En neuropatologías como la lesión cerebral traumática (TBI), la sinapsis se altera o destruye. TBI es una condición que posee una alta incidencia a nivel mundial y es una causa importante de muertes y discapacidad. TBI se caracteriza por cambios de presión intracraneal debido a fuerzas de aceleración inducidas por el golpe, lo que genera un daño primario a nivel de tejido. El daño secundario posterior puede durar por semanas o meses, incluso años dependiendo de la gravedad del trauma. Este daño secundario es en parte mediado por glutamato al estimular receptores NMDA extrasinápticos, lo que desencadena una pérdida de función sináptica y por consiguiente alteración de conductas cognitivas y sociales. El daño mediado por el derrame de glutamato provoca una redistribución de receptores N-methyl-D-aspartic acid (NMDA) hacia sitios extrasinápticos, lo que potenciaría el daño generado por el glutamato extrasináptico. Uno de los componentes asociados a tráfico, exocitosis y mantención de los receptores de glutamato en la sinapsis es el exocisto. El exocisto es un complejo multiproteico constituido por 8 proteínas encargado de la exocitosis de membrana basolateral y de crecimiento de neuritas, así como también del tráfico y exocitosis de receptores de glutamato. A su vez, el exocisto ha sido relacionado a la disponibilidad basal de receptores de glutamato en la sinapsis y por lo tanto regula el umbral de activación de estos. A pesar de que se conoce bastante sobre el complejo exocisto a nivel celular, existe poca información que relacione al exocisto con neuropatologías. Nuestra hipótesis de trabajo es que Exo70 promueve la disponibilidad y señalización sináptica

del receptor NMDA en respuesta a trauma cerebral inducido por golpe, manteniendo así procesos cognitivos. Para poner a prueba esta hipótesis se utilizó un modelo de trauma leve provocado por golpes repetitivos en ratones. Nuestros resultados demuestran que Exo70 es redistribuido hacia la sinapsis en condición TBI, donde el ensamblaje del complejo se incrementa y la interacción con GluN2B se ve favorecida. En esta tesis se logró la sobreexpresión de Exo70 en la región CA1 del hipocampo dorsal previo a la inducción de TBI, lo que nos permitió realizar ensayos conductuales, electrofisiológicos y bioquímicos que responden a la evaluación de la disponibilidad de receptores NMDA en la sinapsis. En estos experimentos encontramos que la previa sobreexpresión de Exo70 protege contra el deterioro cognitivo, acompañado de la estabilización de la transmisión glutamatérgica basal y la potenciación a largo plazo en hipocampo. Finalmente, GluN2B permanece en la sinapsis cuando Exo70 es sobre expresado, promoviendo así la señalización intracelular asociada a receptores NMDA sinápticos. Estos hallazgos revelan el papel que cumple Exo70 en la dinámica intracelular de receptores NMDA en condición de trauma cerebral y sugieren que Exo70 podría ser parte de la maquinaria de distribución sináptica de estos receptores en otras neuropatologías.

ABSTRACT

Synaptic proper functioning is essential to maintain neuronal stability. The synapse is disrupted or destroyed in neuropathologies such as traumatic brain injury (TBI). TBI is a condition that has a high incidence worldwide and is a major cause of death and disability. TBI is characterized by changes in intracranial pressure due to acceleration forces induced by the head strike, which generates primary damage at the tissue level. Subsequent secondary damage can last for weeks or months, even years, depending on the severity of the trauma. This secondary damage is in part mediated by glutamate by stimulating extrasynaptic NMDA receptors, which triggers a loss of synaptic function and consequently alteration of cognitive and social behaviors. The damage mediated by glutamate spillage causes a redistribution of N-methyl-D-aspartic acid (NMDA) receptors towards extrasynaptic sites, which would enhance the damage generated by extrasynaptic glutamate. The exocyst is one of the components associated with trafficking, exocytosis, and maintenance of glutamate receptors in the synapse. The exocyst is a multiprotein complex made up of 8 proteins responsible for the exocytosis of the basolateral membrane and the growth of neurites, as well as the trafficking and exocytosis of glutamate receptors. The exocyst has been related to the availability of glutamate receptors in the synapse and therefore regulates their activation threshold. Although much is known about the exocyst complex at the cellular level, there is little information that relates the exocyst to neuropathologies. Our hypothesis is that Exo70 promotes the availability and synaptic signaling of the NMDA receptor

in response to TBI, thus maintaining cognitive processes. To test this hypothesis, a model of mild trauma caused by repetitive strikes in mice was used. Our results show that Exo70 is redistributed towards the synapse in TBI condition, where the assembly of the complex is increased and the interaction with GluN2B is favored. In this thesis, the overexpression of Exo70 was achieved in the CA1 region of the dorsal hippocampus prior to TBI induction, which allowed us to perform behavioral, electrophysiological and biochemical tests that respond to the evaluation of NMDAR synaptic availability. In these experiments, we found that the prior overexpression of Exo70 protects against cognitive deterioration, alongside the stabilization of basal glutamatergic transmission and long-term potentiation in hippocampus. Finally, GluN2B remains at the synapse when Exo70 is overexpressed, thus promoting intracellular signaling associated with synaptic NMDA receptors. These findings reveal the key role played by Exo70 in the intracellular dynamics of NMDA receptors in TBI and suggest that Exo70 could be part of NMDAR distribution machinery in other neuropathologies.

1.- INTRODUCTION

1.1.- Glutamatergic transmission

In the central nervous system (CNS), the synapses are specialized structures connecting neurons and letting the flux of information between them. The primary excitatory neurotransmitter in the brain is glutamate (Meldrum, 2000), and glutamatergic synapses comprise a presynaptic terminal, a specialized postsynaptic structure called dendritic spine (Hering and Sheng, 2001), and glial cells (Figure 1) in the called tripartite synapse. The presynaptic terminal contains synaptic vesicles where glutamate is stored, and from here, glutamate is released to the synaptic cleft upon electrical stimulation (Hackett and Ueda, 2015). The postsynaptic compartment contains the glutamate receptors, which are transmembrane proteins responsible for transducing the glutamate signal from the extracellular space.

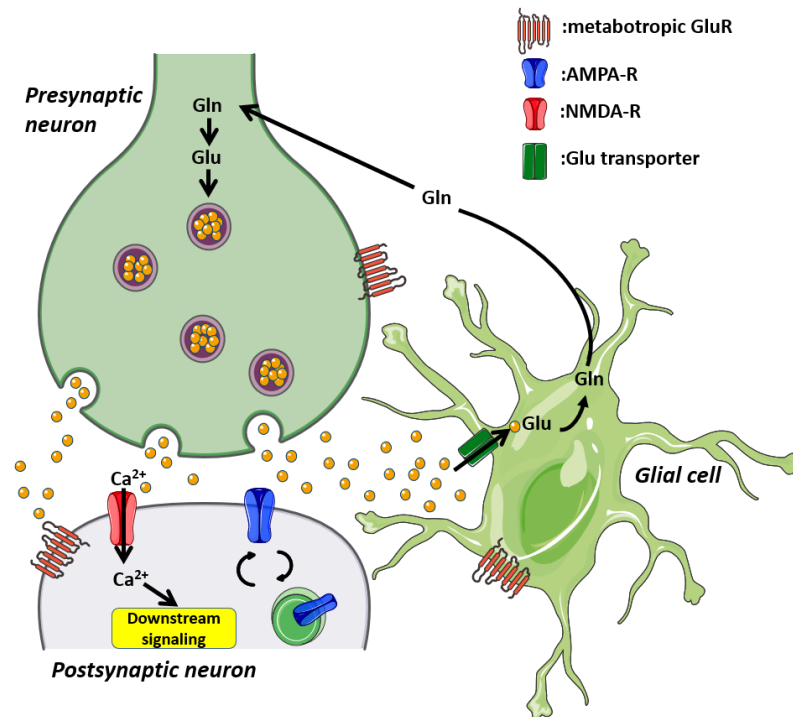


Figure 1. Tripartite excitatory synapse structure. Excitatory synapses are the most common in the central nervous system. It comprises a presynaptic neuron, a postsynaptic neuron, and a glial cell. The presynaptic compartment contains the cellular machinery for tethering, exocytosis, and endocytosis of glutamate-containing vesicles; refilling these vesicles is carried out in this compartment as well. In the postsynaptic compartment, we find glutamate receptors and associated signaling coupled to exocytosis and recycling machinery. Additionally, there are supporting glial cells that maintain this basic synaptic structure. The correct functioning of synapses depends on all three cellular components to maintain physiological activity.

1.1.1.- Glutamate receptors

There are a variety of glutamate receptors, both ionotropic and metabotropic (Blackshaw et al., 2011), that are widely distributed in the brain and spinal cord in both neurons and glia (Jakowec et al., 1998, Sillevs Smitt et al., 2000, Testa et al., 1998, Fukaya et al., 2003, Dunah et al., 1998, Nishi et al., 2001, Habermacher et al., 2019). Ionotropic glutamate receptors, i.e., α -amino-3-hydroxy-5-methyl-4-isoxazole propionic acid (AMPA) receptors, and N-methyl-D-aspartic acid (NMDA) receptors primarily mediate fast excitatory neurotransmission in the CNS (Carvajal et

al., 2016). AMPA receptors are permeable to calcium, sodium, and potassium, with differential permeability depending on subunits compositions. Similar heterogeneity applies to NMDARs. They are mainly calcium-permeable, but like AMPARs, depending on the subunits' composition, their properties change. AMPARs appear to have four agonist sites. Following the binding of the agonist to these binding sites, conformational changes occur, the channel opens, cation enters, and conductance increases, all within milliseconds (Platt, 2007, Traynelis et al., 2010). Once open, the channel suffers rapid desensitization due to small conformational rearrangement in the dimer interface, which closes the pore and diminishes the conductance (Traynelis et al., 2010, Armstrong et al., 2006). NMDARs are more restrictive in gating processes. NMDARs contain four agonist sites for glutamate and for co-agonist glycine (Furukawa et al., 2005). If glycine is not present, the NMDAR opening does not occur. In addition, D-serine has been suggested to be a substitute for glycine in physiological NMDARs activation, mainly by activating synaptic NMDARs (Papouin et al., 2012). Additionally, the NMDAR channel is blocked by Mg^{2+} at physiological conditions. NMDAR opening relies on both agonist binding to their specific site and the release of Mg^{2+} due to AMPAR-mediated depolarization of the postsynaptic membrane (Kristiansen et al., 2007). In doing so, channels allow cation influx and evoke intracellular signaling. NMDARs have slow activation and desensitization compared to AMPARs, leading to the research of these receptors, particularly in synaptic memory after low and high-frequency synaptic inputs (Blancke and VanDongen, 2009).

Glutamate receptors are composed of various subunits, such as GluA1-4 for AMPARs and GluN1-3 for NMDARs, each of them establishing homo or heterotetramers to form active receptors (Wenthold et al., 2003). These subunits are interchangeable, and thus, different subunits combinations grant the receptor diverse channel properties. Due to the receptor's

ability to change their properties (among others) depending on subunit composition, ionotropic glutamate receptors are critical in brain development, synaptic plasticity, and neuropathology.

AMPA and NMDA receptors intrinsically participate in neuronal circuitry by promoting intra- and inter-brain region neuronal communication (Ali et al., 2013). The ionotropic glutamate receptors are part of neuronal activity processes in which long-lasting changes occur in synaptic transmission efficacy. These changes are known as long-term potentiation (LTP) and long-term depression (LTD), where synaptic transmission is potentiated or depressed to modulate electrical signals in the neuronal circuitry (Herring and Nicoll, 2016, Collingridge et al., 2010). Observation of LTP and LTD events throughout decades has led to the conception that they represent cellular correlates of learning and memory because deficits in these cognitive processes commonly are accompanied by impairment of LTP/LTD delivery at a cellular and circuitry level (Stuchlik, 2014, Takeuchi et al., 2014).

Deficits in ionotropic glutamate receptors function and signaling have been widely described in neurodevelopmental (Burnashev and Szepietowski, 2015, Soto et al., 2014), neurodegenerative (Lewerenz and Maher, 2015, Wang and Reddy, 2017), and acute neuropathologies (Carvajal et al., 2016). By being part of the development/maintenance of the disorder or disease, ionotropic glutamate receptors are considered therapeutic targets to delay detrimental effects at a cellular level and clinical symptoms associated with these pathologies.

1.1.2.- Ionotropic glutamate receptor trafficking

As a result of the relevance in physiological and pathological events, the traffic of glutamate receptors toward the synaptic place has been intensively studied. AMPA and NMDA receptor

subunits are synthesized in the endoplasmic reticulum (ER), where dimers are formed, and subsequent tetramers are ensembled (Buonarati et al., 2019, Meddows et al., 2001, Hansen et al., 2010). From there, receptors exit ER to be trafficked through Golgi apparatus. Asparagine residues are glycosylated to further regulate tetramers assembly (Kandel et al., 2018, Skrenkova et al., 2018, Lichnerova et al., 2015), affecting the function of the channel at the plasma membrane. ER-Golgi intermediate compartment (ERGIC) has also shown to be a central structure related to receptor trafficking, particularly in the somatic compartment (Horak et al., 2014), where receptors are rapidly delivered to the plasma membrane. Additionally, palmitoylation occurs at the cytosolic face of Golgi membranes to retain receptors from being surface-expressed (Sohn and Park, 2019). Therefore palmitoylation is part of the internal store regulation of newly synthesized receptors (Mattison et al., 2012). Finally, post-Golgi transport of AMPAR and NMDARs occurs in vesicular organelles. It depends on cytoskeletal structures such as microtubules and actin filaments that run along axons and dendrites. This process is carried out by motor proteins such as kinesins (Hirokawa et al., 2010).

Protein interactions are also essential determinants in ionotropic glutamate receptor trafficking (Figure 2A). AMPAR and NMDAR subunits associates with proteins such as synapse-associated protein 102 (SAP102), stargazing, synapse-associated protein 97 (SAP97), and the exocyst complex, among others, as they traffic toward the neuronal surface (Sans et al., 2001, Horak et al., 2014, Bissen et al., 2019). These proteins ride alongside receptors and stabilize them at the synaptic site, but receptor trafficking *per se* requires specific proteins to carry on the transport. On one hand, AMPARs needs glutamate receptor-interacting proteins (GRIPs), protein interacting with C kinase (PICK1), membrane-associated guanylate kinase family (MAGUKs), transmembrane AMPAR regulatory proteins (TARPs), cornichon proteins

(CNIHs), all of them being the most critical proteins in AMPAR trafficking. On the other hand, NMDAR are trafficked mainly through interactions with MAGUKs proteins such as SAP97, SAP102, and PSD95 with the support of mPins and the exocyst (Horak et al., 2014). Thus, the lack of any of the specific proteins has a strong impact on receptor traffic and delivery, both in basal and stimulating contexts.

AMPA and NMDAR have two options of being transported toward the plasma membrane. One is the canonical secretory pathway at the soma of neurons, and the other is transported through ER–ERGIC–Golgi structures in dendrites (Figure 2B) (Lira et al., 2020). It has been suggested that both receptors continue through the secretory pathway, bypassing the somatic Golgi apparatus, being trafficked to dendritic Golgi outposts alongside adaptor proteins (Lira et al., 2020) illustrating the complexity of the exocytic route for these receptors. In the synapses, ionotropic glutamatergic receptors could be either directly exocytosed at the synapse or first exocytosed into the extrasynaptic membrane, followed by their lateral diffusion at the neuronal surface and trapping at synaptic sites (Carvajal et al., 2016).

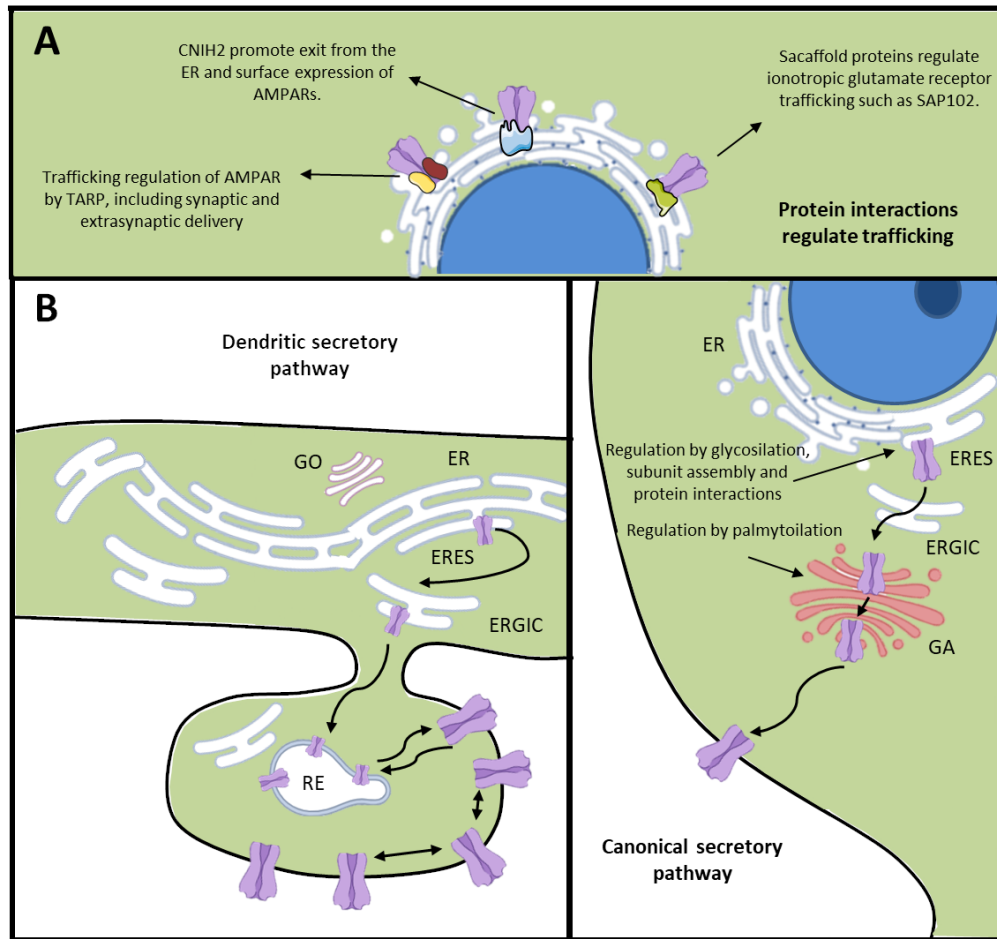


Figure 2. Ionotropic glutamate receptor trafficking. **(A)** Protein interactions regulate exocytic trafficking of ionotropic glutamate receptors, such as TARPs, Cornichon proteins, and scaffolding proteins, among others. **(B)** (Left) Dendritic secretory pathway, indicating the presence of ER, ERES, ERGIC, and GO in the dendrites. Moreover, it shows the action of recycling endosomes in the anterograde secretory pathway for glutamate receptors to the plasma membrane. (Right) Canonical secretory pathway for glutamatergic receptors in the somatic ER, and trafficking through ERGIC and GA. Neurons use both pathways in neuronal development and plasticity. ER: endoplasmic reticulum, ERES: endoplasmic reticulum exits sites, ERGIC: ER–Golgi intermediate compartment, GO: Golgi outpost, GA: Golgi apparatus, TARP: transmembrane α -amino-3-hydroxy-5-methyl-4-isoxazole propionic acid receptor regulatory proteins (Adapted from Lira et al, Cells, 2020).

1.1.3.- Ionotropic glutamate receptors in long term potentiation (LTP)

LTP can be induced by a variety of electrical, pharmacological, and behavioral paradigms. Classical LTP, as initially described (Bliss and Lomo, 1973), can be stable for months. Presumably, a mechanism such as this underlies our own memories, which in human humans can span several decades. LTP is typically induced by high-frequency tetanic stimulation, which leads to Na^+ influx through AMPARs, depolarization of the postsynaptic compartment, and activation of NMDAR to allow Ca^{2+} influx; this sets off a cascade of phosphorylation events to potentiate synaptic transmission (Chater and Goda, 2014).

Glutamate receptor trafficking in and out of synapses is one of the principal mechanisms for rapid changes in the number of functional receptors in synaptic plasticity processes. During LTP induction, AMPAR and NMDAR are grossly increased at synapses (Chater and Goda, 2014), partially by receptor phosphorylation due to an increase in CaMKII, PKA, and PKC activity (Barria et al., 1997, Boehm et al., 2006, Luscher and Malenka, 2012), which leads to augmented synaptic retention of the glutamate receptors. These phosphorylation events enhance channel conductance and opening probability not only in AMPA receptors but NMDA receptors as well, further reinforcing LTP induction (Derkach et al., 1999, Banke et al., 2001, Luscher and Malenka, 2012).

The lack of AMPAR and NMDAR subunits has a strong impact on LTP induction. For example, downregulation of GluA1/2 in neurons results in a total impairment in LTP induction (Terashima et al., 2019, Shimshek et al., 2017), while GluA3/4 lacking neurons suffer reduced LTP induction mostly (Renner et al., 2017, Luchkina et al., 2014). On the other hand, NMDAR-related LTP is abolished when GluN1 or GluN2 subunits are absent (Tsien et al., 1996, Shipton

and Paulsen, 2014). Thus, ionotropic glutamate receptors are essential to LTP induction and expression.

1.1.4.- Ionotropic glutamate receptors in learning and memory

Learning and memory are essential aspects of animal life, including human life, where incoming experiences mainly achieve brain development of the individual. Learning and memory have been intensively studied in human and animal models to gather knowledge at a molecular, cellular, and, therefore, behavioral level. Memory refers to a capability to encode, store and retrieve information to guide behavioral outputs, while learning is considered as acquisition or encoding the information to memory (Stuchlik, 2014).

Initially, learning and memory were associated to forebrain as a whole, where information was processed in a single brain structure. Since then, the research field of memory has concluded that multiple memory systems exist. These systems have specific brain resources (from individual brain zones – to shared capabilities) to fulfill their tasks (Doeller et al., 2008, Lee et al., 2008, Schwabe, 2013) by a strict interplay action between them and memory-related brain zones. Thus, it seems clear that the cognitive system of learning and memory is complex. Given that many interactions and overlaps between those brain resources may occur, it is imperative to comprehend memory consolidation and retrieval.

There are three major classifications of memory: sensory memory, short-term memory, and long-term memory. Information from the world around us begins to be stored by sensory memory, making it possible for this information to be accessible in the future. Short-term memory refers to the data processed by the individual in a short period of time. Working memory performs this processing, and long-term memory allows the storage of information for

long periods (memory consolidation) (Camina and Guell, 2017). But where is memory processed and retained within the brain? Often it is accepted that the hippocampus is responsible for the formation and retrieval of memories. That is the information that structures directly related to the hippocampus (entorhinal, parahippocampal, and perirhinal cortices) yield to the hippocampus, where new memories are generated and can later be retrieved (Brem et al., 2013). The entorhinal cortex is the main interface between the hippocampus and the neocortex; thus, it is associated with the distribution of information to and from the hippocampus. The hippocampus mainly participates in information processing related to declarative memories (usually associated with environmental events), episodic memory, and spatial memories (referenced and working memory) and has been widely used to study spatial memory (Bird and Burgess, 2008).

Glutamate receptors play a significant role in learning and memory processes, particularly ionotropic AMPA and NMDA receptors (Peng et al., 2011). Whether aging- or youth-associated impairment is being discussed, they intrinsically participate in learning and memory processes, which has been discovered by using two approximations: pharmacological and genetic approaches.

Pharmacological inhibition of AMPARs and NMDARs using intrahippocampal administration of antagonists before the cognitive test in murine models evokes memory impairment, while post-testing administration of the same antagonists prior to retesting dimmed behavioral testing for a few days after, these being tested in several learning and memory paradigms such as spatial memory, fear conditioning, odor aversion, among others (Dauvermann et al., 2017). On the other hand, genetic ablation (Knock-out or conditional knock-out) of ionotropic glutamate

receptors on several subzones of the hippocampus produces impairment in learning and memory as well (Morris, 2013), but particularly CA1-specific knock-out severely impair learning and memory (Riedel et al., 2003).

1.2.- Traumatic brain injury

Stable neuronal circuitry and neuronal survival depend on proper synaptic transmission; therefore, it is of utmost importance to study alterations in glutamatergic transmission in both chronic neurodegenerative diseases such as Alzheimer's disease and Parkinson's disease, in which cumulatively damage occurs over a long period of time, as well as in sporadic neuropathologies that are generated by a discrete event, such as traumatic brain injury.

Traumatic brain injury (TBI) is an alteration in brain function and physiology caused by external forces leading to brain movement inside the skull (Menon et al., 2010). It is a critical health problem worldwide that contributes to one-third of all injury-related deaths (Roozenbeek et al., 2013). It has been estimated that by now, in 2021, TBI will become the third leading cause of permanent disability and mortality (Finfer and Cohen, 2001). Indeed, sixty-nine million individuals are estimated to experience TBI nowadays worldwide (Dewan et al., 2018). 1.7 million people suffer from it each year in the United States alone, reaching an annual incidence of 500 in 100,000 (Georges and J, 2021). In Chile, head trauma was the third cause of death amongst young male and female patients between 2000 and 2010 (MINSAL, 2013). Additionally, between 55 and 70% of trauma patients admitted to Chilean emergency rooms comes from traumatic brain injuries caused by car accidents (Ruiz et al., 2013, Franulic et al.,

2004) which leads to high medical costs (Dismuke-Greer et al., 2020), which trigger accumulating interest in research to develop effective treatments.

TBI is considered an acute neuropathology with complex cellular processes that depend on the head trauma severity. Because of this heterogeneity, TBI has been subdivided into three levels of severity, namely mild, moderate, and severe TBI. Mild TBI is the most frequent form accounting for approximately 80% of TBI cases (Blennow et al., 2016, Maas et al., 2008, McCrory et al., 2013). Head trauma can be considered mild when no visible damage is observed in patients or when loss of consciousness, confusion, and disorientation is shorter than 30 minutes (Greenwald et al., 2003). Patients that suffer mild TBI usually present memory loss, headache, dizziness, among others (Blennow et al., 2012). Next, in moderate TBI, we can find similar symptoms than mild TBI, just more intense and lasting for more time. Loss of consciousness can last up to 24 hours, and partial amnesia may appear for seven days (Capizzi et al., 2020). On the other hand, severe TBI is considered the major cause of disability and death within the pathophysiology. Severe TBI can cause permanent physical and mental disability, primarily by being part of polytraumas (Blennow et al., 2016). This type of TBI usually shows abnormal structural brain imaging and loss of consciousness last for at least 24 hours; also, amnesia can occur for several weeks to months (Harrison-Felix et al., 2015, Harrison-Felix et al., 2006). With severe TBI, recovery rate is rather low, with high medical costs involved.

At present, there is a growing concern about severe changes in patients' quality of life that suffer from TBI. The symptoms of TBI are highly variable and can include physical symptoms such as nausea, dizziness, vomiting, and headache; they may also suffer from poor concentration and cognitive deficits (Blennow et al., 2016). In addition, there may be social behavior problems

such as poor emotional integrity, irritability, lack of insight, and judgment in conjunction with aggressiveness (Blennow et al., 2012). Finally, TBI patients can suffer from anxiety and/or depression that can lead to suicide (Silverberg and Iverson, 2011).

Most of the tissue damage in TBI can be classified into two types of harm, focal and diffuse damage. Focal damage results from direct mechanical forces and is usually observed with naked eyes due to physical tissue disruption (Andriessen et al., 2010). Common causes of focal damage include head strikes in car accidents or penetrating head injury, in which the skull is perforated with a severe impact or a gunshot wound (Kazim et al., 2011). On the other hand, diffuse damage is more complex in terms of visibility. Such complexity lies in microscopic cellular damage hardly seen by the naked eye (Andriessen et al., 2010). Therefore, diffuse damage is usually called multifocal damage because head strikes often generate multiple microscopic focal injuries (Su and Bell, 2016). In turn, Diffuse damage results from acceleration, deceleration, and rotational forces gathered in mild TBI. However, it is common for both focal and diffuse damage to occur due to the same event.

1.2.1.- Pathophysiology of TBI

TBI pathophysiology comes in two damage stages. Primary damage is evoked by external forces, which accelerate and deaccelerate brain tissue resulting in cellular damage due to stretch-like events (Blennow et al., 2016). Primary damage also comes when a penetrating wound occurs, and tissue is disrupted as an outcome. On the other hand, secondary damage starts a couple of minutes after the first damage and can last for weeks to months or even years. In this stage, excitotoxicity, neuroinflammation, synaptic injury, oxidative damage, and ultimately cell

death can occur (Figure 3) (Carvajal et al., 2016). In addition, glutamate release/uptake imbalance occurs, and detrimental signaling triggers cell death due to calcium and reactive oxygen species (ROS) buffering impairment (Mira and Cerpa, 2021). Importantly, secondary damage mechanisms are responsible for the persistence of symptoms and increase vulnerability to new brain trauma or other neurodegenerative disorders (Maas et al., 2008).

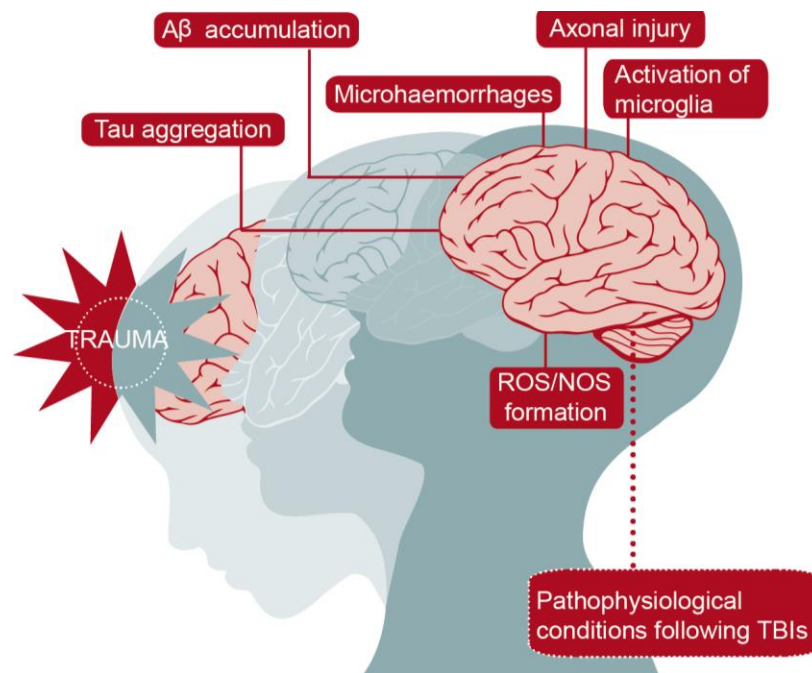


Figure 3.- Scheme depicting cellular and pathophysiological outcomes after TBI induction. Cellular effects comprise tau and A β accumulation, axonal injury, neuroinflammation, excitotoxicity, synaptic damage, and oxidative damage, among others. Pathophysiological alterations in memory, mood, depression, and general daily activities also occur depending on the injury severity (Modified from Blennow et al, 2016).

TBI has commonly been associated with memory loss in patients (Blennow et al., 2016, Blennow et al., 2012). Animal models have replicated these observations with various intensity-related brain injuries. For example, single and repeated mild TBI (typically provoked by closed

head impacts) produces detrimental effects in learning and memory on an array of memory-assessment paradigms (Marschner et al., 2019, Xu et al., 2021, Luo et al., 2017, McInnes et al., 2017). Additionally, severe TBI models resemble long-term memory impairments due to extreme tissue damage (Xu et al., 2019, Mao et al., 2020b), which is not observed in mild TBI. Therefore, depending on the severity of the injury, behavioral outcomes may change, but usually, the damage results in learning and memory impairment.

1.2.2.- Cellular and molecular mechanisms of TBI

Intracellular trafficking of proteins, cargoes, and organelles is of utmost importance for normal cell functioning. Due to head trauma, the brain is compressed and decompressed inside the skull due to head trauma, causing shearing to cells, particularly neurons. This neuronal damage produces microtubule rupture and disconnection that result in hindered intracellular trafficking both in dendrites and axons (McKee et al., 2016, Kaplan et al., 2018, Hill et al., 2016, Siedler et al., 2014), where bulbs are formed because of the trafficking impairments, and thus, hampering the delivery of cargoes to target sites such as synapses.

At the molecular level, proteomics studies have shown that multiple molecular systems in the brain are altered following TBI, being neurons and glia the most studied cells (Zou et al., 2018, Sowers et al., 2018, Chen et al., 2018). For example, synaptic protein levels are decreased, such as brain-derived-neurotrophic factor (BDNF) (Krishna et al., 2019) and the scaffold protein PSD-95 (Rehman et al., 2018). Conversely, glial fibrillary acidic protein (GFAP) and calcium-binding adapter molecule 1 (Iba1), among others, have shown to be altered as well (Manek et al., 2018). Given that protein expression changes with TBI, it is common to observe alterations

in a wide array of signaling pathways within most brain zones. To name some of them, ER-stress, oxidative stress, inflammatory, apoptotic, necroptotic, or even glutamate and gamma-aminobutyric acid (GABA) signaling pathways could be altered depending on TBI severity (Rana et al., 2019, Carvajal et al., 2016).

At the synaptic level, dendritic spines are one of the main cellular structures that are affected by TBI induction (Maiti et al., 2015). Dendritic spine degeneration is commonly observed in TBI patients and murine models, which eventually triggers damped synaptic function and concomitant loss of spines (Xiong et al., 2019). Synaptic malfunction is observed after TBI as a decrease in basal excitatory synaptic transmission (Titus et al., 2016, Xu et al., 2019) in the hippocampus and other zones (Carron et al., 2016), as well as synaptic plasticity in the form of LTP and LTD (Aungst et al., 2014, Schwarzbach et al., 2006).

1.2.3.- Ionotropic glutamate receptors in TBI

Ionotropic glutamate receptors have been extensively studied in several TBI models with proteomics, electrophysiological, and behavioral approaches (Blennow et al., 2016, Blennow et al., 2012, Carvajal et al., 2016). Basal synaptic transmission and plasticity are decreased upon TBI induction (Mira et al., 2020, Zhang et al., 2011), which is accompanied by a reduction in glutamate binding to receptors (Miller et al., 1990) and ultimately their internalization. GluR2 is internalized, and GluN2B availability at synapses is reduced after TBI induction (Bell et al., 2009, Park et al., 2013). Both events trigger downstream signaling that eventually causes a detrimental impact on neurons, and cell death is induced (Carvajal et al., 2016).

AMPA and NMDA receptors can be found both in synaptic and extrasynaptic membranes, and the appropriate balance between their specific localization is responsible for the correct

functioning of the synapse. If we focus on NMDA receptors, glutamate binds this receptor after being released from the presynaptic terminal and triggers downstream signaling. Synaptic NMDARs activate Akt (Papadia et al., 2008) and ERK (Chandler et al., 2001, Papadia et al., 2005), which in turn phosphorylates and activates the transcription factor CREB (Hardingham et al., 2001), thus contributing to neuronal survival. On the other hand, extrasynaptic NMDARs activation elicits ERK dephosphorylation and inactivation (Ivanov et al., 2006) with afterward CREB inactivation (Hardingham et al., 2002), which triggers detrimental effects to neurons. TBI-evoked NMDAR movement outside of synapses produces a disbalance between synaptic and extrasynaptic associated downstream signaling, inducing the effects already presented (Figure 4).

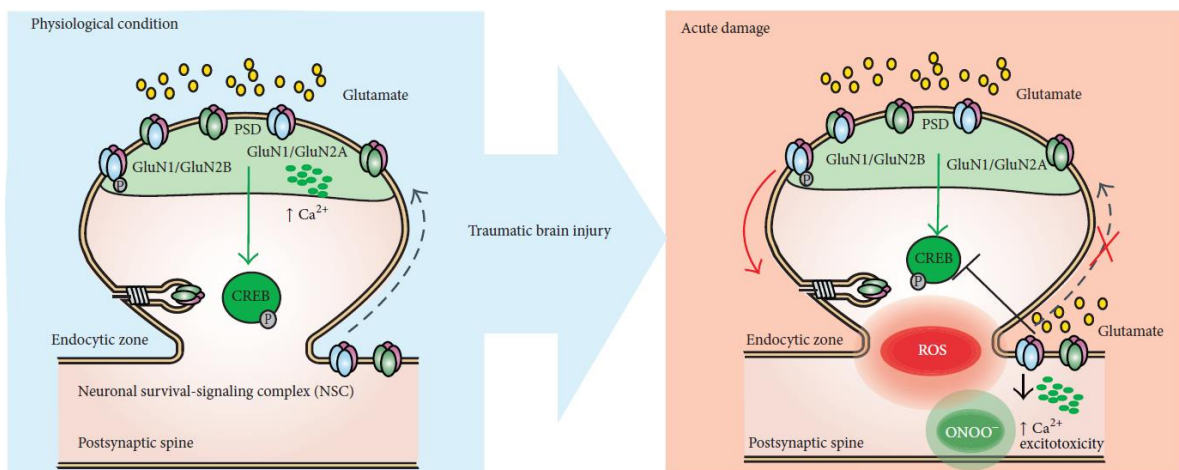


Figure 4.- Dysregulation of NMDARs performance in TBI. Under physiological conditions, synaptic NMDARs are activated as well as antiapoptotic cell pathways preventing excitotoxicity by targeting CREB. After acute damage, including TBI, there is a decrease in CREB activation, increased activation of extrasynaptic NMDARs, and ROS/NOS generation (Adapted from Carvajal et al., *Neural Plast.*, 2016).

1.3.- The exocyst complex

Exocytosis is the process by which eukaryotic cells can release substances into the extracellular space and deliver proteins or lipids to the plasma membrane through the fusion of cargo vesicles. During this process, vesicles (e.g., Golgi-derived vesicles, recycling endosomes, and lysosomes) are transported through microtubules and actin tracks toward specific and polarized areas of the plasma membrane, where vesicles are tethered before fusion to the plasma membrane. Target membrane recognition constitutes an essential mechanism for the specificity of membrane fusion processes in exocytosis. Golgi-derived vesicles are docked and tethered by the exocyst complex (Pfeffer, 1999, Whyte and Munro, 2002, Guo et al., 2000). The exocyst is an evolutionarily conserved complex composed of eight subunits (Sec3, Sec5, Sec6, Sec8, Sec10, Sec15, Exo70, and Exo84) (Figure 5) (TerBush et al., 1996, Guo et al., 1999, Hsu et al., 1996) first identified in yeast and then characterized in multicellular organisms. Many cellular functions have been associated with this complex; these functions include cellular growth, division, migration, signaling, cell–cell contact, Exo/endocytosis of membranes and proteins, morphogenesis of tissues, and cell invasion of fungi, plant, yeast, and mammal organisms (Martin-Urdiroz et al., 2016).

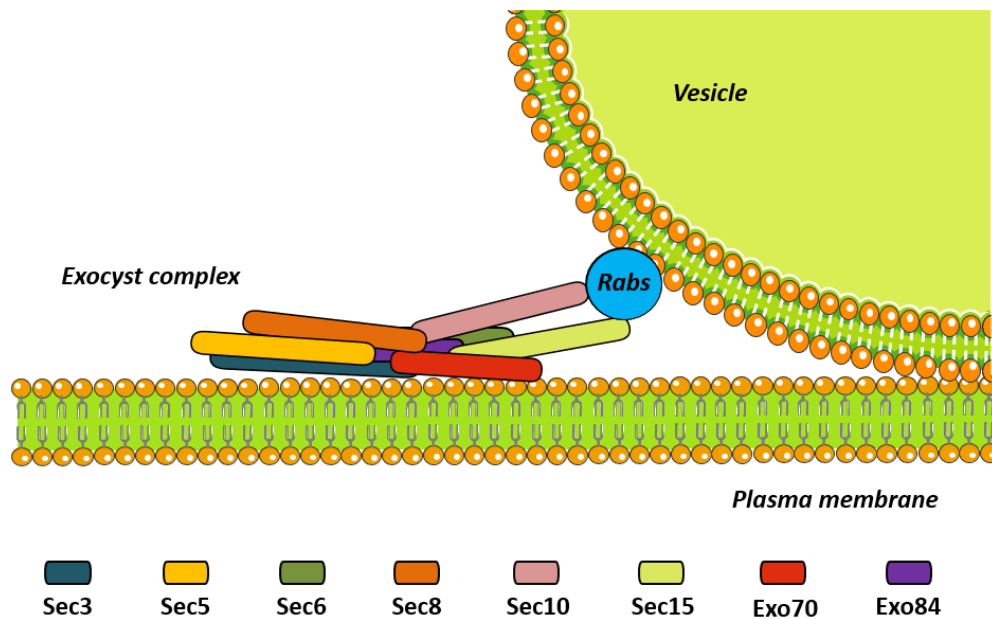


Figure 5.- The exocyst complex. The exocyst acts by tethering secretory vesicles to the plasma membrane in specific sites where the cargo is needed. The model shows a rod-like molecular structure of the subunits. In this model, Sec3 and Exo70 target the exocyst to the plasma membrane. An opposite positioning of Sec10 and Sec15 is observed compared to Sec3 and Exo70; this positioning is vital to the contact of the exocyst with the vesicles where Sec15 interacts with several Rabs to be its effector protein (Adapted from Lira et al., Cells, 2020).

In neurons, the exocyst has been identified in neurite growth cones (Vega and Hsu, 2001) and multiple domains throughout the axon in equidistant patches (Hazuka et al., 1999). Remarkably, the exocyst participates in synapse formation/stabilization from a postsynaptic perspective (Lira et al., 2019, Gerges et al., 2006), while a role in neurotransmitter release has not been discovered yet (Murthy et al., 2003, Andrews et al., 2002). An impairment of neuronal cell polarity and neurite outgrowth is achieved in the absence of native exocyst subunits (Vega and Hsu, 2001, Murthy et al., 2003, Peng et al., 2015).

Exo70 is one of the most studied exocyst subunits. Exo70 is localized at the plasma membrane and can directly interact with regions containing phosphoinositol-4,5-bisphosphate (PI(4,5)P₂) through a phospholipid-binding motif located in its C-terminus (Liu et al., 2007, Moore et al., 2007). In doing so, it mediates the exocyst targeting to the plasma membrane (Hamburger et al., 2006). Exo70 has been shown to participate in neurite development and synapse formation/stabilization (Dupraz et al., 2009, Lira et al., 2019). Its intracellular localization is important to carry on its tethering and exocytosis functions (Inoue et al., 2003, Vega and Hsu, 2001, Pommereit and Wouters, 2007) and particularly its plasma membrane localization promotes the activity of the complex (Inoue et al., 2006, Zhang et al., 2016, Fujimoto et al., 2019). Thus, Exo70 is considered to be a limiting factor in the exocyst complex activity (Ren and Guo, 2012, Zhang et al., 2016).

1.3.1.- Exocyst in ionotropic glutamate receptor trafficking and delivery

When it comes to the exocyst—a complex related to traffic, recycling, and exocytosis—several reports have intended to elucidate how it may function in delivering and recycling AMPA and NMDA receptors. First, it is essential to note that interactions between the exocyst and AMPA/NMDA receptors have been detected both *in vivo* and in a heterologous cell system. Positive interactions in brain and synaptosome preparation were detected between Sec8, Sec6, and GluN2B (Sans et al., 2003). In addition, Sec8 and Exo70 interact with GluR1-3 and GluN1 (Gerges et al., 2006). This interaction occurs early in the ER, where the exocyst recruits newly synthesized receptors to be ridden through actin cables (Sans et al., 2003), and this interaction is essential to the delivery of the receptors to the plasma membrane. Blocking this interaction through the Sec8-PDZ domain deletion results in cell surface delivery impairment. GluN1 and

GluN2B trafficking toward the cell surface are carried out in a trimeric complex, which includes SAP102, Sec8, and the receptors in heterologous cells and neurons (Sans et al., 2003, Mellone and Gardoni, 2013). Reaching the plasma membrane, Sec8 controls the directional movement of AMPA receptors to the synapse through PDZ domains, and Exo70 mediates the insertion of the receptor to the plasma membrane. An interference of Exo70 function with Exo70 dominant-negative (DN) lacking a C terminal domain results in the accumulation of AMPA receptors within the spine, forming an associated complex that has not been fused to the plasma membrane (Gerges et al., 2006). This DN impairs the delivery of GluR1 to the dendritic spines surface in cultured hippocampal neurons, suggesting a synaptic transmission malfunction. Indeed, Exo70 DN reduced the AMPAR excitatory postsynaptic currents, while Sec8 DN affected both AMPAR and NMDAR currents (Gerges et al., 2006).

GluR2 trafficking into distal dendrites is effected when Sec8 DN is expressed but not with Exo70 DN expression, indicating that AMPARs transport along dendrites does not require a fully functional Exo70 subunit (Gerges et al., 2006). In addition, expression of Sec8 DN is related to a reduction in AMPAR EPSC, supporting its involvement in trafficking (Gerges et al., 2006).

NMDAR trafficking toward cell surface employs a large protein complex containing GluN1, GluN2B, SAP102, mPins, and Sec8 (Sans et al., 2003, Sans et al., 2005, Petralia et al., 2009). NMDAR travels through dendrites bound to SAP102, which in turn binds to Sec8. Both NMDAR and Sec8 bind SAP102 in the same region containing PDZ domains (Sans et al., 2003). Expression of Sec8 DN that lacks the PDZ-binding domain impair Sec8–SAP102 binding, thus preventing the delivery of NMDARs to the cell surface. This provides evidence that NMDAR

surface delivery needs both Sec8 and SAP102. This transport complex also binds Sec6 and Exo70, suggesting that some or the entirety of the complex travel with ensembled NMDARs toward the cell surface and synapse (Sans et al., 2003). A schematic summary is shown in Figure 6.

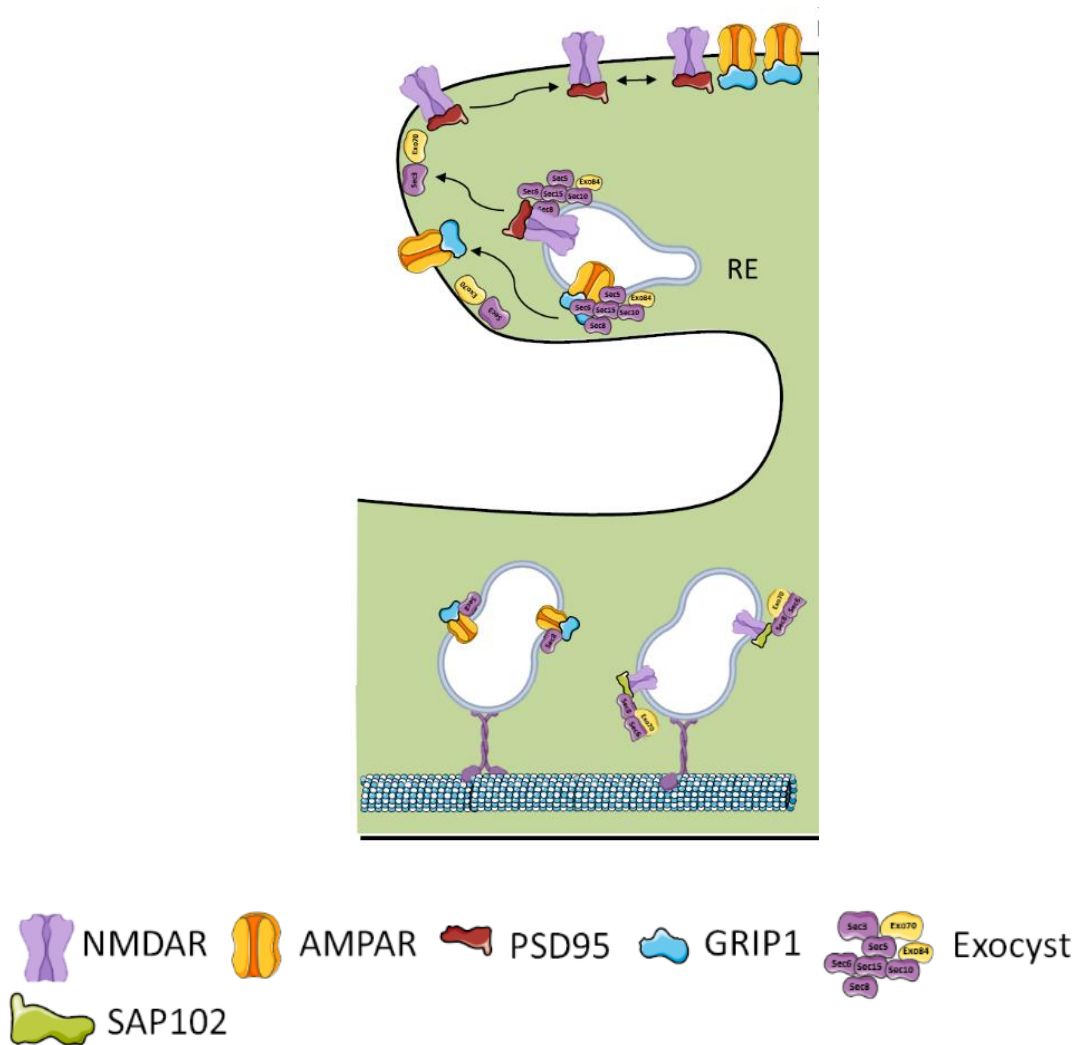


Figure 6. Exocyst in glutamatergic receptors trafficking. (Left) In basal conditions, AMPARs are trafficked along with the GRIP1 scaffold protein and the Sec8 subunit of the exocyst complex. NMDARs, on the other hand, are trafficked in vesicles along with SAP102 scaffold protein and subunits of the exocyst complex such as Sec8, Sec6, and Exo70 (Adapted from Lira et al., Cells, 2020).

1.3.2.- The exocyst complex in brain pathologies.

The knowledge of exocyst's involvement in brain pathologies is very limited. First of all, the exocyst participates in neuronal development and migration within the brain, being part of the machinery that drives polarized cell migration (Das et al., 2014, Letinic et al., 2009). Three case reports point that Sec15 downregulation and the genetic anomaly are involved in neurodevelopmental abnormalities affecting ultimately intellectual ability, language delay, and speech capacity (Fruhmesser et al., 2013, Wen et al., 2013, Borsani et al., 2008). Pathogenic variants of Sec5 affect brain development, produce seizures with minor epileptic episodes, evokes large white matter loss, and presents severe hypoplastic hippocampi (Van Bergen et al., 2020). SEC8 is a candidate gene involved in Meckel-Gruber syndrome, which is a multiple congenital malformation syndrome characterized by an occipital encephalocele (among others phenotypes) evoked by neural tube closure impairment (Shaheen et al., 2013). Biallelic mutations in the SEC6 gene cause downregulation of Sec6 protein and evokes brain development impairment, primarily in the cerebellum (Shalata et al., 2019). Finally, Sec6 has been associated with brain glucose metabolism abnormalities presented in Alzheimer's disease patients, presumably by affecting intracellular transport (Miller et al., 2018).

2.- Hypothesis and objectives

2.1.- Hypothesis

NMDARs can be found in both postsynaptic and extrasynaptic compartment, granting a balance by which NMDAR-mediated synaptic signaling and function is regulated. In TBI, GluN2B leaves the postsynaptic density and is redirected into the extrasynaptic compartment, evoking a signaling imbalance, detrimental effects on synaptic transmission and cognition. This suggests that a trafficking impairment occurs to NMDAR when a head trauma occurs. One of the components of NMDAR trafficking towards the synapse is the exocyst complex. The exocyst, especially Exo70 and Sec8 subunits, are of utmost importance to allow NMDAR trafficking and delivery into the synapse at the basal level. Additionally, Exo70 is considered as a limiting factor in the exocyst's function in intracellular trafficking. Therefore, we pose the following hypothesis:

“The synaptic localization of NMDA receptors mediated by Exo70 counteracts cognitive damage in a model of mild traumatic brain injury.”

2.2.- General objective

To determine whether Exo70 acts as a compensatory mechanism to promote the synaptic localization of NMDA receptors and counteract cognitive damage produced by brain trauma.

2.3.- Specific objective

- **1.-** To determine if mTBI changes Exo70 expression.
 - 1a.- To evaluate Exo70 presence in the forebrain, cortex, and hippocampus in mice.
 - 2a.- To determine whether Exo70 protein level is altered upon mTBI induction.

- **2.-** To evaluate Exo70 subcellular localization after mTBI.
 - 2a.- To evaluate subcellular localization in forebrain, cortex, and hippocampus of mTBI mice.
 - 2b.- To evaluate Exo70's proximity to the plasma membrane after mTBI induction.
 - 2c.- To determine if exocyst's assembly is altered upon mTBI induction.

- **3.-** To determine if Exo70 gain of function rescues learning/memory and NMDAR synaptic availability after mTBI induction.
 - 3a.- To determine whether Exo70 overexpression rescues learning and memory upon mTBI induction.
 - 3b.- To determine if Exo70 gain of function restores the synaptic function of mice subjected to mTBI.
 - 3c.- To evaluate whether Exo70 overexpression normalizes the intracellular signaling associated with synaptic NMDA receptors.

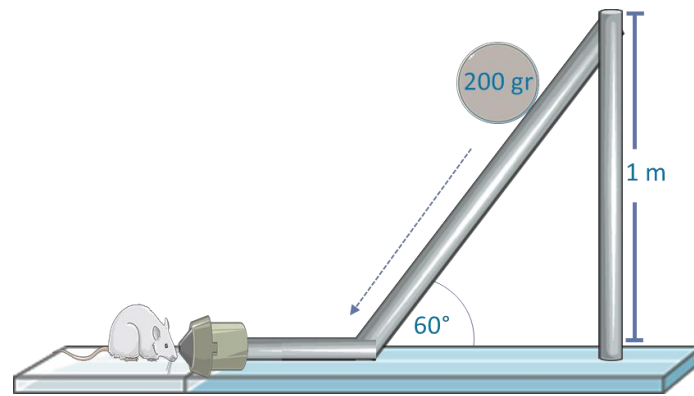
3.- MATERIALS AND METHODS

3.1.- Animals

One and two months old C57BL/6 J male mice were used in this study. Animals were housed up to 4 mice per cage with a 12:12 h light/dark cycle (light on at 8:00 am) and provided food and water ad libitum. Animals were obtained from CEBIM-UC (Center for Innovation in Biomedical Experimental Models from the Pontificia Universidad Católica de Chile). Animals were handled according to the National Institutes of Health guidelines (NIH Publications No. 8023). The Bioethical and Biosafety Committee of the Faculty of Biological Sciences of the Pontificia Universidad Católica de Chile approved all experimental procedures (N° 180814017)

3.2.- Traumatic brain injury procedure

To induce mTBI, we used a modified Maryland's weight drop model used for rats (Kilbourne et al., 2009). For this purpose, we adapted the impact device to fit mice anatomy (Mira et al., 2020, Carvajal and Cerpa, 2021). The impact energy was obtained from a 180 grams steel ball accelerated by gravity along a 1 m rail disposed at a 60° angle from the horizontal. The rail curved at the bottom end to redirect the ball onto a chamber where it struck a coupling arm. The arm then accelerated to impact the malar processes bilaterally with 2 pistons. The energy of impact delivered was calculated as follows: $E_{\text{impact}} = E_{\text{total}} - E_{\text{rotational}}$, (Figure 7), resulting in 1.1 Joule.



$$E_{\text{impacto}} = E_{\text{total}} - E_{\text{rotacional}}$$

$$E_{\text{impacto}} = \frac{1}{2} \cdot m \cdot v^2 - \frac{1}{2} \cdot I \cdot \omega^2$$

$$E_{\text{impacto}} = 1,1 \text{ J} - 0,087 \text{ j}$$

$$E_{\text{impacto}} = 1,1 \text{ J}$$

$V = \text{velocidad} = (2 \cdot g \cdot h)^{1/2}$, donde $g = 9,8 \text{ m/s}^2$

$I = \text{momento de inercia} = \frac{2}{5} \cdot m \cdot r^2$

$\omega = \text{velocidad angular} = 2 \cdot \pi \cdot f$, donde $f = 1/2 \cdot \pi \cdot r/t$

$M = \text{masa de la bola} = 0,180 \text{ Kgrs}$

$r = \text{radio de la bola} = 0,0155 \text{ m}$

$h = \text{altura vertical de la rampa} = 1 \text{ m}$

$L = \text{longitud de la rampa} = 1,32 \text{ m}$

$T = \text{tiempo de la bola en la rampa} = 0,6 \text{ s}$

Figure 7.- Frontal impact device is shown. Impact energy is calculated as shown in the equation.

Animals were randomly assigned to receive either sham or mTBI. Mice were anesthetized with isoflurane using the open-drop method (Risling et al., 2012). Animals were then gently restrained in position onto the impact device using an elastic belt placed across the dorsal thorax leaving the head free. Mice were subjected to 5 sessions of 3 blasts, each with a 2-day interval in a frontal weight impact device. After each session, mice were carefully monitored until the anesthesia effect was finalized and returned to their home cage. Then, animals were kept in their home cage for 7 days before analysis (Figure 8). Orally administered Tramadol (30 mg/kg every 24 hours) was used as analgesic. Sham animals were subjected to all procedures except injury induction.

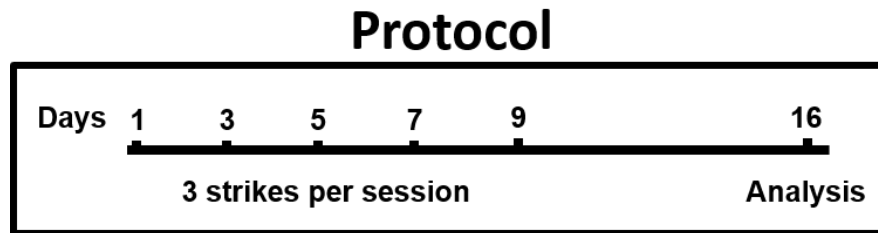


Figure 8.- Protocol for repeated mTBI induction is shown. The scheme depicts the interval of the strikes session and the analysis time after the protocol is initiated.

3.3.- Biochemical analyses

3.3.1.- Immunoblot

Protein concentration was determined using a BCA protein assay kit (Pierce, ThermoFisher Scientific, USA). Samples were resolved by SDS-PAGE and transferred to PVDF membranes. Protein quantity and polyacrylamide gel percentage are indicated in each figure legend. Membranes were blocked with BSA 5% in PBS-tween 0.1% for 1 hour and incubated overnight with primary antibodies at 4 °C (Table 1). Then, membranes were washed 3 times with PBS-tween 0.1% and incubated with the appropriate secondary antibody for 1 hour. Blots were developed using a chemiluminescence detection kit. Images were obtained with a G:BOX Chemi XT4 Gel imaging system (Syngene). Membranes were stripped for 30 min at room temperature using a stripping buffer (6 M GnHCl, 0.2% NP-40, 100 mM β -mercaptoethanol, 20 mM Tris-HCl, pH 7.5) and washed thoroughly 4 times with PBS containing 0.1% Tween-20. After stripping, membranes were tested again with chemiluminescence to confirm that membranes were properly stripped, and no signal was detected. Up to four stripping was carried out to each membrane, carefully managing that secondary antibody host was intercalated between mouse and rabbit.

Table 1.- Antibody List

Antibody	Company	Dilution
Exo70	Proteintech	WB 1:2000; IHC 1:300
GAPDH	Santa Cruz Biotechnology	WB 1:1000
Tubulin	Santa Cruz Biotechnology	WB 1:1000
PSD-95	Santa Cruz Biotechnology	WB 1:1000
Synaptophysin	Santa Cruz Biotechnology	WB 1:1000
PDI	Santa Cruz Biotechnology	WB 1:1000
β -Actin	Sigma	WB 1:2000
PMCA1	Santa Cruz Biotechnology	WB 1:1000
GluR1	NeuroMabs	WB 1:1000
GluR2	Santa Cruz Biotechnology	WB 1:1000
GluN2A	NeuroMabs	WB 1:1000
GluN2B	ThermoFisher Scientific	WB 1:1000
GluN2B p1472	Cell Signaling	WB 1:1000
GluN2B p1336	Invitrogen	WB 1:1000
Sec6	Santa Cruz Biotechnology	WB 1:500
Sec10	Santa Cruz Biotechnology	WB 1:500
GFP	NovusBiologicals	WB 1:2000; IHC 1:200
HA	Cell Signaling	WB 1:1000
pCREB	NovusBiologicals	WB 1:1000
pERK1/2	ThermoFisher Scientific	WB 1:1000
ERK1/2	ThermoFisher Scientific	WB 1:1000
Fyn	Santa Cruz Biotechnology	WB 1:500

3.3.2.- Subcellular fractionation

For subcellular fractionation, the sucrose gradient was performed. Tissues were rapidly dissected on cold PBS. Samples were homogenized in buffer A containing 5 mM Hepes, pH 7.4; 320 mM sucrose supplemented with a protease and phosphatase inhibitor mixture (Protease: Amresco, VWR Life Science; Phosphatase: 25 mM NaF, 100 mM Na_3VO_4 and 30 μM $\text{Na}_4\text{P}_2\text{O}_7$). Homogenization was done using a potter S by delivering 10 up and down strokes. Cell debris were removed by centrifugation for 10 min at 1,000 g (P1) and the supernatant (S1) was centrifuged for 20 min at 20,000 g obtaining S2 (cytosol and microsomes) and P2 fractions. In order to isolate microsomes, the S2 fraction was centrifuged for 2 h at 100,000 \times g. P2 fraction was loaded on top of a 0.32/0.85/1.0/1.2 M sucrose gradient and centrifuged for 2 h at 100,000 \times g and synaptosomes were obtained from 1.0/1.2 M interface. Synaptosomes were then resuspended in Triton buffer (20 mM HEPES, 100 mM NaCl, 0.5% Triton X-100, pH 7.2) and rotated for 20 min before centrifugation at 20,000 \times g for 20 min to obtain PSD and nonPSD fractions. PSD pellet was resuspended with PBS unless otherwise mentioned. A scheme of the conducted fractionation is shown in Figure 9. All manipulations were carried out on the ice or at 4 °C. Samples were stored at -80 °C until use. Proteins (30 μg per well) were resolved in 10% SDS-PAGE and analyzed by Western blot.

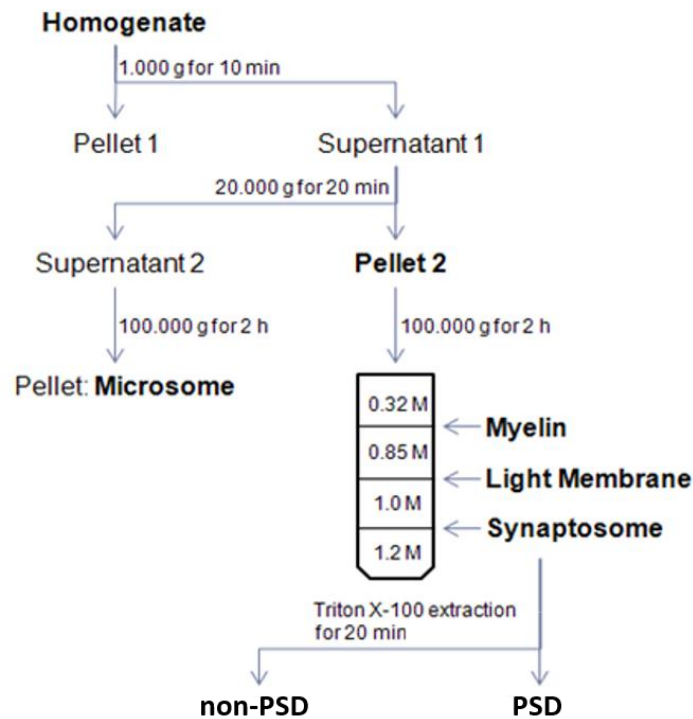


Figure 9.- Schematic representation of the steps followed in the subcellular fractionation.

3.3.3.- Co-immunoprecipitation

Co-immunoprecipitation experiments were carried out as follows. Both hippocampi from each mouse were dissected and PSD and nonPSD fractions were prepared as described above with minor modifications. PSD fractions were resuspended in RIPA buffer (25 mM Tris-Cl, pH 7.6, 150 mM NaCl, 1% NP-40, and 0,1% SDS) and rotated for 20 min for immunoprecipitation. Samples were quantified using the BCA Protein assay kit (Pierce, ThermoFisher Scientific, USA). 50 µg of PSD and 300 µg of nonPSD protein samples were incubated with 1 µg of Exo70 antibody overnight at 4 °C followed by incubation with Protein A/G agarose beads (30 µl; Santa Cruz Biotechnology, USA) for 1 h at 4 °C. Normal rabbit IgG was used as a control for

immunoprecipitation. Then, beads were recovered by brief centrifugation and washed three times with PBS. Proteins were eluted with a 2X protein loading buffer, resolved in a 6% SDS-PAGE, and transferred to PVDF membranes. Membranes were cut to allow the proper probing of receptors and exocyst's subunits in the same membrane. Membranes were stripped up to four times. The absence of signal was determined after each stripping (appendix A, right panel).

3.3.4.- Cell surface biotinylation

Hippocampal slices were prepared as follows. Brains were quickly removed, and transverse slices (300 μm) were cut under cold artificial cerebrospinal fluid (ACSF, in mM: 124 NaCl, 2.6 NaHCO₃, 10 D-glucose, 2.69 KCl, 1.25 KH₂PO₄, 2.5 CaCl₂, 1.3 MgSO₄, and 2.60 NaHPO₄) using a vibratome (BSK microslicer DTK-1500E, Ted Pella, Redding, CA, USA) and incubated in a resting chamber for 1 h with a 95% O₂/5% CO₂ saturation. Brain slices were transferred to an incubation chamber at 4 °C supplemented with O₂ and CO₂. Then, slices were incubated with EZ-Link Sulfo-NHS-Biotin (1 mg/ml in ACSF, ThermoScientific) for 45 min at 4 °C to biotinylate surface proteins. Excess biotin was removed by washing the slices three times (5 min) with a quenching solution (Glycine 100 mM) and then washing three times with cold ACSF. Hippocampal slices were dissected under a binocular microscope (Amscope, Irvine, CA, USA). Slices were homogenized in modified RIPA buffer (150 mM NaCl, 20 mM HEPES, 1% Triton X-100, 0.5% SDS, and 2 mM EDTA, pH 7.4) supplemented with a mixture of protease and phosphatase inhibitors. Sample homogenates (total fraction) were collected, and cell debris was removed by centrifugation for 10 min at 12,000 g. Next, supernatant proteins were quantified using a BCA protein assay kit (Pierce, ThermoFisher Scientific, USA). 500 μg of protein were incubated overnight at 4 °C with Neutravidin Agarose beads (50 μl ; Pierce,

ThermoFisher Scientific, USA). Beads were recovered by brief centrifugation and washed three times with ice-cold PBS. Proteins were eluted with a 2X protein loading buffer and resolved in a 10% SDS-PAGE.

3.4.- Immunohistochemistry

Mice were perfused intracardially with saline solution and PFA 4%. Brains were removed and post fixated for 6 hours in PFA 4%. 30 μ m thick brain slices were cut in a cryostat and stored -20 °C with OLMOS solution. Slices were permeabilized with 0.2% (v/v) Triton X-100 in PBS (PBS-T) for 30 min. Then, a 30 min incubation was carried out with 0.15 M Glycine and 10 mg/ml NaBH₄ (for immunofluorescence) and H₂O₂ 3% (for chromogenic immunohistochemistry). Slices were washed with PBS-T three times and blocked with 3% BSA for 1 h at room temperature. Slices were incubated overnight at 4 °C with primary antibodies diluted in PBS-T containing 3% BSA. After three PBS-T washes, slices were incubated with respective secondary antibody in PBS-T containing 3% BSA for 2 h at room temperature. Slices were then washed three times with PBS and distilled water. Chromogenic staining was developed using DAB kit (ThermoFisher Scientific, USA). Finally, slices were mounted on gelatin-coated slides using the appropriate mounting media and images were captured in an Olympus BX51 microscope equipped with a Micro-publisher 3.3 RTV camera (QImaging, Surrey, BC, Canada) using Q-imaging software.

3.5.- Intrahippocampal lentiviral injection

Third-generation lentiviral particles were packaged and acquired in Applied Biological Materials (ABM, Canada) based on the bicistronic lentiviral construct FUG-1D/2A-W (Figure 10). 1 μ l of high titer (1×10^9 IU/ml) lentiviral particles were injected bilaterally into the CA1 *stratum radiatum* region of the dorsal hippocampus from 4 weeks old C57BL/6 J mice using a stereotaxic device. Coordinates from bregma were 1.8 mm caudal, 1.5 mm lateral and 1.5 mm ventral. The injection rate was 0.5 μ l/min. After surgery, mice were carefully observed in their recovery process in a thermal pad at 37 °C. Lentiviral expression was carried out for 4 weeks prior to mTBI induction.

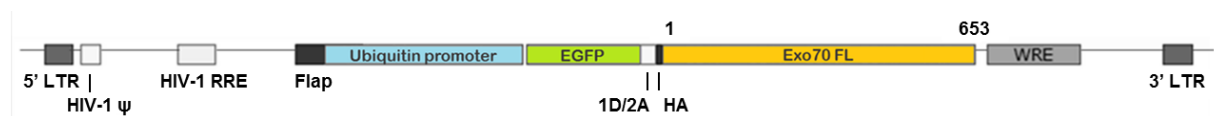


Figure 10.- Map of the bicistronic lentiviral construct. The construct have the self-cleavage signal 1D/2A from the foot and mouth disease virus that allows the synthesis of two soluble individual proteins (Lira et al., 2019).

3.6.- Behavioral analysis

3.6.1.- Spatial memory

The Morris water maze (MWM) task was used as a spatial memory behavioral test. Mice were trained in a 1.1 m diameter circular pool (opaque water, 50 cm deep) filled with 19–21 °C water. A submerged 9-cm platform (1 cm below the surface, invisible to the animal) was used for training, with a maximum trial duration of 60 s and 10 s on the platform at the end of the trials. Mice were placed into the water facing the side walls, being transported there by hand from a holding cage. Each animal was trained to locate the platform. The test was performed with three

trials per day for 5 days, and a probe test was carried out on day 6 where the platform was removed. Swimming was monitored using an automatic tracking system (ANY-maze video tracking software, Stoelting Co, Wood Dale, IL, USA). This system was used to measure the latency time (in seconds) required for the animal to reach the platform and the time spent in each quadrant (in seconds). After testing, the mouse was gently removed from the maze and returned to its cage.

3.6.2.- Memory flexibility

The week after MWM was performed, memory flexibility was tested using a modified MWM paradigm. Each animal was trained for one pseudo-random location of the platform per day for 4 days, with a new platform location each day. Up to 15 training trials were performed per day until the criterion of 3 successive trials with an escape latency of <20 s was met (intertrial delay time = 20 min). Upon testing completion, mice were gently removed from the maze and returned to its cage. The animals were tested for the next location on the following day. Data were collected using a water maze video tracking system (ANY-maze video tracking software, Stoelting Co, Wood Dale, IL, USA).

3.7.- Electrophysiology

Transverse slices (400 μm) from the dorsal hippocampus were cut under cold ACSF using a Vibratome (BSK microslicer DTK-1500E, Ted Pella, Redding, CA, USA) and incubated in ACSF for 1 hour at room temperature. In all experiments, 10 μM PTX was added to suppress inhibitory GABAA transmission. Slices were transferred to an experimental chamber (2 ml), superfused (3 ml/min, at room temperature) with gassed ACSF (using 95% O_2 /5% CO_2) and visualized by trans-illumination with a binocular microscope (Amscope, Irvine, CA, USA). To

evoke field excitatory post synaptic potentials (fEPSPs), Schaffer collaterals were stimulated with bipolar concentric electrodes (Tungsten, 125 μm OD diameter, Microprobes) connected to an isolation unit (Isoflex, AMPI, Jerusalem, Israel). The stimulation was performed in the *stratum radiatum* within 100–200 μm from the recording site. Recordings were filtered at 2.0–3.0 kHz, sampled at 4.0 kHz using an A/D converter (National Instrument, Austin, TX, USA), and stored with the WinLTP program. The basal excitatory synaptic transmission was measured using an input/output curve protocol with 10 s of interval between stimuli. To generate LTP, we used high-frequency stimulation (HFS) protocol, which consisted of 3 trains at 100 Hz of stimuli with an inter-train interval of 10 s. In order to isolate NMDAR fEPSP, slices were incubated with 20 μM NBQX 30 min before testing started and the antagonist were kept throughout the recording. Data were collected and analyzed offline with pClamp 10 software (Molecular Devices, San Jose, CA, USA).

3.8.- Dorsal hippocampus isolation

Characterization of lentiviral expression were carried out in dorsal hippocampal samples. Brains were cut with a vibratome (BSK microslicer DTK-1500E, Ted Pella, Redding, CA, USA) and the dorsal hippocampus were isolated. Two 300 μm thick dorsal hippocampal slices per brain hemisphere were homogenized in RIPA buffer and analyzed by immunoblot.

Western blot analysis of Sham and mTBI mice injected with lentiviral particles was carried out using dorsal hippocampal slices employed in the electrophysiological analyses. Hence, after synaptic transmission analyses were finished, the slices were stored at $-80\text{ }^{\circ}\text{C}$ until required. Samples were homogenized and resolved in a 10% SDS-PAGE.

3.9.- Statistical analysis

Data were analyzed using unpaired t-test where 2 experimental groups was presented. For multiple-grouped experiments, statistical analysis was calculated using one-way ANOVA or two-way ANOVA with Bonferroni correction for multiple comparisons. All data is shown as mean \pm SEM. A $p < 0.05$ value was considered significant. GraphPad Prism 8 was used to carry statistical analysis.

4.- RESULTS

4.1.- Objective 1: To determine if mTBI changes Exo70 expression

4.1.1.- Evaluation of Exo70 expression

Exo70 expression has been reported in rat and mouse forebrain (Chernyshova et al., 2011, Lira et al., 2019). Nevertheless, a more profound description in structures like cortex or hippocampus is yet to be described. Cortical and hippocampal slices of 2 months old C57BL/6J mice were analyzed for Exo70 expression and localization. By immunohistochemistry, Exo70 is observed in mostly all cortical layers. Most of the signal comes from II to III layers and the immunoreactivity is reduced in inner layers V and VI (Figure 11A). Hippocampus also shows Exo70 expression throughout all hippocampal zones (Figure 11B). Exo70 immunoreactivity is predominantly observed in CA1 and CA3 *stratum pyramidale*, although some Exo70-positive cells in *stratum oriens* and *stratum radiatum* are found (Figure 11C and D, lower panels). Finally, dentate gyrus Exo70 expression is predominantly observed in the granule cell layer (Figure 11E) and immunoreactivity is detected in hilus-located cells (Figure 11C, lower panels). Next, protein extracts were obtained from the forebrain, cortex, and hippocampus from 2-month-old mice, and samples were analyzed by immunoblot. The analysis shows that Exo70 is expressed on the forebrain, cortex, and hippocampus (Figure 11F), supporting immunohistochemistry results.

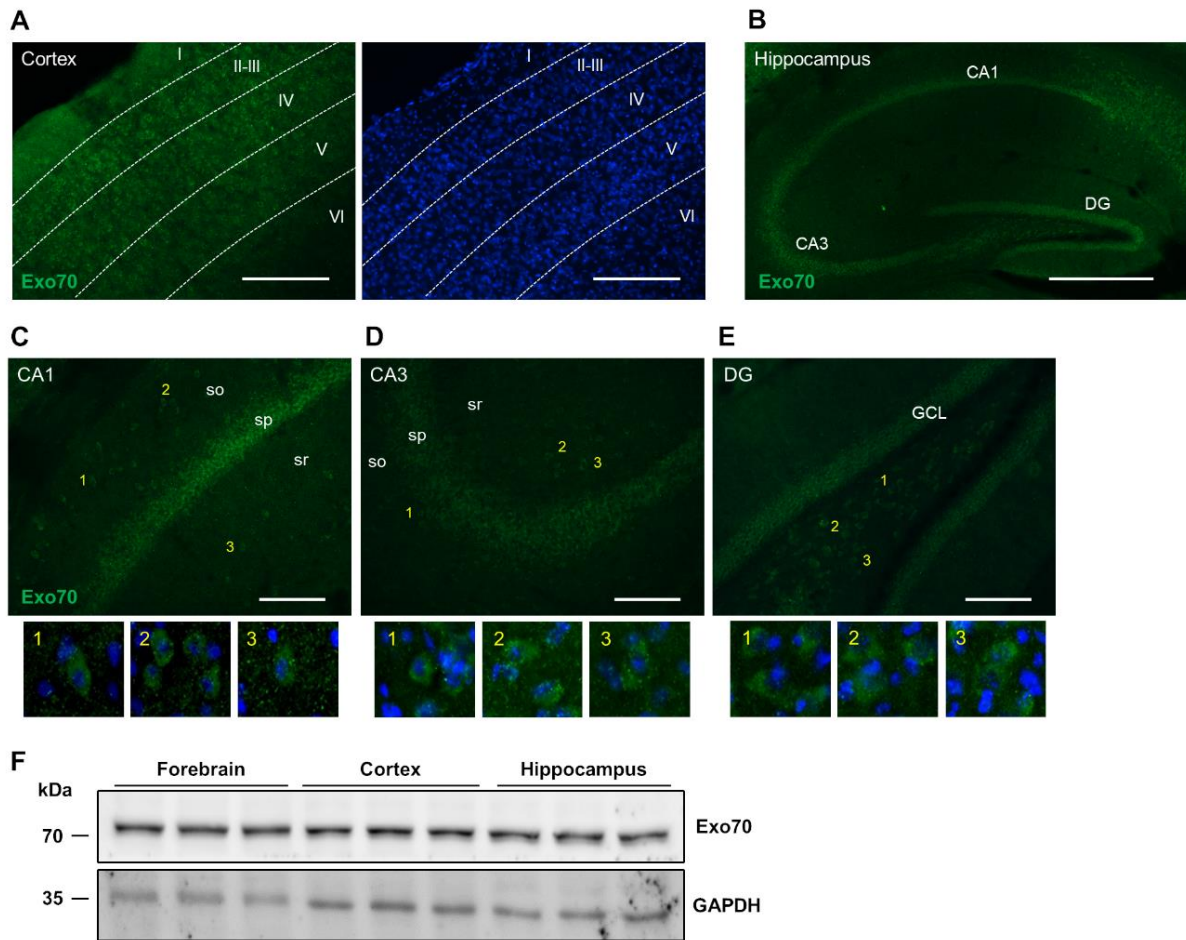


Figure 11.- Evaluation of Exo70 expression in the brain, cortex, and hippocampus. Two-month-old male mice were perfused and 30 μm thick brain slices were prepared. **(A and B)** Representative images of slices were obtained between 1.8 and 2 mm caudal from bregma. Slices were stained with an Exo70 specific polyclonal antibody and Hoechst to label the nucleus. Cortical layers and hippocampal zones are depicted in the images. Scale bars: cortex 300 μm , hippocampus 400 μm . **(C, D, E)** Hippocampal zones CA1, CA3, and DG are shown. so: Stratum oriens; sp: Stratum pyramidale; sr: Stratum radiatum. Scale bars: 100 μm . **f** Western blot analysis of brain, cortex, and hippocampus protein extracts. Samples were resolved in 10% SDS-PAGE. 30 μg of protein samples were loaded in each well. $n = 3$ mice per group.

4.1.2.- Evaluation of Exo70 expression after mTBI

To date, no study has been conducted to evaluate the contribution of exocyst complex in neurodegenerative diseases or particularly in acute neuropathologies like mTBI. To induce mTBI, we used a modified Maryland's weight drop model used for rats (Kilbourne et al., 2009) to fit mouse anatomy. This model uses a repeated scheme (see methods) in which brain damage is achieved. Our model induces diffuse damage in the cortex that eventually reaches the hippocampus provoking impaired synaptic transmission (Mira et al., 2020) and cognitive decline (Carvajal and Cerpa, 2021). Initially, it was asked whether mTBI alters Exo70 expression in the forebrain, cortex, and hippocampus. Protein samples were obtained and analyzed by Western blot. The analysis showed that Exo70 protein level was not altered when mice were subjected to mTBI in all anatomical regions (Figure 12).

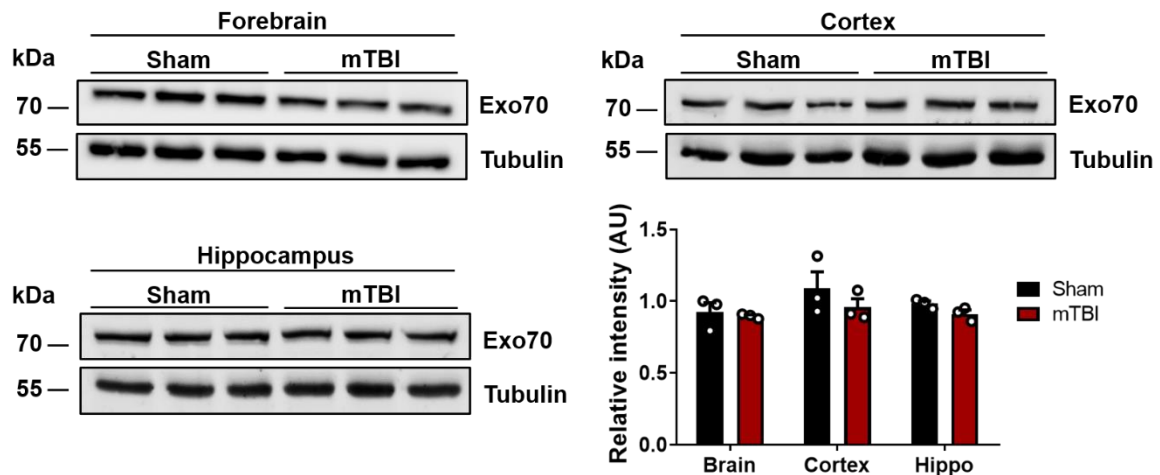


Figure 12.- Exo70 protein levels are not altered after mTBI induction. Two-month-old male mice were subjected to mTBI, and protein extracts were prepared from the forebrain, cortex, and hippocampus. Protein samples were resolved in 10% SDS-PAGE and transferred to PVDF membrane. Western blot analysis was carried out using Exo70 and Tubulin antibodies. The graph shows the Exo70 densitometric analysis normalized with the Tubulin signal. Values represent means \pm SEM, $n = 3$ mice per experimental group. Statistical differences were determined by an unpaired t-test comparing Sham and mTBI. Brain $p = 0.18$, Cortex $p = 0.29$, Hippocampus $p = 0.37$.

4.2.- Objective 2: To evaluate Exo70 subcellular localization after mTBI.

4.2.1.- Exo70 compartmentalization following mTBI

Exo70, as part of the exocyst complex, has shown to have several functions. Most of them related to membrane trafficking and exocytosis (Martin-Urdiroz et al., 2016), particularly localized near the plasma membrane (Inoue et al., 2006, Zhang et al., 2016). Indeed, the correct function of Exo70 strictly depends on its subcellular localization (Inoue et al., 2003, Dupraz et al., 2009, Zhang et al., 2016, Fujita et al., 2013). To study this, a classic biochemical approach was used to assess if mTBI changes the subcellular patterning in tissue. Forebrain subcellular fractionation was carried out using a well-established protocol (see figure 9 in methods section) (Lira et al., 2019, Smalla et al., 2013) to obtain cytosol, microsome, and P2 crude membrane fraction. P2 is then further fractionated to obtain synaptosomes. Samples were processed and analyzed by immunoblot (Figure 13A). As expected, the major postsynaptic scaffolding protein PSD95 was mainly distributed in synaptosomes (Figure 13B). Synaptophysin, a synaptic vesicle protein, was highly distributed in microsomes and synaptosomes (Figure 13B). Protein disulfide-isomerase (PDI) is an endoplasmic reticulum-resident protein and therefore is distributed in microsome fractions. GAPDH, a cytosolic protein, was distributed in cytosolic fractions (Figure 13B). Hence, the distribution of those proteins validates the biochemical preparations. Exo70 was present in cytosol, microsome, and synaptosome fractions from the forebrain and was highly distributed in microsomal fraction (Figure 13B). Then, mice were subjected to mTBI, and forebrains were fractionated to obtain microsomal and synaptosomal fractions (Figure 13C). In these fractions, Exo70 localization was increased on mTBI mice

compared to Sham mice (Figure 13D), suggesting that Exo70 may increase its functionality upon mTBI induction.

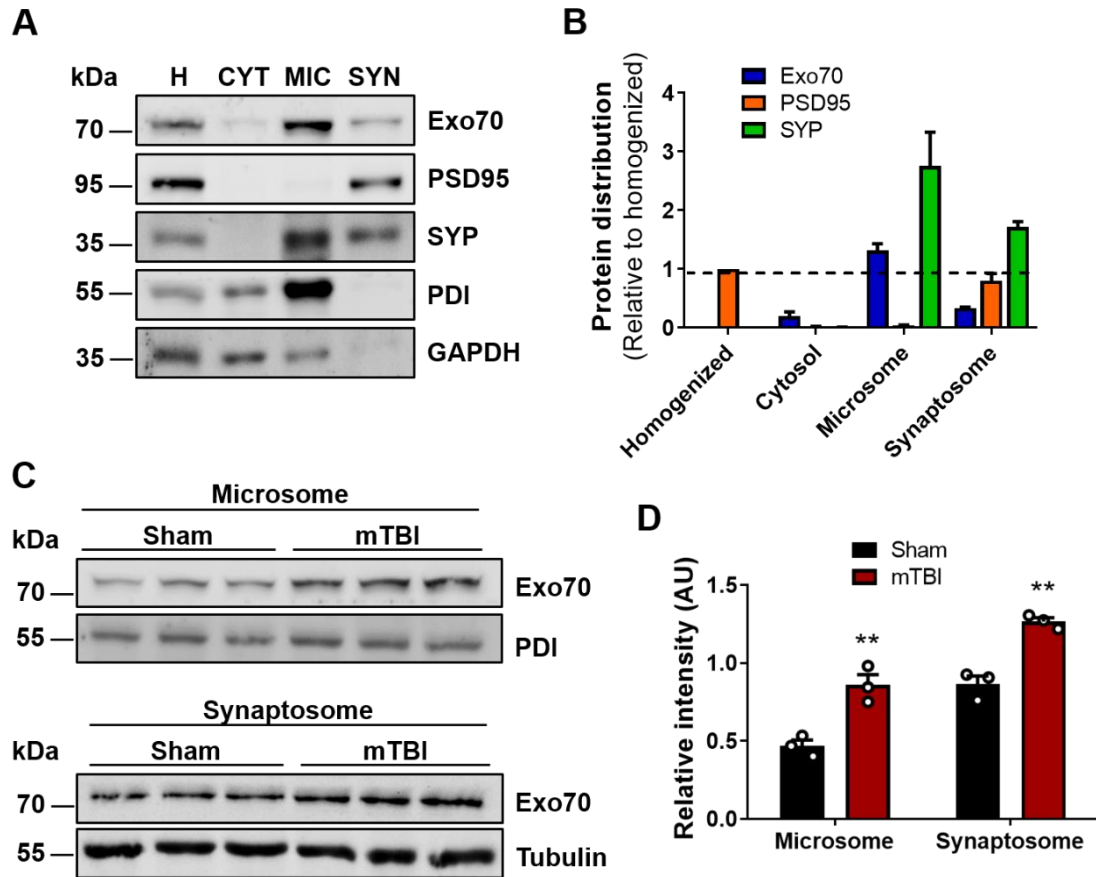


Figure 13.- Exo70 localization is increased in forebrain synapses upon mTBI induction. **(A)** Forebrains from two-month-old male mice were obtained and subcellular fractionation was carried out. Homogenized (H), cytosol (CYT), microsome (MIC), and synaptosome (SYN) fractions were obtained. 20 μ g of protein samples were resolved in a 10% SDS-PAGE and transferred to PVDF membranes. Membranes were incubated with the respective antibodies shown in the figure. Membranes were stripped and tested again with the indicated antibodies. **(B)** Protein distribution was analyzed with densitometric analysis by comparing signal intensity from each fraction with homogenized. Mean values \pm SEM are shown. **(C)** Two-month-old male mice were subjected to mTBI and microsome and synaptosome fractions were obtained. 30 μ g of protein samples were analyzed. PDI/Tubulin was used as loading controls. **(D)** The graph shows the Exo70 densitometric analysis normalized with loading controls. Values represent means \pm SEM, $n = 3$ mice per experimental group. Statistical differences were determined by an unpaired t-test comparing Sham and mTBI. ** $p < 0.01$.

Because the damage induced by mTBI can reach the hippocampus passing through the cortex, it was intended to determine if Exo70 subcellular distribution would behave similarly between both cortex and hippocampus. To test this, subcellular fractionation was carried out using the same protocol for the forebrain and analyzed it again by immunoblot. An example of hippocampi subcellular fractions is shown in Figure 14A. In these experiments, synaptosome fraction was treated with Triton X-100 and further fractionated to obtain PSD and nonPSD fractions (Figure 14A). PSD95 showed that it is highly distributed in PSD and excluded from nonPSD fraction (Figure 14B). Contrary to this, Synaptophysin was highly distributed in nonPSD and excluded from PSD fraction (Figure 14B), indicating that synaptosome fractionation worked as expected. Exo70 was again highly distributed in microsomes (Figure 14B). However, it was present in PSD and nonPSD fractions, although most of the synaptosomal Exo70 was present in nonPSD. Next, subcellular fractionation was performed of cortex and hippocampus obtained from Sham and mTBI mice. Exo70 distribution was analyzed in microsome, PSD, and nonPSD fractions by immunoblot (Figure 15). No Exo70 distribution changes were observed on the cortex (Figure 15A), while Exo70 distribution in the hippocampus was altered upon mTBI induction. Specifically, Exo70 localization was reduced on microsome and increased in PSD fraction (Figure 15B), suggesting that Exo70 is redistributed from microsome to PSD following mTBI.

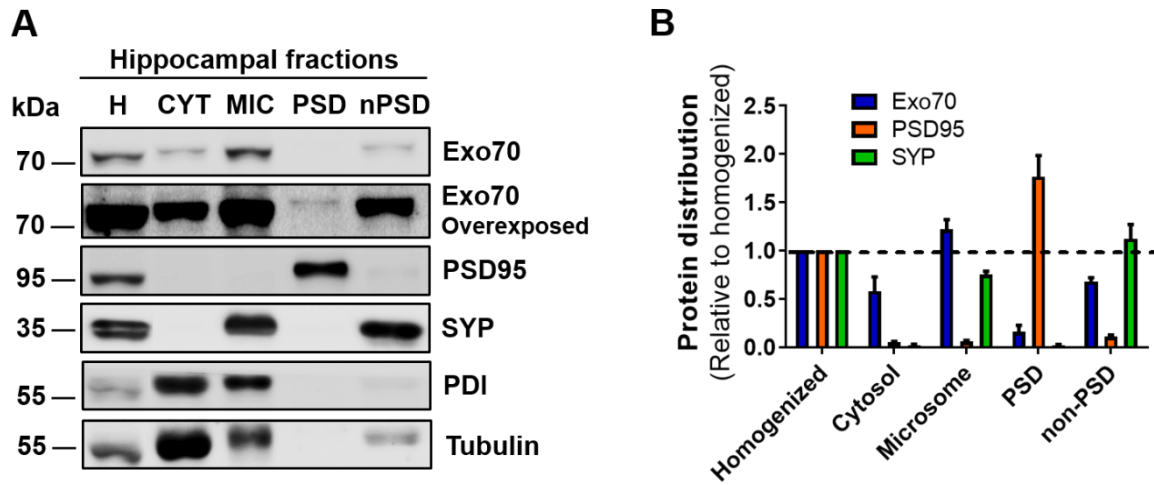


Figure 14.- Hippocampal subcellular fractionation. Hippocampus from two-month-old male mice was fractionated and microsome, PSD, and nonPSD fractions were obtained. 20 μ g of protein samples were resolved in a 10% SDS-PAGE and transferred to PVDF membranes (**A**). Membranes were incubated with the respective antibodies shown in the figure. Membranes were stripped and tested again with the indicated antibodies. (**B**) Proteins distributions were analyzed with densitometric analysis by comparing signal intensity from each fraction with homogenized. Mean values \pm SEM are shown. N = 3 mice.

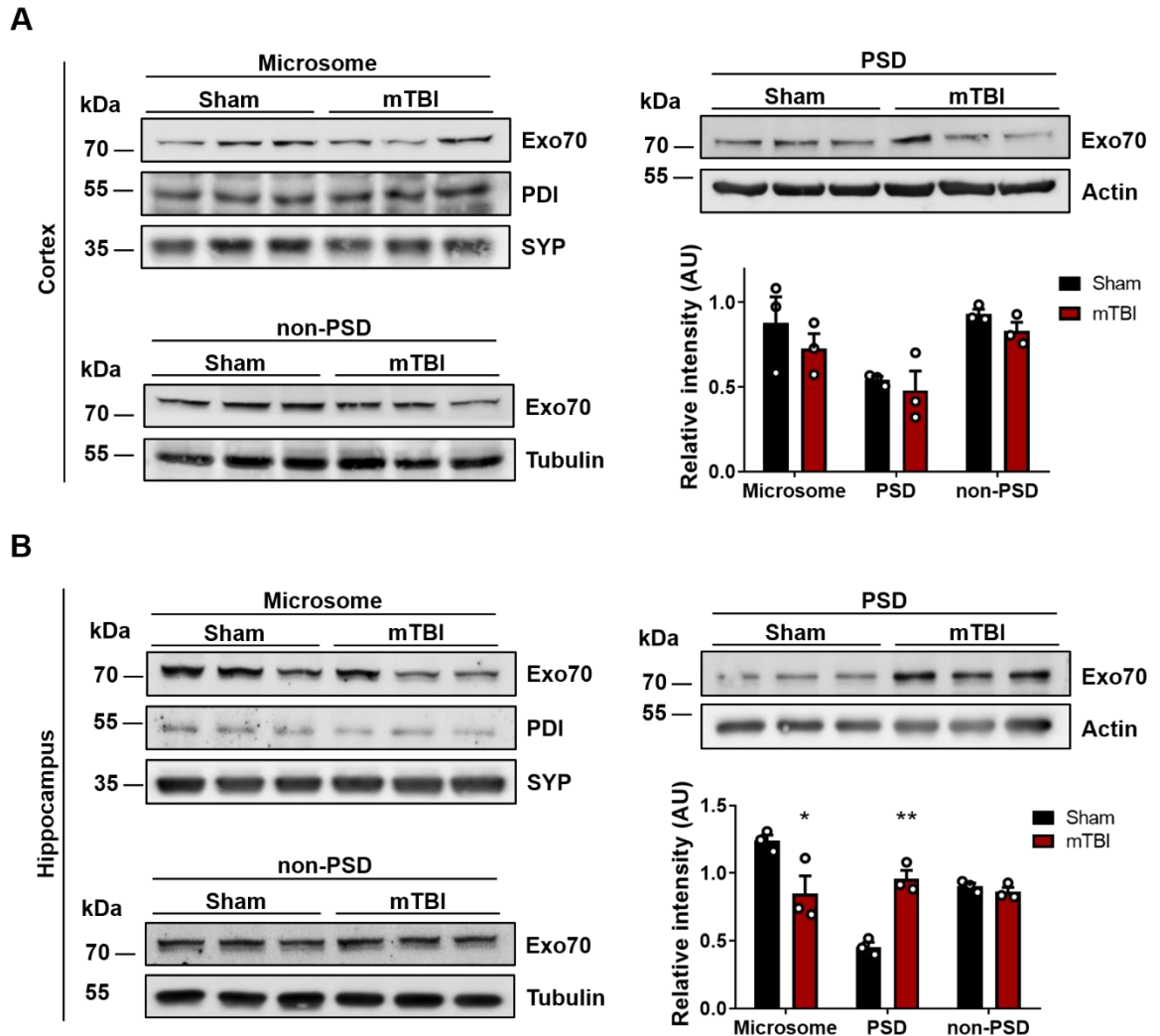


Figure 15.- Exo70 is redistributed into PSD in the hippocampus of mTBI mice. (A) Cortex and Hippocampus (B) from Sham and mTBI mice were fractionated and analyzed by western blot using Exo70, PDI, Actin, and Tubulin antibodies. PDI/Actin/Tubulin was used as loading controls. 30 μ g of protein samples were resolved in a 10% SDS-PAGE and transferred to PVDF membranes. The graph shows the Exo70 densitometric analysis normalized with loading controls. Values represent means \pm SEM, $n=3$ mice per experimental group. Statistical differences were determined by an unpaired t-test comparing Sham and mTBI. * $p < 0.05$, ** $p < 0.01$.

4.2.2.- Exo70 membrane proximity following mTBI

Exo70 is mainly found in the microsomal fraction, as shown above. Microsome fraction contains endoplasmic reticulum, Golgi apparatus, synaptic vesicles, and plasma membrane (Sandoval et al., 2013). As Exo70 is predominantly located at the plasma membrane (Liu et al., 2007, Moore et al., 2007, Zhang et al., 2016), it was asked if Exo70 membrane localization is altered following mTBI. To test this, an ex vivo approach was used by which plasma membrane proteins are isolated using biotin. Brain from Sham and mTBI mice were cut to obtain slices, and biotinylation was carried out (see methods). After biotinylation, hippocampal slices were dissected and homogenized, and biotinylated proteins were captured using NeutrAvidin. Using this approach, it was able to isolate most of the membrane fraction as shown by the plasma membrane calcium ATPase PMCA1, a typical plasma membrane marker, while cytosolic GAPDH showed absence in this fraction (Figure 16A), indicating that the protocol worked as expected. Membrane-proximal Exo70 showed to be nearly 30% of total Exo70 (Figure 16B). Interestingly, after mTBI induction, Exo70 surface proximity was reduced by 36% (Figure 16C and D), suggesting that Exo70 redistribution towards PSD observed in fractionation experiments comes from the plasma membrane.

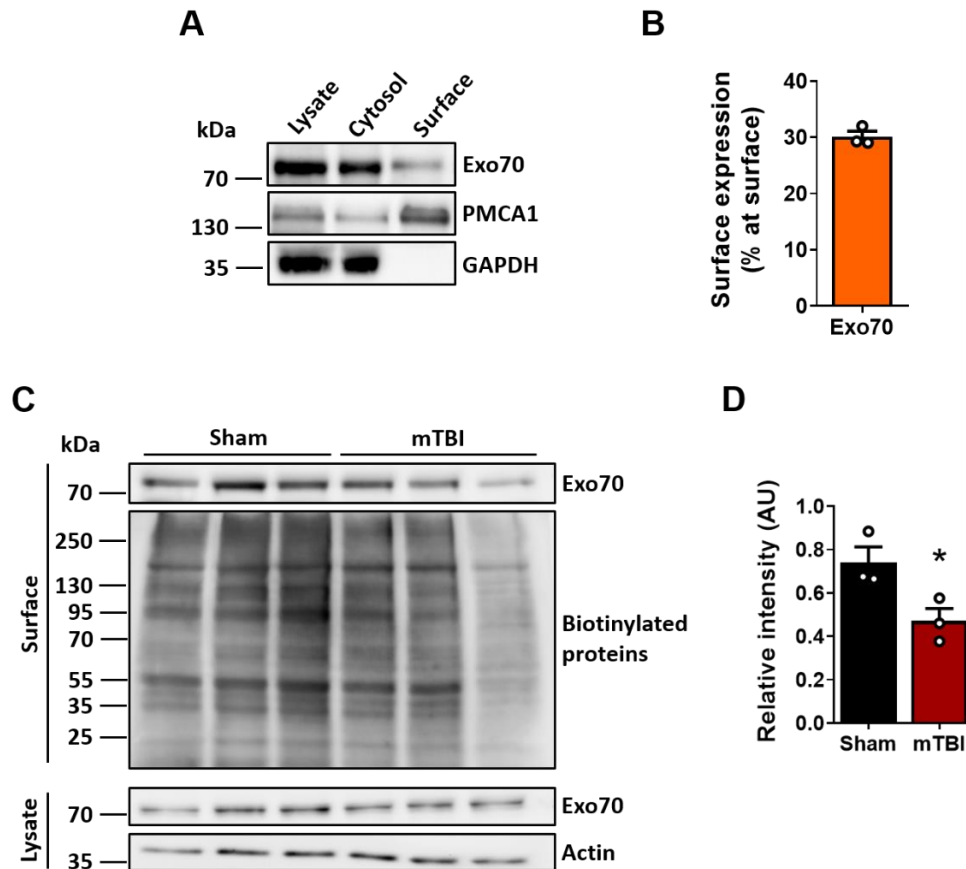


Figure 16.- Exo70 proximity to the plasma membrane decreases after mTBI induction. **(A)** Brains from two-month-old mice were cut in 300 μ m thick slices. Biotinylation was carried out and the hippocampus was dissected. Hippocampal slices were homogenized in a modified RIPA buffer (see methods). 500 μ g of protein samples were incubated with NeutrAvidin overnight at 4 $^{\circ}$ C and beads were obtained by brief centrifugation. 200 μ g (40%) of total protein samples were loaded alongside cytosolic (unbound) and eluted samples from NeutrAvidin precipitation assays. Samples were resolved in 10% SDS-PAGE and transferred to PVDF membranes. Membranes were incubated with the antibodies indicated in the figure. Membranes were stripped and tested again with the indicated antibodies. **(B)** Exo70 proximity to the plasma membrane was described as follows: Combined cytosolic and surface Exo70 band intensities were considered as 100%. Then Exo70 proximity was calculated using the band intensity combination. The graph shows that nearly 30% of the Exo70 total pool is proximal to the plasma membrane. Mean \pm SEM is shown, $n = 3$ hippocampi from different mice. **(C)** Two-month-old male mice were subjected to mTBI, and hippocampal slices were prepared and biotinylated. 500 μ g of protein samples were incubated with NeutrAvidin overnight at 4 $^{\circ}$ C, and beads were obtained by brief centrifugation. Lysates were analyzed using 30 μ g of proteins. **(D)** Exo70 densitometric analysis. Protein lysates were used to normalize band intensities. 4 Hippocampal slices from each mouse were used. Values represent means \pm SEM, $n = 3$ mice per experimental group. Statistical differences were determined by an unpaired t-test comparing Sham and mTBI. * < 0.05 .

4.2.3.- Exocyst assembly following mTBI

Exo70 has been proposed as the nucleating factor of the exocyst complex establishing the site where the complex should be directed (Lira et al., 2019, Picco et al., 2017, Ahmed et al., 2018, Lipschutz and Mostov, 2002). Also, the level of assembly of the complex through Exo70 denotes its activity on exocytosis (Ren and Guo, 2012, Mao et al., 2020a, Lu et al., 2016). Therefore, it was asked if the assembly of the exocyst complex is altered on mTBI mice. In order to do that, hippocampal PSD and nonPSD fractions from Sham and mTBI mice were prepared as above, and Exo70 was immunoprecipitated using a specific polyclonal antibody. Experiments were analyzed using Sec6 and Sec10 antibodies (Figure 17A and C). In PSD, Exo70 interaction with Sec6 and Sec10 was increased, indicating that the complex's assembly is increased following mTBI (Figure 17B). On the other hand, Exo70 interaction with Sec6 and Sec10 was reduced in the nonPSD fraction (Figure 17D). These results suggest that the complex assembly occurs in hippocampal PSD after mTBI induction. Crude data is observed in appendix A, left panel.

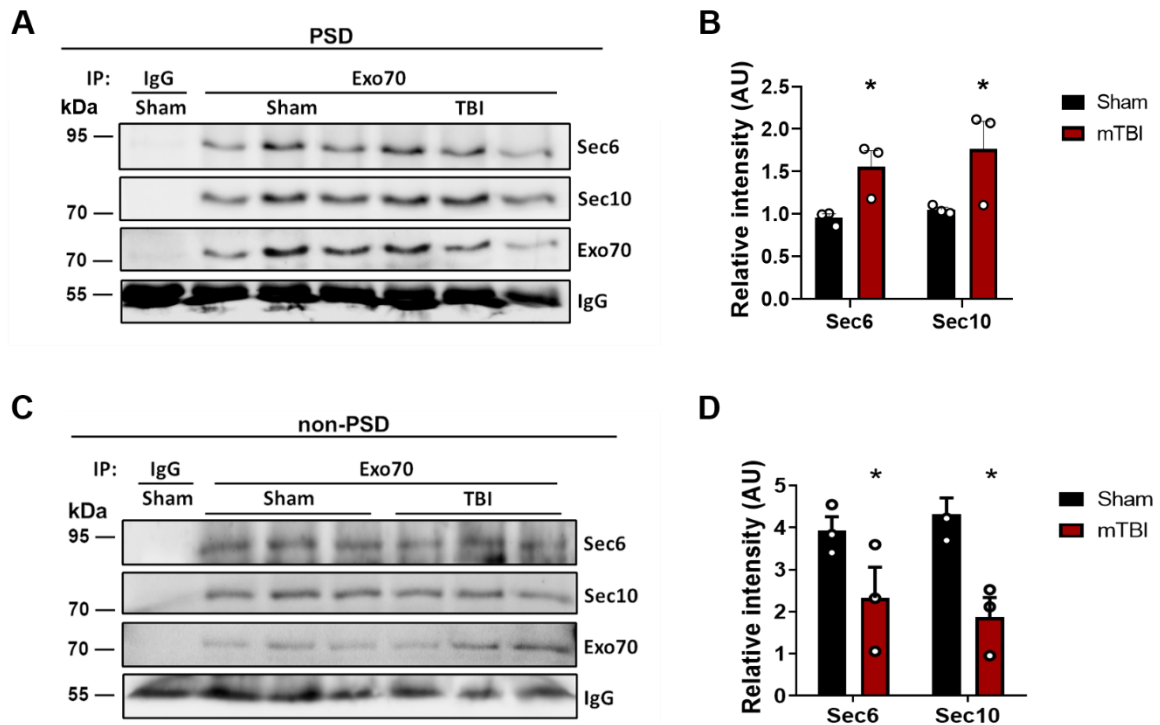


Figure 17.- mTBI increases exocyst complex assembly in the PSD fraction. **(A and C)** Two-month-old male mice were subjected to mTBI and hippocampal PSD/nonPSD fractions were obtained. 50 and 300 μ g of PSD and nonPSD protein samples, respectively, were immunoprecipitated using a specific Exo70 polyclonal antibody. Beads were recovered by brief centrifugation. Samples were resolved in 6% SDS-PAGE and transferred to PVDF membranes. Both hippocampi of each mouse were used. Membranes were stripped and tested again with the indicated antibodies. **(B and D)** Sec6 and Sec10 densitometric analysis from PSD and nonPSD immunoprecipitations. Signal intensity was normalized with Exo70 band intensity. The analysis shows the assembly level of the exocyst complex is increased after mTBI. Values represent means \pm SEM, $n = 3$ mice per experimental group. Statistical differences were determined by an unpaired t-test comparing Sham and mTBI. * $p < 0.05$.

The exocyst has been related to AMPA and NMDA receptors trafficking and delivery into the synapse (Gerges et al., 2006, Sans et al., 2003) by being in the same protein complex, thus modulating the availability of these receptors on PSD. In this case, it was asked if mTBI could change the level of interaction between Exo70 and both types of ionotropic glutamate receptors in hippocampal PSD and nonPSD fractions. To address this, hippocampal PSD and nonPSD

fractions were prepared, and Exo70 was again immunoprecipitated. In these experiments, GluR1/GluR2 from the AMPA receptors and GluN2A/GluN2B from the NMDA receptors were assessed by immunoblot (Figure 18A). The analysis showed that Exo70 didn't change its interaction with both GluR1 and GluR2 AMPAR subunits in PSD when mTBI was induced (Figure 18B). When it comes to the NMDA receptors, Exo70 interaction is increased only with the GluN2B subunit and not with GluN2A (Figure 18B). Null interaction was detected between Exo70 and AMPA/NMDA subunits in nonPSD fraction (not shown). This prompts the idea that the assembly of the exocyst complex favors the interaction with GluN2B in the hippocampus upon mTBI induction. It is then suggested that Exo70 redistribution into PSD to increase its interaction with GluN2B is probably a compensatory mechanism by which GluN2B gets stabilized in PSD to diminish mTBI detrimental neuronal effects.

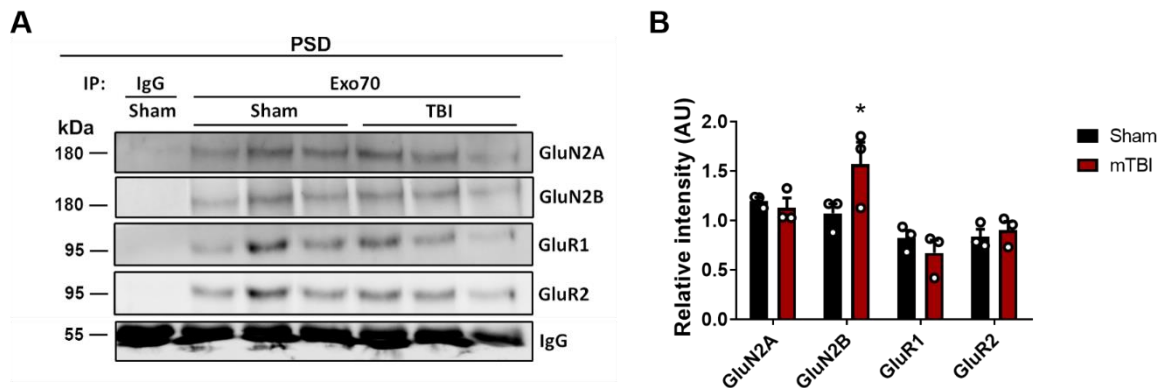


Figure 18.- mTBI increases Exo70-GluN2B interaction in the PSD fraction. GluN2A, GluN2B, GluR1, GluR2 densitometric analysis from PSD and nonPSD immunoprecipitations. Samples were resolved in a 10% SDS-PAGE and transferred to PVDF membranes. Signal intensity was normalized with Exo70 band intensity. Exo70-GluN2B increased interaction after mTBI. Values represent means \pm SEM, $n = 3$ mice per experimental group. Statistical differences were determined by an unpaired t-test comparing Sham and mTBI. * $p < 0.05$.

4.3.- Objective 3: To determine if Exo70 gain of function rescues learning/memory and NMDAR synaptic availability after mTBI induction.

From this point, the experimental strategy adopted to evaluate this objective is a lentiviral infection of CA1 neurons with lentiviral particles that overexpress Exo70. The lentivirus used in this thesis is based on the human immunodeficiency virus genome with a third-generation system, which grants a high biosafety level due to the lack of viral replication capacity (Dull et al., 1998, Lois et al., 2002). This system allows long-term stable expression of the protein of interest and does not considerably affect neuronal network activity (Minerbi et al., 2009). Mice injected with lentiviral systems have demonstrated stable lentiviral expression for months, showing even cognitive changes (Jeon et al., 2018, Kanninen et al., 2009, Barbash et al., 2013) and is a reliable tool to use in the research of TBI physiology (Farook et al., 2013).

4.3.1.- Intrahippocampal lentiviral injection

Mice were bilaterally injected on postnatal day 30 with 1 μ l of lentiviral suspension (approximately 1×10^6 lentiviral particles), and the expression was analyzed 30 days after. The lentiviral construct expresses a single transcript (GFP + Exo70), which is then translated and processed with the self-cleavage sequence 1D/2A located between GFP and Exo70 ORF; thus, generating both proteins separately with an HA tag fused to Exo70 in the N-terminal end (Figure 19). Lentiviral expression was first evaluated in HEK293 cells by immunoblot. The analysis showed that GFP is only expressed in transduced cells, while no GFP signal was detected in non-transduced cells (Figure 20A). Soluble GFP bands showed two molecular weights, one at 25 kDa corresponding to control LV-GFP lentivirus, and the other at ~27 kDa. The former being expressed by a control lentivirus that doesn't express the HA tag (Figure 20A, arrowhead), and

the latter being expressed by HA-tagged Exo70 lentiviral virus Figure 20A, asterisk). The self-cleavage site likely adds residues to the GFP protein and therefore slight increase in molecular weight is observed. Additionally, a GFP-positive, ~96 kDa band, was detected only in samples transduced with LV-Exo70, in agreement with what has been reported (Torres et al., 2010, Lira et al., 2019) that approximately 5% of the one-pieced translated protein stays as a single protein without being self-cleaved (Figure 20A, arrow). After 72h, Exo70 overexpression was achieved only in LV-Exo70 transduced cells (Figure 20B). Next, *in vivo* Exo70 overexpression was assessed using dorsal hippocampal samples from injected mice. Similar to HEK293 cells, the analysis showed that GFP is expressed in mice injected with control lentivirus (LV-GFP) and the overexpression lentivirus (LV-Exo70) but was absent in non-injected animals (Figure 20C); both 25 and 27 kDa bands were observed in these samples as well. The HA tag was only detected in samples from LV-Exo70 mice, indicating that Exo70 is being overexpressed; indeed, 1 month of expression was sufficient to increase the Exo70 protein level in the dorsal hippocampus of LV-Exo70, but not LV-GFP injected mice (Figure 20D). By immunohistochemistry, GFP+ cells were found in both LV-GFP and LV-Exo70 injected mice in a wide area of the CA1 region from the dorsal hippocampus (Figure 20C).

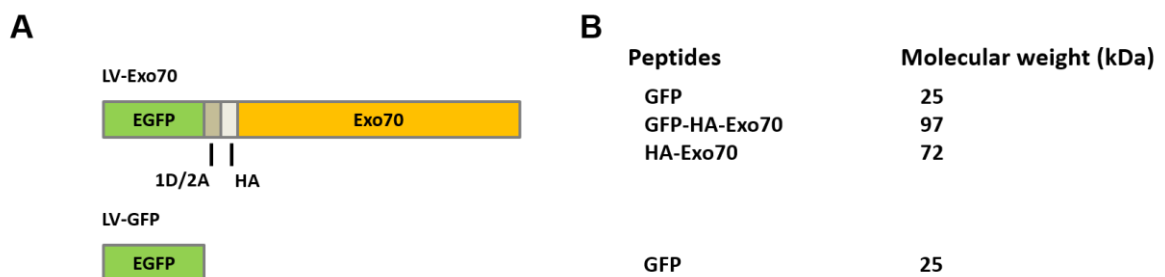


Figure 19.- (A) Schematic representation of protein expressed by the lentiviral system. (B) Peptides expressed and their expected molecular weights.

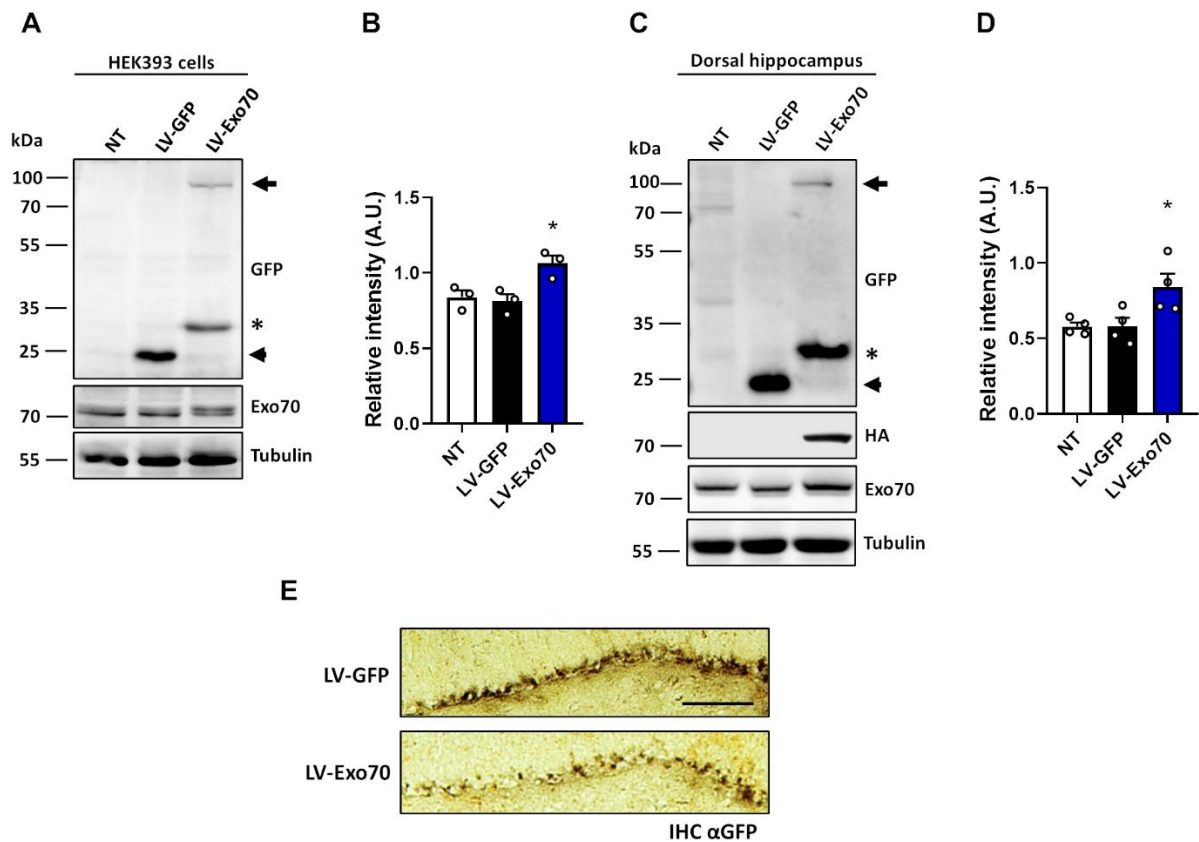


Figure 20.- Characterization of the lentiviral system expressing Exo70. One month old mice were injected intrahippocampally with 1 μ L of LV-GFP, LV-Exo70 lentiviral suspension or PBS (NT: non transduced). LV-GFP construct expresses only GFP, while LV-Exo70 expresses GFP and Exo70. Expression was carried out for 30 days. Immunoblot analysis of **(A)** transduced HEK293 cells and **(C)** dorsal hippocampal samples from injected mice. 30 μ g of protein samples were resolved in 10% SDS-PAGE and transferred to PVDF membranes. Membranes were stripped and tested again with the indicated antibodies. **(B and D)** Densitometric analysis of Exo70. Signal intensity was normalized with Tubulin band intensity. The analyses show Exo70 overexpression only in LV-Exo70 transduced samples. Values represent means \pm SEM. $n = 3$ independent experiments with HEK293 cells, $n = 4$ mice per experimental group. Statistical differences were determined by an unpaired t-test comparing LV-GFP and LV-Exo70 samples. $*p < 0.05$. **(E)** Classical IHC was carried out using a GFP antibody. Representative images of CA1 hippocampal region showing GFP signal. Scale bar: 100 μ m.

4.3.2.- Learning and memory

TBI has been shown to diminish spatial learning and memory (Marschner et al., 2019, Xu et al., 2021). The hippocampal function was tested using the Morris Water Maze (MWM) spatial

memory test. For this task, mice are required to learn the location of a hidden platform based on external cues. The swimming speed of experimental groups was measured in order to detect possible motor problems. However, no significant differences were observed between the groups (Figure 21A). Sham-GFP mice showed a normal learning curve as expected for non-injured animals, and mTBI was able to increase escape latency on day 3 and day 4 during the test, while Exo70 overexpression returned escape latency to normal (Figure 21B). Exo70 overexpression in Sham mice did not have any effect on escape latency. Interestingly, cumulative latency showed that Exo70 overexpression was able to reduce the escape time of both LV-Exo70 Sham/mTBI mice as compared to control Sham-GFP mice (Figure 21C), suggesting that Exo70 overexpression might enhance learning processes in the MWM test. Specifically, on day 4, the results show that Exo70 overexpression rescues the escape latency as shown in Figure 21D, where representative swimming paths are shown as well. Figure 21E shows the relationship between spatial acuity and the average escape latency of animals from the different experimental groups. The graph shows that mTBI-GFP mice are located in a region of the graph that corresponds to high-escape latency values and low-spatial acuity scores. In contrast, Sham-GFP and Sham-Exo70 mice show low-escape latency values and high spatial acuity scores. Exo70 overexpression was able to rescue spatial acuity (Figure 21E). On day 6 of the memory task, the platform was removed in a probe test that measures the time mice spend swimming in the former area, near the initial platform location (a circular area with twice the platform radius). Sham-GFP and Sham-Exo70 mice spend more time in the platform area than TBI-GFP mice, while Exo70 overexpression was able to rescue the memory deficit, demonstrating the inability of mTBI mice to remember the platform location and the improvement that suffered TBI-Exo70 mice (Figure 21F).

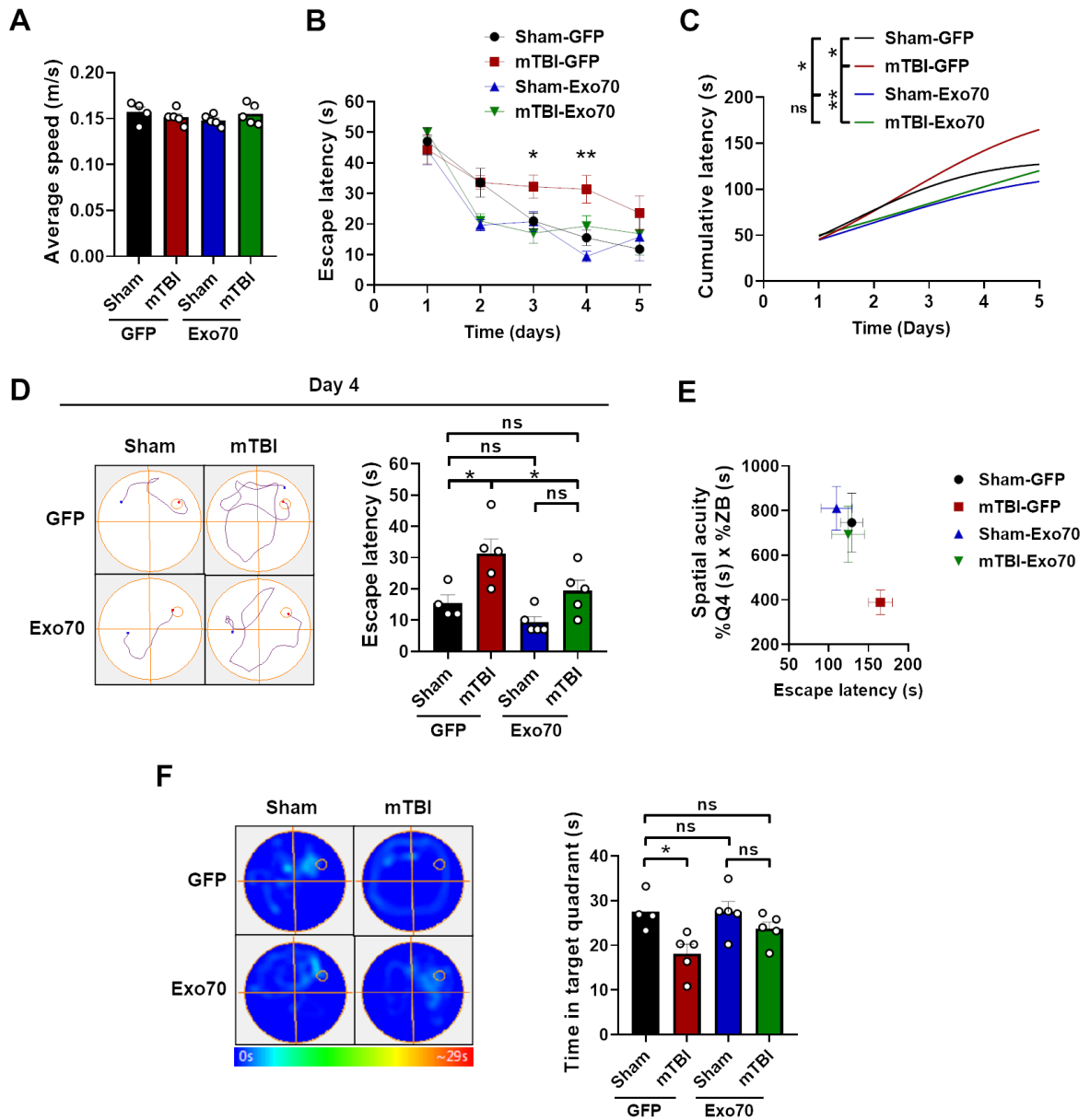


Figure 21.- Learning and memory impairment is prevented by Exo70 overexpression in mTBI-induced mice. Behavioral performance was tested using the MWM test. **(A)** Average swimming speed. **(B)** Escape latency (time to reach the hidden platform) of Sham and mTBI mice expressing GFP or Exo70. **(C)** Cumulative latency throughout the 6 days of the test. **(D)** Representative swimming trajectories and escape latency for all experimental groups on day 4. **(E)** Spatial acuity for Sham and mTBI mice with or without Exo70 overexpression after 6 days of training. **(F)** Representative heat map and analysis of the time mice spent swimming in the area near the platform when it was removed on day 6. Values represent means \pm SEM, $n = 5$ mice per experimental group. Statistical differences were calculated by ANOVA, followed by post hoc Bonferroni's test. Curves were analyzed by Repeated Measures ANOVA. * $p < 0.05$, ** $p < 0.01$.

Additionally, animals' cognitive performance was evaluated using a modified spatial memory paradigm associated with episodic memory (memory flexibility) that has been shown to be more sensitive in detecting hippocampal dysfunction (Carvajal et al., 2018). The analysis of behavioral performance indicates that, in almost every day, mTBI-GFP mice required more trials to achieve the learning criterion (see Methodology) than control Sham-GFP mice, while Exo70 overexpression was able to rescue the learning and memory impairment (Figure 22).

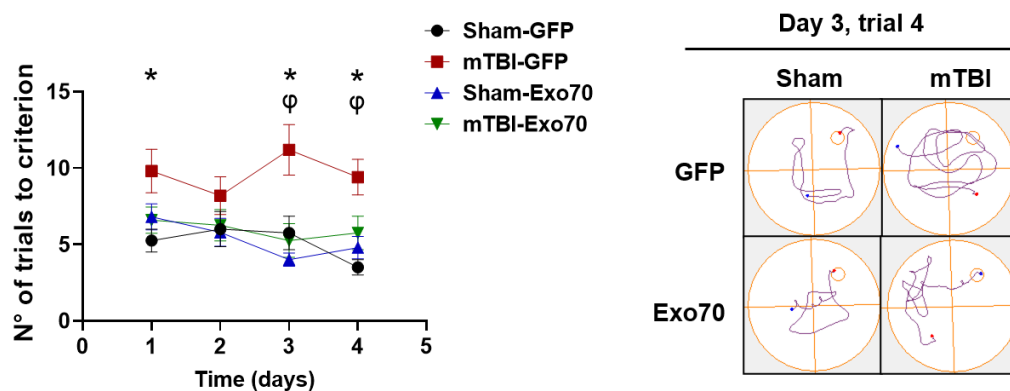


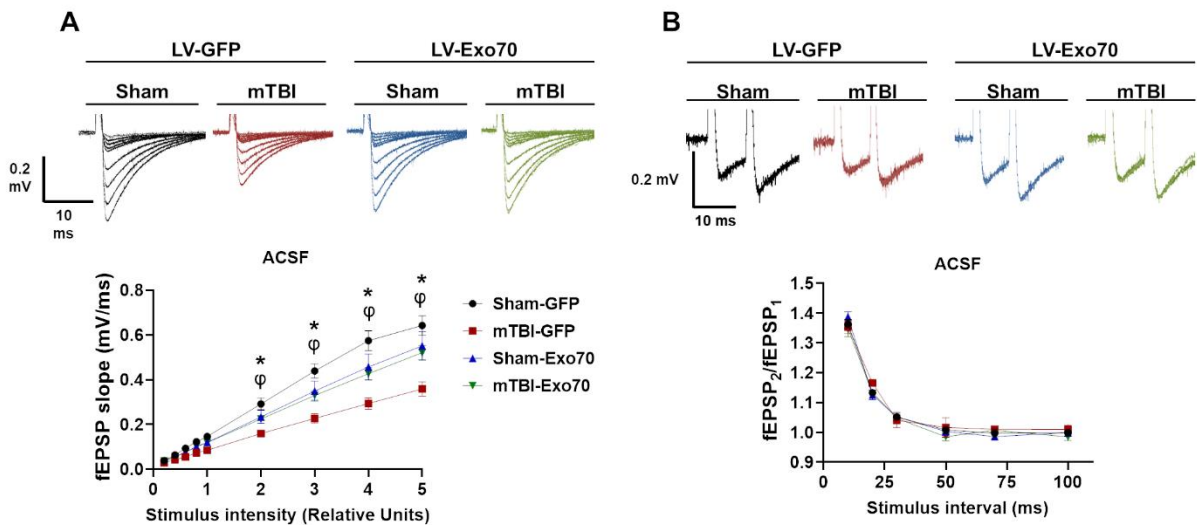
Figure 22.- Memory flexibility test. Behavioral performance was tested using a modification of the MWM test, the memory flexibility test (see methods). Memory flexibility was performed the week after MWM test was carried out. Representative swimming trajectories for trial 4 on day 3 of the test are shown. Values represent means \pm SEM, $n = 5$ mice per experimental group. Statistical differences were calculated by repeated measures ANOVA, followed by post hoc Bonferroni's test. Sham-GFP/TBI-GFP comparison: $*p < 0.05$. TBI-GFP/TBI-Exo70 comparison: $\phi p < 0.05$.

4.3.3.- Synaptic transmission

One of the TBI cellular hallmarks is that synaptic transmission is altered upon injury induction, both in basal and stimulated transmission. To study this, total synaptic strength was evaluated using input/output curves by stimulating schaffer collaterals with crescent stimuli. A significant decrease in total response to different stimulus intensities was found in mTBI-GFP compared to

Sham-GFP mice (Figure 23A), which was partially rescued by Exo70 intrahippocampal overexpression. Complementary studies were made to evaluate presynaptic function using the paired-pulse facilitation assay and no differences were found between any of the experimental groups (Figure 23B).

Figure 23.- Basal synaptic transmission in hippocampus from mTBI mice expressing GFP or Exo70. (A) fEPSP slope induced by the input-output protocol to record total responses of CA3-



CA1 synapses. Responses were recorded by crescent stimuli. (B) Paired pulse facilitation (PPF) of fEPSP shows no alterations in presynaptic activity in CA3-CA1 synapses. Values represent means \pm SEM, $n = 6$ slices per experimental group. Statistical differences were calculated by repeated measures ANOVA, followed by post hoc Bonferroni's test. Sham-GFP/TBI-GFP comparison: $*p < 0.05$. TBI-GFP/TBI-Exo70 comparison: $\phi p < 0.05$.

NMDAR-dependent response in basal synaptic transmission was also assessed by incubating slices with $20 \mu\text{M}$ NBQX, an AMPAR antagonist, and recording input/output curves. Similar to total response recording, mTBI decreased NMDAR-dependent synaptic response, while overexpression of Exo70 totally rescued synaptic strength in all stimuli applied (Figure 24A). Next, synaptic plasticity was evaluated by studying LTP magnitude in hippocampal CA3-CA1 transmission, which also correlates with learning and memory (Whitlock et al., 2006). By the

usage of a high-frequency stimulation protocol (3 trains at 100 Hz), it was found that LTP induction was compromised in TBI-GFP when compared with Sham-GFP control mice (Figure 24B). TBI-GFP mice showed potentiation but were unable to maintain LTP and Sham-Exo70 mice had the ability to induce LTP at a similar proportion as control animals did. Finally, TBI-Exo70 mice were able to induce and maintain LTP throughout the protocol (Figure 24B). These results reinforce the rescued memory of the mTBI animals injected with LV-Exo70.

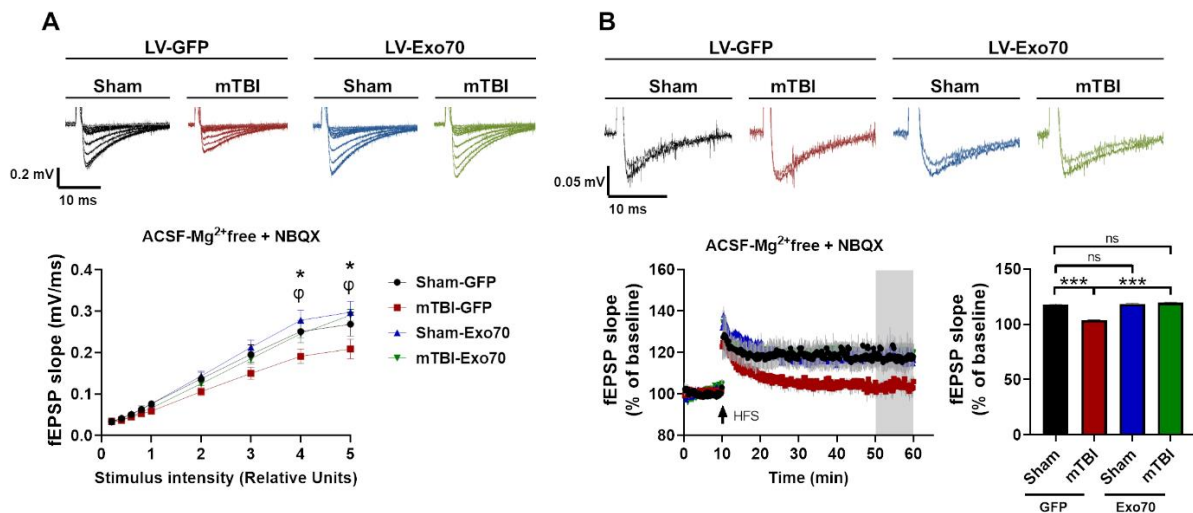


Figure 24.- NMDAR-related synaptic transmission in hippocampus from mTBI mice expressing GFP or Exo70. Recordings were made by incubating slices with 20 μ M NBQX. **(A)** fEPSP slope induced by the input-output protocol to record NMDAR responses of CA3-CA1 synapses. Responses were recorded by crescent stimuli. **(B)** LTP was generated by high-frequency stimulation (HFS) in the hippocampal CA1 area, and the recording was carried out for 50 min. The graph shows fEPSP slope in the last 10 minutes of the recording. Values represent means \pm SEM, $n = 6$ slices per experimental group. Statistical differences were calculated by repeated measures ANOVA, followed by post hoc Bonferroni's test. Sham-GFP/TBI-GFP comparison: * $p < 0.05$. TBI-GFP/TBI-Exo70 comparison: $\phi p < 0.05$. Bar graph was analyzed using one-way ANOVA with Bonferroni's correction. *** $p < 0.001$.

4.3.4.- NMDAR synaptic availability

One of the features of NMDAR, is that they could be found both in synaptic and extrasynaptic membranes. Several reports demonstrate that tyrosine phosphorylation of the NMDARs GluN2B subunit is strongly associated with the surface expression of this receptor. For instance, phosphorylation on tyrosine 1472 determines the surface expression of NMDARs in the synaptic zone (Xu et al., 2006), and phosphorylated tyrosine 1336 is associated with enrichment of the receptor in extrasynaptic membranes (Goebel-Goody et al., 2009). Thus, it was asked whether Exo70-GluN2B increased interaction (Figure 18) could be part of a compensatory mechanism by which GluN2B is intended to be stabilized in the synapse since learning/memory and its NMDAR-associated synaptic transmission rescue was allowed by Exo70 overexpression. First, samples from the dorsal hippocampus were analyzed by immunoblot to evaluate the proper expression of the lentiviral construct. Soluble GFP was present in mice from all experimental groups but only GFP-Exo70 was found in both Sham and mTBI mice injected with LV-Exo70 (Figure 25A); again, both expected GFP bands (see Figure 20) were observed in all hippocampal samples. Accordingly, only HA-Exo70 was observed in LV-Exo70 samples indicating Exo70 overexpression (Figure 25B).

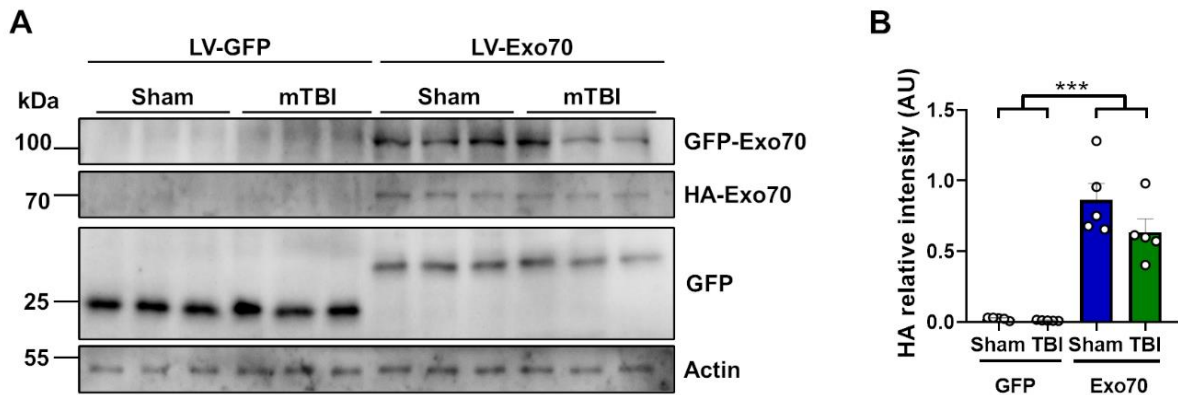


Figure 25.- Characterization of the lentiviral expression in all experimental groups. **(A)** Samples from dorsal hippocampus were analyzed by western blot using GFP and HA antibodies. 30 μ g of protein samples were resolved in a 10% SDS-PAGE and transferred to PDVF membrane. **(B)** The graph shows the densitometric analysis of HA-Exo70 band intensity normalized with Actin as loading control. Values represent means \pm SEM, $n=5$ mice per experimental group. Statistical differences were calculated by one-way ANOVA, followed by post hoc Bonferroni's test, $***p < 0.005$.

Using GluN2B p1472 and p1336 antibodies, it was detected that mTBI reduced p1472 signal as compared to control, whereas TBI-Exo70 samples showed a restored signal (Figure 26). Exo70 overexpression in Sham mice did not alter the phosphorylation state of Y1472. Contrary to p1472, mTBI was able to increase phosphorylation of Y1336, which was partially decreased by Exo70 overexpression (Figure 26B). Sham-Exo70 mice showed an apparent increase in p1336 signal but without statistical significance. GluN2B total protein levels didn't change in any of the experimental groups (Figure 26B). These results not only suggest that a disbalance of synaptic/extrasynaptic GluN2B occurs with mTBI, but also suggest that Exo70 overexpression is able to rebalance the synaptic distribution of this NMDAR subunit.

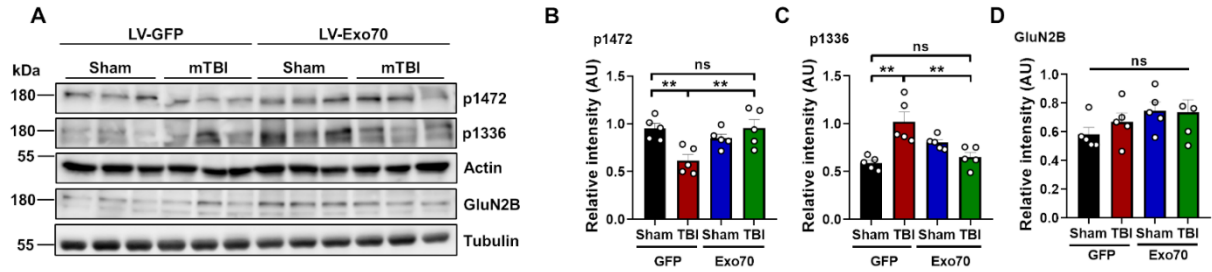


Figure 26.- NMDAR synaptic localization after mTBI overexpressing Exo70. (A) Samples from dorsal hippocampus were analyzed by western blot using GluN2B p1472, GluN2B p1336 and total GluN2B antibodies. 30 μ g of protein samples were resolved in a 10% SDS-PAGE and transferred to PDVF membranes. Membranes were stripped and reprobbed for phosphorylation testing. Actin and Tubulin were used as loading controls. (B -D) The graphs show the densitometric analysis normalized with loading controls prior to normalization with Sham-GFP control samples. Values represent means \pm SEM, n=5 mice per experimental group. Statistical differences were calculated by one-way ANOVA, followed by post hoc Bonferroni's test, $**p < 0.01$.

Because an NMDAR synaptic/extrasynaptic disbalance was found. It was asked whether these results could correlate with the downstream synaptic signaling through ERK1/2 and CREB. Thus, samples were analyzed using specific antibodies showing phosphorylation of residues that are related to NMDAR synaptic activity (Figure 27A). pERK1/2 signal was reduced in mTBI-GFP mice compared to control animals, while TBI-Exo70 mice showed restored signal (Figure 27B). Similar results were observed with pCREB antibody, where Exo70 overexpression rescued the phosphorylation state of this protein (Figure 27C). Finally, neither pERK1/2 nor pCREB signal were altered with Exo70 overexpression in Sham animals (Figure 27B and C). These results support the idea that mTBI evokes an exit of GluN2B from the synapse and that the synaptic/extrasynaptic disbalance is restored when Exo70 is overexpressed.

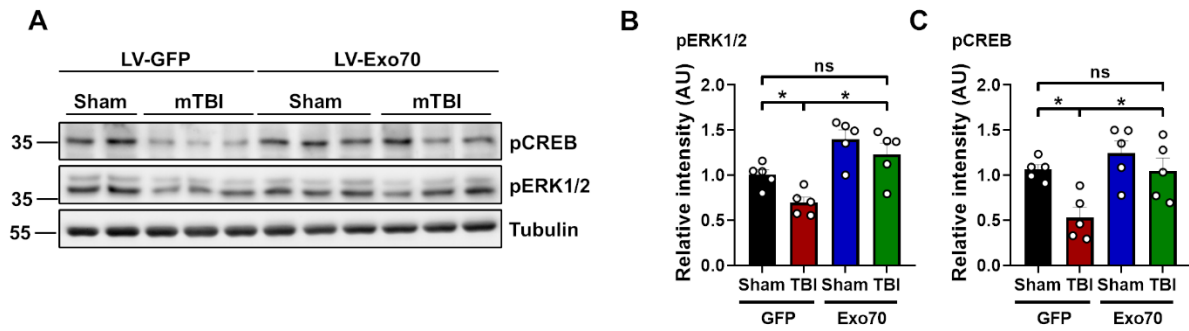


Figure 27.- NMDAR synaptic signaling after mTBI induction in Exo70-overexpressing mice. **(A)** Samples from dorsal hippocampus were analyzed by western blot using pCREB and pERK1/2 antibodies. 30 μ g of protein samples were resolved in a 10% SDS-PAGE and transferred to PDVF membranes. Membranes were stripped and re probed for phosphorylation testing. Tubulin was used as loading control. **(B and C)** The graph shows the densitometric analysis normalized with loading controls prior to normalization with Sham-GFP control samples. Values represent means \pm SEM, $n=5$ mice per experimental group. Statistical differences were calculated by one-way ANOVA, followed by post hoc Bonferroni's test, $*p < 0.05$.

5.- DISCUSSION

5.1.- First part: Objectives 1 and 2

The exocyst complex basic function is the tethering of secretory vesicles during the process of membrane addition for polarized outgrowth (Wu and Guo, 2015), and its protein components have been involved in specialized membrane processes in neurons. As it so, the complex acts as a unit giving the molecular machinery to carry on trafficking and exocytosis related processes (Martin-Urdiroz et al., 2016). In this thesis, it was found that Exo70 is redistributed in the hippocampus of mice subjected to mTBI and that the exocyst function might be altered on hippocampal synapses. In the present work, a modified Maryland's weight drop model was used, which was fitted to mice anatomy. Brain injury was developed with a closed head frontal impact device using a repeated strike paradigm (see methods). The usage of this weight drop model grants the ability to induce repeated strikes which is associated with accumulative damage (Blennow et al., 2016). The first injury is associated with the release of excitotoxic neurotransmitters, neurometabolic crisis, inflammation, and axonal dysfunction (Blennow et al., 2012). A second TBI, that occurs before the resolution of the pathophysiological changes induced by the first TBI, adds cumulative damage to the brain and prolongs the recovery from the second injury (Blennow et al., 2016, Guskiewicz et al., 2003, Slobounov et al., 2007). The protocol lacks any craniotomy procedures and consists of 5 days strike with a 2-day-interval which consequently adds damage to an already damaged system. In the end, the protocol resembles severe brain damage without any aggressive surgical procedures (Mira et al., 2020, Carvajal and Cerpa, 2021).

Exo70 expression has been reported on many mono and multicellular organisms including mammals and it is considered as a ubiquitous protein expressed in most cell types including brain cells (Martin-Urdiroz et al., 2016). Several reports have indicated that Exo70 is present in brain tissue and specifically in neurons (Gerges et al., 2006, Sans et al., 2003, Dupraz et al., 2009, Lira et al., 2019, Letinic et al., 2009, Coulter et al., 2020, Brymora et al., 2001), but none have studied its expression patterning in the cortex and hippocampus. We showed that Exo70 is expressed both in the cortex and hippocampus by western blot (Figure 11). By immunochemistry, Exo70 appears to be expressed in most of the cortical layers (Figure 11). In the hippocampus, Exo70 is expressed mainly in *stratum pyramidale* which contains most of the neuronal soma present in CA1-CA3 hippocampal zones and thus it is believed that Exo70 is predominantly expressed in neurons, although some Exo70-positive cells were detected outside of *stratum pyramidale*. The exocyst has been related in neurodevelopmental disorders, but non study has determined whether this complex is part of the cellular mechanisms associated with pathophysiological conditions in neurodegenerative diseases or acute neuropathologies such as traumatic brain injury. Therefore, as a first approach, Exo70 expression changes were searched in the forebrain, cortex, and hippocampus upon mTBI induction, and no disturbances were found (Figure 12).

The lack of expression disturbances doesn't necessarily mean that Exo70 has no changes in mTBI. Exo70's function is strictly related to its subcellular localization and changes in this localization have shown to be important to developing Exo70 malfunction (Inoue et al., 2003, Dupraz et al., 2009, Vega and Hsu, 2001, Pommereit and Wouters, 2007, Zhao et al., 2013). As no expression changes were found upon mTBI induction, it was asked whether Exo70 subcellular distribution is altered after mTBI. A well-established protocol to isolate subcellular

organelles was used. This protocol allows the isolation of cytosolic, microsomal, and synaptic fractions, among others. Microsomal fraction is mainly composed of cellular membranes related to intracellular trafficking, such as endoplasmic reticulum, Golgi apparatus, plasma membrane, and synaptic vesicles, whereas the synaptic fraction is composed of presynaptic Active Zone and exocytic machinery, recycling machinery and postsynaptic density among others (Sandoval et al., 2013). Exo70 showed to be mainly located at microsomes followed by synaptic localization, which has also been seen in the rat brain (Lira et al., 2019), supporting the idea that Exo70 function is related to these subcellular compartments. We observed that in the forebrain, Exo70 increased its localization in microsome and synaptosome fractions upon TBI induction (Figure 13). Particularly Exo70 functions have been described in these processes where cargoes are transported with the exocyst complex (Lira et al., 2020). Still, whether mTBI shows alterations in dendritic trafficking related to these fractions, it's not totally understood. One possibility is that TBI induces Exo70 accumulation into these membrane fractions to change trafficking through Exo70 and the exocyst complex as a result of the pathophysiology development, and the other possibility is that Exo70 could be part of a compensatory mechanism to counteract damage development. The forebrain contains many zones where different biological processes are carried out; thus, our results can't determine which possibility is the correct one for forebrain fractionation.

TBI causes neuronal damage principally in the cortex (Kilbourne et al., 2009, Carron et al., 2016, Johnstone et al., 2015) but also the damage reaches the hippocampus eventually (Kilbourne et al., 2009, Mira et al., 2020, Ibrahim et al., 2016, Winston et al., 2013, Ariza et al., 2006, Girgis et al., 2016). Consequently, we sought to determine whether Exo70 distribution gets differentially affected between cortex and hippocampus. In this regard, synaptosomal

fractions were further fractionated to obtain PSD and non-PSD fractions (Triton X-100 insoluble and soluble fractions). Using differential centrifugation, ultrastructural analysis and flow cytometry as tools, it is known that synaptosome shows a size between 1.5 and 4.5 μm and that approximately 50-60 % of synaptosomal volume is comprised of the presynaptic compartment (Gyls et al., 2000, Gyls et al., 2004a, Gyls et al., 2004b), therefore, nearly half of our non-PSD fraction should be composed by the postsynaptic cytosolic fraction.

It is worth noting that differences are observed in Exo70 subcellular distribution between the forebrain and hippocampi. In the forebrain, Exo70 was barely seen in the cytosolic fraction, whereas more presence was observed in the hippocampal cytosolic fraction. All of this despite Exo70 being highly distributed in microsomes in both samples. It is likely that forebrain, as a multizone tissue, englobes many Exo70 subcellular distribution patterns, while Exo70 hippocampal distribution is essentially granted to an isolated zone. Regarding TBI, it was determined that Exo70 is redistributed into synapse only in the hippocampus and that this pool might come from microsomal fraction (Figure 15). Diminishing Exo70 localization in microsomes would allow cellular systems to provide the pool of Exo70 necessary to the redistribution into the postsynaptic density in the synaptic compartment. This redistribution found in the hippocampus was not seen in the cortex. Therefore, there might be some tissue-specific alterations related to Exo70 in the TBI context. The fact that Exo70 distribution doesn't change in the cortex raises the question: Is Exo70 important in the development of TBI pathology? It is then suggested that Exo70 localization is altered to modify its function, probably providing the site where the exocyst must be redirected to play a role in the development of the pathology that has not been discovered yet. Forebrain fractionation showed that Exo70 localization in microsomes is increased, contrary to the reduction observed in hippocampal

microsomes of mice subjected to our repeated mTBI protocol. This difference relies on the forebrain (without the cerebellum) being composed of many zones, which number in its entirety could obscure an event occurring in specific tissues such as the hippocampus.

Microsome fraction is a technical fraction obtained only by subcellular fractionation and thus is not a “real” cellular compartment. As tissue homogenization is carried out with an isotonic buffer, membranous organelles remain fairly untouched and thus several organelles are isolated together. Microsome fraction contains endoplasmic reticulum, Golgi apparatus, synaptic vesicles, and plasma membrane (Sandoval et al., 2013). In our TBI model, it was found that Exo70 localization is reduced in microsomal fraction (Figure 15) and that Exo70 is mainly located on this fraction on Sham animals. As Exo70 is predominantly located at the plasma membrane (Liu et al., 2007, Moore et al., 2007, Zhang et al., 2016), it was hypothesized that the reduction of Exo70 in microsomes is due to a decrease in plasma membrane localization after mTBI. In this case, a biotinylation protocol, that can isolate plasma membrane proteins, was used. This protocol biotinylated extracellular portions of those proteins and therefore intracellular proteins should not be biotinylated (Figure 16) (Dennis et al., 2011, Heise et al., 2018). It is important to note that Exo70 is an intracellular protein. Nevertheless, this biotinylation protocol has been used to evaluate the membrane localization of intracellular proteins such as Fyn kinase and Tau (Attiori Essis et al., 2015) due to the ability of these proteins to interact with surface biotinylated partners. Indeed, Fyn is an intracellular kinase that interacts and phosphorylates NMDAR (Carvajal et al., 2016, Nada et al., 2003, Tezuka et al., 1999). Additionally, exocyst subunits and other “cytosolic” proteins have also been detected in surface membrane fraction in cortical tissue (Smolders et al., 2015). Exo70, as an exocytic protein, is thought to interact with several membrane proteins and there is some evidence of it (Gerges et

al., 2006, Sans et al., 2003, Inoue et al., 2003, Inoue et al., 2006, Wang et al., 2019) and thus we consider this protocol suitable for assessing Exo70 membrane localization. Finally, Exo70 membrane proximity is reduced on the hippocampus when mTBI was induced (Figure 16), suggesting that the pool of Exo70 that is redistributed from the microsome into synapses comes from the plasma membrane. Altogether, our biochemical experiments showed that Exo70 function might be altered in the mTBI context.

The mammalian exocyst is a multimeric complex that has been shown to have two subcomplexes. Subcomplex 1 (SC1) comprises Sec3, Sec5, Sec6 and Sec8; subcomplex 2 (SC2) comprises Sec10, Sec15, Exo70 and Exo84 (Ahmed et al., 2018). When SC1 and SC2 assembly is induced, the complex is activated. In this thesis, Sec6 and Sec10 was analyzed. Both Exo70 and Sec10 lays on SC2 while Sec6 is present in SC1; therefore, our immunoblot analysis to Sec6 and Sec10 is suitable to evaluate the assembly of the exocyst. This approach has been used before on biochemical experiments with a similar aiming on exocyst assembly and activity (Ren and Guo, 2012, Mao et al., 2020a, Lu et al., 2016, Rossi et al., 2020). The exocyst is a complex widely distributed intracellularly (Sans et al., 2003, Lira et al., 2019), so immunoprecipitating Exo70 in hippocampal protein extracts would add several difficulties in assessing the particular assembly on synapses. It was then decided to narrow down the possibilities and isolate synaptosomes to address this issue. Hippocampal synaptosomes were Triton-treated and PSD/nonPSD fractions were obtained before Exo70 immunoprecipitation. The results showed that upon mTBI induction, exocyst assembly increased only on PSD and decreased in nonPSD fraction (Figure 17). This suggests that the Exo70 redistribution towards PSD provides a site where the exocyst complex can increase its assembly and probably its activity, triggering the redirection of nonPSD ensembled complex into PSD. The activity of the complex has been

shown to depend on its assembly, and therefore we suggest that the activity of the complex is increased after mTBI on hippocampal PSD. Due to this increased activity specifically in PSD, one could speculate that the exocyst could reinforce the stabilization of the PSD structure by providing with cargoes that are required to stabilize synapses from the postsynaptic compartment.

One possibility is that the exocyst could provide the machinery to modulate the availability of glutamate receptors at PSD. The exocyst has been related to traffic and delivery of AMPA and NMDA receptors into the synapse (Gerges et al., 2006, Sans et al., 2003, Lira et al., 2020). These studies suggested that Sec6, Sec8, and Exo70 might be in the same protein complex with AMPAR subunits such as GluR1 and GluR2 (Gerges et al., 2006). Additionally, NMDAR subunits GluN1/GluN2B also has been detected in the same complex with Sec6, Sec8, and Exo70 (Sans et al., 2003). Glutamate receptors have been extensively studied in several traumatic brain injury models with proteomic, electrophysiological, and behavioral approaches (Blennow et al., 2016, Carvajal et al., 2016, Blennow et al., 2012). Basal synaptic transmission and plasticity are decreased upon TBI induction (Mira et al., 2020, Zhang et al., 2011), accompanied by a reduction in glutamate binding to the NMDA receptor (Miller et al., 1990) and ultimately internalization of glutamate receptors. GluR2 is internalized after TBI (Bell et al., 2009). GluN2B availability at synapses is reduced dramatically upon TBI induction (Park et al., 2013, Carvajal and Cerpa, 2021). Both events trigger downstream signaling that ultimately induces cell death (Carvajal et al., 2016). Thus, given the fact that Exo70 and the exocyst are part of AMPAR/NMDAR trafficking and delivery machinery (Lira et al., 2020), one could speculate that the induction of exocyst assembly on PSD is likely a compensatory event by which glutamate receptors are maintained in the synapse to diminish TBI detrimental signaling.

To test this, Exo70 binding to GluR1, GluR2, GluN2A, and GluN2B subunits was assessed (Figure 18). The results showed that only GluN2B increased its interaction with Exo70 on PSD. The same interactions were tested on nonPSD fraction, and no signal was detected, suggesting that the exocyst function through Exo70 towards PSD in order to maintain synapse stability. This has been proven at least in hippocampal neuron cultures (Lira et al., 2019). It was then suggested that exocyst assembly favors Exo70-GluN2B interaction to develop a compensatory mechanism by which GluN2B gets stabilized in the PSD rather than an evoked increase of this receptor at the PSD (Figure 28). This, in turn, prevents the development of neuronal dysfunction.

All the biochemical analysis were carried out with a $n = 3$. It is known that this number of sample size are in the lower limit of acceptable. For this reason, power analysis was carried out in order to determine statistical power. Power was calculated to discard the null hypothesis using PASS 2019 Power Analysis and Sample Size Software (NCSS, LLC. Kaysville, Utah, USA). Each data shown with significant differences was ran into power analysis and results are as follows: Figure 13, microsome and synaptosome 100% of power; figure 15, microsome 99,53% and PSD 100% of power; figure 16, biotinylation 99.48% of power. Finally, power analysis of immunoprecipitation results are as follows for PSD: GluN2B 97.74%, Sec6 95.72%, and Sec10 85.44%. For nonPSD: Sec6 91.33% and Sec10 96.05%. The minimum power accepted for animal experiments in biological sciences is 80% (Gosselin, 2019), thus our sample size is sufficient to reach the minimum power of 0.8. Additionally, this power analysis was presented in a paper that has been peer-reviewed and published (Lira et al., 2021).

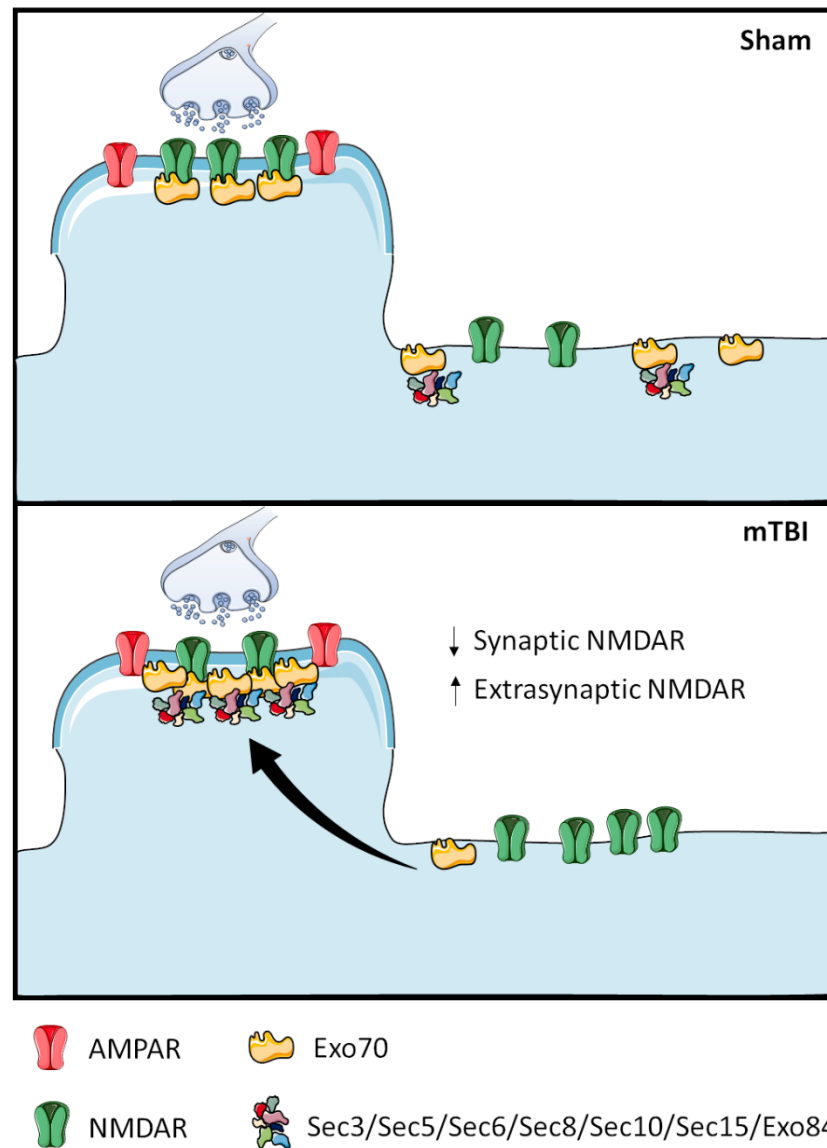


Figure 28.- Scheme depicting Exo70 redistribution after traumatic brain injury. mTBI is able to redistribute Exo70 from plasma membrane into the postsynaptic density, where promotes the assembly of the exocyst and increase its interaction with GluN2B.

5.2.- Second part: Objective 3

To test whether Exo70 redistribution into synapses, where increases its interaction with GluN2B, could be a compensatory mechanism to counteract TBI synaptic pathology, we decided to use a lentiviral tool to overexpress Exo70 in CA1 neurons in dorsal hippocampus, which is related to spatial memory processes (Lee et al., 2019). Lentiviral expression, alongside adeno-associated viruses, are one of the most used tools to produce knock-in and knock-down of genes in animal models (Sung and Kim, 2019), but contrary to adeno-associated virus, lentivirus allows long-term stable expression of the protein of interest and does not considerably affect neuronal network activity (Minerbi et al., 2009), which makes this tool suitable for this thesis. Indeed, around 2 months after the injection, Exo70 overexpression was consistently found in dorsal hippocampal samples. The FUG lentiviral plasmid (Lois et al., 2002) was constructed in order to create new genetic mice models by injecting these viruses into germline cells. Nevertheless, this lentiviral system is being used to assess brain function such as learning and memory and neuronal plasticity that are related to neuron (Wang et al., 2021). As lentiviral particles were injected in the CA1 *stratum pyramidale* zone, neuronal cells from this region were most efficiently transduced. This is in agreement with previous reports showing mainly neuronal transduction by this lentiviral construct (Dittgen et al., 2004, Wang et al., 2021). The transduction radius of effectively transduced cells was not determined. However, a single 0.5-1 μ l injection of lentiviral particles has shown to transduce a 400 μ m area, 200 μ m in every direction from the injection site, where the majority of the reporter intensity is detected (Barbash et al., 2013, Fricano-Kugler et al., 2016). In this same context, 1 μ l of lentiviral injection grants the ability to assess differences in behavioral analysis such as Morris Water Maze (Barbash et al., 2013).

NMDAR synaptic/extrasynaptic balance is of utmost importance in proper synaptic functioning because the intracellular signaling associated with this balance is strictly related to neuronal activity and survival (Carvajal et al., 2016). In animals subjected to mTBI, we found a decrease in the synaptic form of NMDARs (measured by tyrosine 1472 phosphorylation of the GluN2B subunit) and an increase in the population of extrasynaptic NMDARs (measured by tyrosine phosphorylation 1336 of the GluN2B subunit) supporting the idea that NMDARs mTBI promotes its exit from the synapse. This observation agrees with what have been observed previously directly by phospho-Y1472 measurement (Park et al., 2013) and synaptic compartment localization (Carvajal and Cerpa, 2021). When comes to Exo70 overexpression in sham animals, results showed an enhanced phospho-Y1336 signal suggesting that a large amount of GluN2B is present in the extrasynaptic compartment; as it so, Exo70 should promote GluN2B exocytosis in extrasynaptic membranes. Exo70 mediates AMPAR insertion directly within the postsynaptic density, rather than extrasynaptic membranes (Gerges et al., 2006), while NMDAR are inserted into extrasynaptic membranes prior to be laterally diffused into the synapse. It is then likely that Exo70 has a role in GluN2B insertion at extrasynaptic membranes, which has already been proposed (Lira et al., 2020), both in basal and stimulated NMDAR trafficking. Additionally, Exo70 prior overexpression in mTBI mice reverted the synaptic/extrasynaptic localization imbalance to what was found in control mTBI mice, suggesting that synaptic trafficking is reinforced by Exo70 activity, at least in TBI pathophysiology. The observation that Exo70 is redistributed into synapse upon mTBI induction, where it increases its interaction with GluN2B, also support the statement made in this thesis that Exo70 is acting as a compensatory mechanism to relieve TBI detrimental effects by modulating GluN2B synaptic availability.

As said before, synaptic and extrasynaptic NMDAR have prominent downstream signalings. Synaptic NMDAR low activity induces a decrease in phosphorylation levels in CREB, target of the ERK pathway, reducing neuronal survival (Hardingham et al. 2001; Hardingham and Bading 2002; Hardingham et al. 2002). In TBI, intracellular signaling is complicated to study, and the outcome varies between acute or chronic exposure to trauma-related damage. For example, analysis shortly after the trauma is induced, typically an increase in pCREB signal is observed (Lu et al., 2015). In contrast, days to weeks after the insult has occurred, pCREB signal is strongly dimmed, indicating reduced neuronal survival (Rehman et al., 2019, Zhang et al., 2020, Atkins et al., 2009, Titus et al., 2016). In our chronic TBI model, we've found a substantial reduction in pCREB and pERK1/2 levels one week after mice were subjected to brain trauma, which agrees with the previous reports already discussed. These results show that downstream signaling to the activation of synaptic NMDARs is altered, which also correlates to GluN2B exit from synapse discussed above. Furthermore, Exo70 overexpression is able to return the phosphorylation signal in both proteins, supporting the synaptic/extrasynaptic rebalance process of GluN2B (Figure 29).

MAPK/ERK signaling is a converging point for several signaling pathways (Wu et al., 2020), which is not substantially different in TBI context at a global level (Walker et al., 2013, Lu et al., 2017, Rai et al., 2019). By observing at a cellular level, ERK signaling is responsible for ATP signaling (released after membrane disturbance due to trauma) mostly in glial cells (Neary, 2005), while neurons are more affected by glutamate-related ERK signaling (Neary and Kang, 2005) suggesting that glutamate-related ERK signaling is more important in neurons than glial cells in TBI context. Thus, the results presented in this thesis are reinforced by the latter statement due to changes in synaptic NMDAR downstream signaling after mTBI induction.

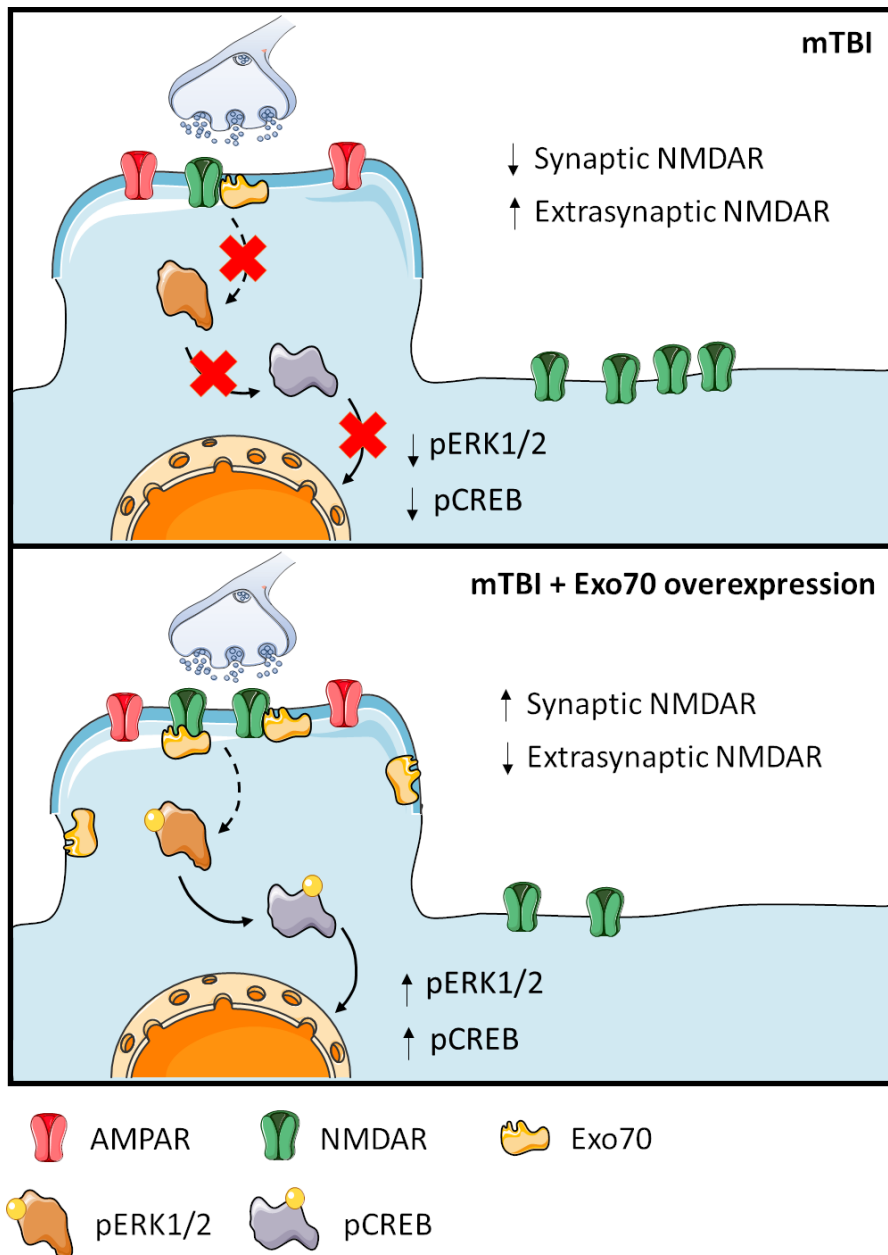


Figure 29.- Schematic representation of synaptic NMDAR signaling following traumatic brain injury. The scheme shows that synaptic NMDAR signaling through pERK1/2 and pCREB is reduced with an insult such as mTBI, resembling the exit of NMDAR from the synapse. On the other hand, Exo70 overexpression is able to prevent this exit and therefore it impedes the blockade of the synaptic signaling.

Synaptic function is essential for the proper performance of the neuronal network. In TBI, hippocampal neuronal circuits are severely affected (Krishna et al., 2020, Schumm et al., 2020), which results in impaired basal synaptic transmission (Titus et al., 2016, Xu et al., 2019) as shown in this thesis (Figures 23 and 24). The fact that Exo70 overexpression in the hippocampus was able to prevent hippocampal synaptic transmission loss in mTBI animals shows that the molecular machinery responsible for the appropriate synaptic functioning is reconstituted in active synapses. On the other hand, Exo70 is a ubiquitous protein that is present both in pre- and postsynaptic structures (Lira et al., 2019), suggesting that not only Exo70 carries out a post synaptic task, but a presynaptic function might be part of the mechanism as well. In this scenario, we didn't detect any differences in presynaptic function between all the experimental groups using the paired pulse facilitation protocol; thus, only the postsynaptic compartment is affected upon mTBI induction in our model, and prevention of damage to synaptic transmission is achieved when Exo70 is overexpressed. Likewise, NMDAR-dependent basal synaptic transmission behaves similarly in mTBI-subjected LV-GFP mice, where transmission is diminished, but only integral prevention is accomplished in NMDAR-dependent transmission as compared to total synaptic transmission where partial protection is observed. These results suggest that NMDARs are prominent in the development of the pathophysiology and that Exo70 is undoubtedly acting as a compensatory mechanism to maintain synaptic function in TBI context.

Another aspect of synaptic dysfunction related to TBI is dendritic spine loss/degeneration (Xiong et al., 2019, Maiti et al., 2015). These observations have been tightly associated with synaptic transmission impairment (Jamjoom et al., 2021). Furthermore, several reports have shown the relationship between spine morphology/function and the exocyst complex. First and

foremost, Exo70 is responsible for spine formation and stabilization in cultured hippocampal neurons (Lira et al., 2019), while the recruitment of the exocyst complex to the postsynaptic compartment by synaptic stimulation triggers the formation of new active synapses (Teodoro et al., 2013). Of note, Exo70 is long thought to be the subunit that leads the exocyst to the site where it is required. These exocyst's characteristics suggest that Exo70 overexpression might enhance synapse formation before the damage takes place. Nevertheless, we didn't find any changes in basal synaptic transmission when Exo70 was overexpressed in sham mice. Thus, only an insult such as TBI would activate the exocyst complex in order to diminish the detrimental effects caused to basal synaptic function. This is supported by the fact that Exo70 is redistributed into the synapse only after mTBI was delivered and promoted the assembly of the exocyst with GluN2B.

One of the hallmarks of TBI neuropathology, is that learning and memory processes are altered upon injury induction. In this regard, NMDARs takes part of the memory impairment in several TBI models (Han et al., 2009, Gabrieli et al., 2021, Biegon et al., 2004). It is important to note that learning and memory has a strong correlation with synaptic plasticity in form of LTP (Whitlock et al., 2006), that is also reduced in mild TBI context (Aungst et al., 2014, Schwarzbach et al., 2006). Our lab have found that NMDAR-related postsynaptic potentials and LTP are reduced upon mTBI induction (Carvajal and Cerpa, 2021) which is in concordance with preceding work in the CA1 zone of the hippocampus (Schwarzbach et al., 2006). This thesis replicated those outcomes and showed that Exo70 overexpression was able to prevent NMDAR-related LTP impairment, suggesting that NMDAR synaptic availability is favored when Exo70 is overexpressed in our mTBI model. However, it is unclear if only GluN2B synaptic stability is responsible for these observations. As synaptic trafficking is enhanced following LTP

induction and the exocyst is a known NMDAR trafficking partner (Lira et al., 2020), it is plausible to hypothesize that Exo70 is enhancing NMDAR synaptic trafficking in mTBI context. Further experiments could address this. Additionally, hippocampal-dependent memory impairment evoked by TBI is associated with the inappropriate activation of the NMDA receptor (Han et al., 2009, Cigel et al., 2021) and its restored activity promotes neuroprotection after TBI (Sonmez et al., 2015).

We assessed spatial learning and memory using Morris Water Maze. This behavioral test relies on spatial learning with cues that evaluates the working memory in spatial navigation activities (Vorhees and Williams, 2006). In our hands, the acquisition phase showed that mTBI-GFP mice learned where the platform was more slowly within each day of the test, whereas Exo70 overexpression prevented the cognitive damage at the acquisition phase. Additionally, Exo70 overexpression in Sham animals slightly enhanced learning in the experimental group, likely due to Exo70's ability to participate in synapse formation, maturation and maintenance (Lira et al., 2019, Gerges et al., 2006). The same statement applies to Exo70 overexpression in mTBI animals, allowing the protection of cognition processes. Moreover, we assessed reference memory with a probe trial 24h after the last acquisition day to ensure memory consolidation in long-term memory was being tested, independent of the memory of the last acquisition session. In this probe trial, Exo70 again protected against cognitive damage and spatial acuity alterations provoked by mTBI. These results suggest that we have found a new Exo70 function in learning and memory processes. More behavioral tests need to be done in other to determine which type of test is more sensitive than MWM. Furthermore, we used a MWM test that conduct reversal phases serially (Vorhees and Williams, 2006), changing the platform to the adjacent quadrant each day of testing, allowing the examination of the animal's flexibility in their ability to learn

across multiple phases of new learning (Williams et al., 2003). In this regard, memory flexibility -a more sensitive test to evaluate hippocampal dysfunction- is reduced with our mTBI model (Carvajal and Cerpa, 2021) and this thesis showed that the impairment is prevented with Exo70 overexpression. It's then likely that in our mTBI model, Exo70 overexpression prevented learning and memory impairments through a cellular process that impedes the exit of NMDAR from the synapse, which keeps synaptic plasticity normal in front of an insult such as TBI.

To resume (Figure 30), our repeated mTBI protocol induces the exit of GluN2B from synapses, damping its synaptic related downstream signaling. Additionally, the diminished NMDAR synaptic localization reduces not only total basal glutamatergic transmission and synaptic plasticity, but also NMDAR related synaptic transmission and plasticity. The diminished synaptic activity correlates with spatial learning and memory deficits found in mTBI-GFP mice. On the other hand, synaptic NMDAR localization and signaling when is retained when Exo70 is overexpressed prior to mTBI induction. This restored signaling pathway, in turn, brings back "normal" neuronal activity and survival, granting neurons the ability to act properly in the neuronal CA3-CA1 network as seen by population spikes in LTP analysis. This, in turn, recover cognition processes.

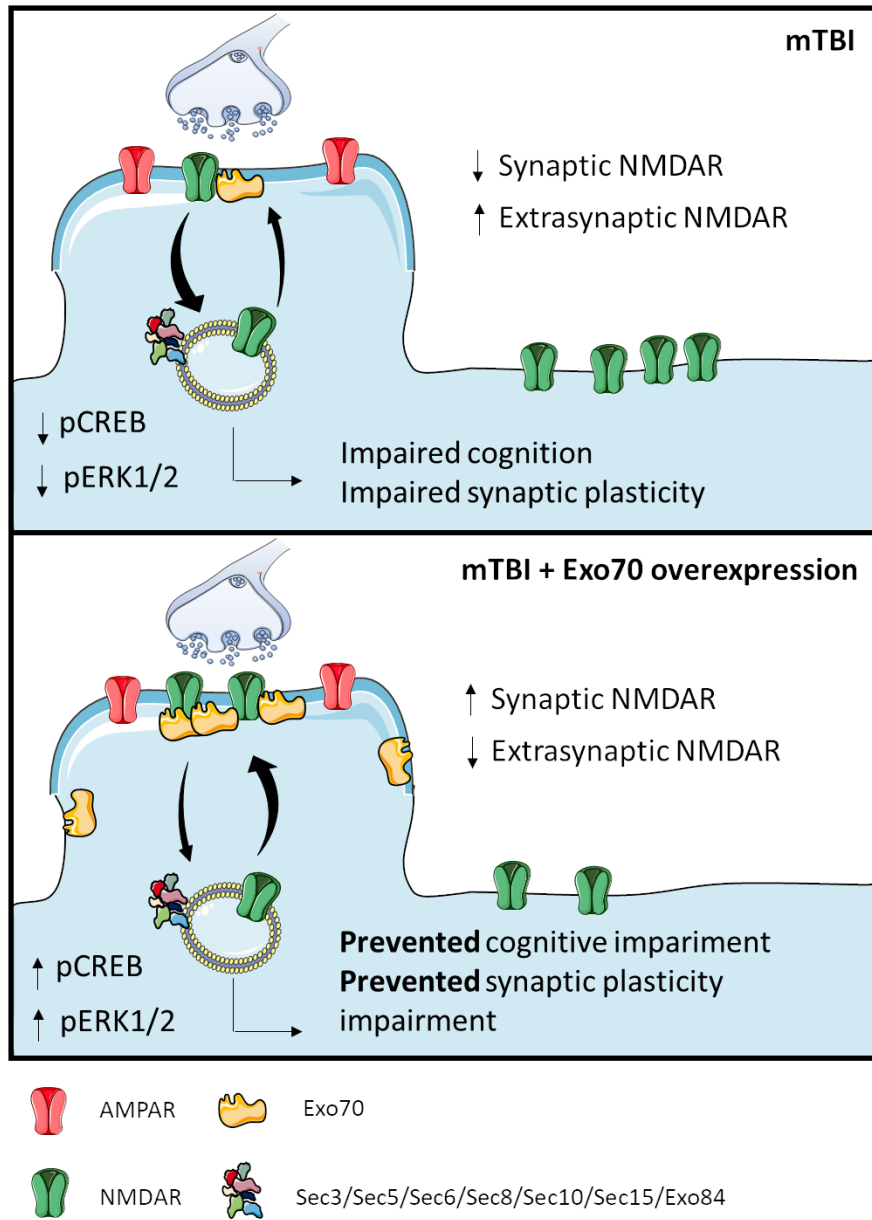


Figure 30.- Schematic summary of Exo70 overexpression effects in our mTBI model.

6.- CONCLUSION

The research question posed in this thesis was whether or not Exo70 participates in the development of TBI pathophysiology. This question was prompted by the fact that TBI affects intracellular trafficking of glutamate receptors and the exocyst is one of the complexes that oversees post-Golgi trafficking. We found that Exo70 is part of a cellular mechanism that stabilizes NMDAR receptors in the synapse, where they can overcome the detrimental effects that neurons suffer upon TBI induction. These findings are in light of a neuronal population effect that occurred in our model, but what occurs at a single-neuron level is not understood. Future work could examine the effects of Exo70 overexpression on NMDAR dynamics and electrical properties within TBI pathophysiology. Finally, we are the first to describe the involvement of Exo70 in an acute neuropathology such as TBI.

7.- REFERENCES

- AHMED, S. M., NISHIDA-FUKUDA, H., LI, Y., MCDONALD, W. H., GRADINARU, C. C. & MACARA, I. G. 2018. Exocyst dynamics during vesicle tethering and fusion. *Nat Commun*, 9, 5140.
- ALI, D. W., CUNNINGHAM, M. E. & ROY, B. 2013. Glutamate Receptors and Synaptic Physiology in Developing Neural Circuits. In: NGUYEN, P. (ed.) *Multidisciplinary Tools for Investigating Synaptic Plasticity*. Totowa, NJ: Humana Press.
- ANDREWS, H. K., ZHANG, Y. Q., TROTTA, N. & BROADIE, K. 2002. Drosophila sec10 is required for hormone secretion but not general exocytosis or neurotransmission. *Traffic*, 3, 906-21.
- ANDRIESEN, T. M., JACOBS, B. & VOS, P. E. 2010. Clinical characteristics and pathophysiological mechanisms of focal and diffuse traumatic brain injury. *J Cell Mol Med*, 14, 2381-92.
- ARIZA, M., SERRA-GRABULOSA, J. M., JUNQUE, C., RAMIREZ, B., MATARO, M., POCA, A., BARGALLO, N. & SAHUQUILLO, J. 2006. Hippocampal head atrophy after traumatic brain injury. *Neuropsychologia*, 44, 1956-61.
- ARMSTRONG, N., JASTI, J., BEICH-FRANDBEN, M. & GOUAUX, E. 2006. Measurement of conformational changes accompanying desensitization in an ionotropic glutamate receptor. *Cell*, 127, 85-97.
- ATKINS, C. M., FALO, M. C., ALONSO, O. F., BRAMLETT, H. M. & DIETRICH, W. D. 2009. Deficits in ERK and CREB activation in the hippocampus after traumatic brain injury. *Neurosci Lett*, 459, 52-6.
- ATTIORI, S., LAURIER-LAURIN, M. E., PEPIN, E., CYR, M. & MASSICOTTE, G. 2015. GluN2B-containing NMDA receptors are upregulated in plasma membranes by the sphingosine-1-phosphate analog FTY720P. *Brain Res*, 1624, 349-358.
- AUNGST, S. L., KABADI, S. V., THOMPSON, S. M., STOICA, B. A. & FADEN, A. I. 2014. Repeated mild traumatic brain injury causes chronic neuroinflammation, changes in hippocampal synaptic plasticity, and associated cognitive deficits. *J Cereb Blood Flow Metab*, 34, 1223-32.
- BANKE, T. G., GREENWOOD, J. R., CHRISTENSEN, J. K., LILJEFORS, T., TRAYNELIS, S. F., SCHOUSBOE, A. & PICKERING, D. S. 2001. Identification of amino acid residues in GluR1 responsible for ligand binding and desensitization. *J Neurosci*, 21, 3052-62.
- BARBASH, S., HANIN, G. & SOREQ, H. 2013. Stereotactic injection of microRNA-expressing lentiviruses to the mouse hippocampus ca1 region and assessment of the behavioral outcome. *J Vis Exp*, e50170.
- BARRIA, A., MULLER, D., DERKACH, V., GRIFFITH, L. C. & SODERLING, T. R. 1997. Regulatory phosphorylation of AMPA-type glutamate receptors by CaM-KII during long-term potentiation. *Science*, 276, 2042-5.
- BELL, J. D., PARK, E., AI, J. & BAKER, A. J. 2009. PICK1-mediated GluR2 endocytosis contributes to cellular injury after neuronal trauma. *Cell Death Differ*, 16, 1665-80.
- BIEGON, A., FRY, P. A., PADEN, C. M., ALEXANDROVICH, A., TSENTER, J. & SHOHAMI, E. 2004. Dynamic changes in N-methyl-D-aspartate receptors after closed head injury in mice: Implications for treatment of neurological and cognitive deficits. *Proc Natl Acad Sci U S A*, 101, 5117-22.
- BIRD, C. M. & BURGESS, N. 2008. The hippocampus and memory: insights from spatial processing. *Nat Rev Neurosci*, 9, 182-94.
- BISSON, D., FOSS, F. & ACKER-PALMER, A. 2019. AMPA receptors and their minions: auxiliary proteins in AMPA receptor trafficking. *Cell Mol Life Sci*, 76, 2133-2169.
- BLACKSHAW, L. A., PAGE, A. J. & YOUNG, R. L. 2011. Metabotropic glutamate receptors as novel therapeutic targets on visceral sensory pathways. *Front Neurosci*, 5, 40.
- BLANKE, M. L. & VANDONGEN, A. M. J. 2009. Activation Mechanisms of the NMDA Receptor. In: VAN DONGEN, A. M. (ed.) *Biology of the NMDA Receptor*. Boca Raton (FL).

- BLENNOW, K., BRODY, D. L., KOCHANEK, P. M., LEVIN, H., MCKEE, A., RIBBERS, G. M., YAFFE, K. & ZETTERBERG, H. 2016. Traumatic brain injuries. *Nat Rev Dis Primers*, 2, 16084.
- BLENNOW, K., HARDY, J. & ZETTERBERG, H. 2012. The neuropathology and neurobiology of traumatic brain injury. *Neuron*, 76, 886-99.
- BLISS, T. V. & LOMO, T. 1973. Long-lasting potentiation of synaptic transmission in the dentate area of the anaesthetized rabbit following stimulation of the perforant path. *J Physiol*, 232, 331-56.
- BOEHM, J., KANG, M. G., JOHNSON, R. C., ESTEBAN, J., HUGANIR, R. L. & MALINOW, R. 2006. Synaptic incorporation of AMPA receptors during LTP is controlled by a PKC phosphorylation site on GluR1. *Neuron*, 51, 213-25.
- BORSANI, G., PIOVANI, G., ZOPPI, N., BERTINI, V., BINI, R., NOTARANGELO, L. & BARLATI, S. 2008. Cytogenetic and molecular characterization of a de-novo t(2p;7p) translocation involving TNS3 and EXOC6B genes in a boy with a complex syndromic phenotype. *Eur J Med Genet*, 51, 292-302.
- BREM, A. K., RAN, K. & PASCUAL-LEONE, A. 2013. Learning and memory. *Handb Clin Neurol*, 116, 693-737.
- BRYMORA, A., VALOVA, V. A., LARSEN, M. R., ROUFOGALIS, B. D. & ROBINSON, P. J. 2001. The brain exocyst complex interacts with RalA in a GTP-dependent manner: identification of a novel mammalian Sec3 gene and a second Sec15 gene. *J Biol Chem*, 276, 29792-7.
- BUONARATI, O. R., HAMMES, E. A., WATSON, J. F., GREGER, I. H. & HELL, J. W. 2019. Mechanisms of postsynaptic localization of AMPA-type glutamate receptors and their regulation during long-term potentiation. *Sci Signal*, 12.
- BURNASHEV, N. & SZEPETOWSKI, P. 2015. NMDA receptor subunit mutations in neurodevelopmental disorders. *Curr Opin Pharmacol*, 20, 73-82.
- CAMINA, E. & GUELL, F. 2017. The Neuroanatomical, Neurophysiological and Psychological Basis of Memory: Current Models and Their Origins. *Front Pharmacol*, 8, 438.
- CAPIZZI, A., WOO, J. & VERDUZCO-GUTIERREZ, M. 2020. Traumatic Brain Injury: An Overview of Epidemiology, Pathophysiology, and Medical Management. *Med Clin North Am*, 104, 213-238.
- CARRON, S. F., ALWIS, D. S. & RAJAN, R. 2016. Traumatic Brain Injury and Neuronal Functionality Changes in Sensory Cortex. *Front Syst Neurosci*, 10, 47.
- CARVAJAL, F. J. & CERPA, W. 2021. Regulation of Phosphorylated State of NMDA Receptor by STEP61 Phosphatase after Mild-Traumatic Brain Injury: Role of Oxidative Stress. *Antioxidants (Basel)*, 10.
- CARVAJAL, F. J., MATTISON, H. A. & CERPA, W. 2016. Role of NMDA Receptor-Mediated Glutamatergic Signaling in Chronic and Acute Neuropathologies. *Neural Plast*, 2016, 2701526.
- CARVAJAL, F. J., MIRA, R. G., ROVEGNO, M., MINNITI, A. N. & CERPA, W. 2018. Age-related NMDA signaling alterations in SOD2 deficient mice. *Biochim Biophys Acta Mol Basis Dis*, 1864, 2010-2020.
- CHANDLER, L. J., SUTTON, G., DORAIRAJ, N. R. & NORWOOD, D. 2001. N-methyl D-aspartate receptor-mediated bidirectional control of extracellular signal-regulated kinase activity in cortical neuronal cultures. *J Biol Chem*, 276, 2627-36.
- CHATER, T. E. & GODA, Y. 2014. The role of AMPA receptors in postsynaptic mechanisms of synaptic plasticity. *Front Cell Neurosci*, 8, 401.
- CHEN, M., SONG, H., CUI, J., JOHNSON, C. E., HUBLER, G. K., DEPALMA, R. G., GU, Z. & XIA, W. 2018. Proteomic Profiling of Mouse Brains Exposed to Blast-Induced Mild Traumatic Brain Injury Reveals Changes in Axonal Proteins and Phosphorylated Tau. *J Alzheimers Dis*, 66, 751-773.

- CHERNYSHOVA, Y., LESHCHYNS'KA, I., HSU, S. C., SCHACHNER, M. & SYTNYK, V. 2011. The neural cell adhesion molecule promotes FGFR-dependent phosphorylation and membrane targeting of the exocyst complex to induce exocytosis in growth cones. *J Neurosci*, 31, 3522-35.
- CIGEL, A., SAYIN, O., GURGEN, S. G. & SONMEZ, A. 2021. Long term neuroprotective effects of acute single dose MK-801 treatment against traumatic brain injury in immature rats. *Neuropeptides*, 88, 102161.
- COLLINGRIDGE, G. L., PEINEAU, S., HOWLAND, J. G. & WANG, Y. T. 2010. Long-term depression in the CNS. *Nat Rev Neurosci*, 11, 459-73.
- COULTER, M. E., MUSAEV, D., DEGENNARO, E. M., ZHANG, X., HENKE, K., JAMES, K. N., SMITH, R. S., HILL, R. S., PARTLOW, J. N., MUNA, A.-S., KAMUMBU, A. S., HATEM, N., BARKOVICH, A. J., AZIZA, J., CHASSAING, N., ZAKI, M. S., SULTAN, T., BURGLIN, L., RAJAB, A., AL-GAZALI, L., MOCHIDA, G. H., HARRIS, M. P., GLEESON, J. G. & WALSH, C. A. 2020. Regulation of human cerebral cortical development by EXOC7 and EXOC8, components of the exocyst complex, and roles in neural progenitor cell proliferation and survival. *Genet Med*, 22, 1040-1050.
- DAS, A., GAJENDRA, S., FALENTA, K., OUDIN, M. J., PESCHARD, P., FENG, S., WU, B., MARSHALL, C. J., DOHERTY, P., GUO, W. & LALLI, G. 2014. RalA promotes a direct exocyst-Par6 interaction to regulate polarity in neuronal development. *J Cell Sci*, 127, 686-99.
- DAUVERMANN, M. R., LEE, G. & DAWSON, N. 2017. Glutamatergic regulation of cognition and functional brain connectivity: insights from pharmacological, genetic and translational schizophrenia research. *Br J Pharmacol*, 174, 3136-3160.
- DENNIS, S. H., JAAFARI, N., CIMAROSTI, H., HANLEY, J. G., HENLEY, J. M. & MELLOR, J. R. 2011. Oxygen/glucose deprivation induces a reduction in synaptic AMPA receptors on hippocampal CA3 neurons mediated by mGluR1 and adenosine A3 receptors. *J Neurosci*, 31, 11941-52.
- DERKACH, V., BARRIA, A. & SODERLING, T. R. 1999. Ca²⁺/calmodulin-kinase II enhances channel conductance of alpha-amino-3-hydroxy-5-methyl-4-isoxazolepropionate type glutamate receptors. *Proc Natl Acad Sci U S A*, 96, 3269-74.
- DEWAN, M. C., RATTANI, A., GUPTA, S., BATICULON, R. E., HUNG, Y. C., PUNCHAK, M., AGRAWAL, A., ADELEYE, A. O., SHRIME, M. G., RUBIANO, A. M., ROSENFELD, J. V. & PARK, K. B. 2018. Estimating the global incidence of traumatic brain injury. *J Neurosurg*, 1-18.
- DISMUKE-GREER, C., HIRSCH, S., CARLSON, K., POGODA, T., NAKASE-RICHARDSON, R., BHATNAGAR, S., EAPEN, B., TROYANSKAYA, M., MILES, S., NOLEN, T. & WALKER, W. C. 2020. Health Services Utilization, Health Care Costs, and Diagnoses by Mild Traumatic Brain Injury Exposure: A Chronic Effects of Neurotrauma Consortium Study. *Arch Phys Med Rehabil*, 101, 1720-1730.
- DITTGEN, T., NIMMERJAHN, A., KOMAI, S., LICZNERSKI, P., WATERS, J., MARGRIE, T. W., HELMCHEN, F., DENK, W., BRECHT, M. & OSTEN, P. 2004. Lentivirus-based genetic manipulations of cortical neurons and their optical and electrophysiological monitoring in vivo. *Proc Natl Acad Sci U S A*, 101, 18206-11.
- DOELLER, C. F., KING, J. A. & BURGESS, N. 2008. Parallel striatal and hippocampal systems for landmarks and boundaries in spatial memory. *Proc Natl Acad Sci U S A*, 105, 5915-20.
- DULL, T., ZUFFEREY, R., KELLY, M., MANDEL, R. J., NGUYEN, M., TRONO, D. & NALDINI, L. 1998. A third-generation lentivirus vector with a conditional packaging system. *J Virol*, 72, 8463-71.
- DUNAH, A. W., LUO, J., WANG, Y. H., YASUDA, R. P. & WOLFE, B. B. 1998. Subunit composition of N-methyl-D-aspartate receptors in the central nervous system that contain the NR2D subunit. *Mol Pharmacol*, 53, 429-37.
- DUPRAZ, S., GRASSI, D., BERNIS, M. E., SOSA, L., BISBAL, M., GASTALDI, L., JAUSORO, I., CACERES, A., PFENNINGER, K. H. & QUIROGA, S. 2009. The TC10-Exo70 complex is essential for membrane expansion and axonal specification in developing neurons. *J Neurosci*, 29, 13292-301.

- FAROOK, J. M., SHIELDS, J., TAWFIK, A., MARKAND, S., SEN, T., SMITH, S. B., BRANN, D., DHANDAPANI, K. M. & SEN, N. 2013. GADD34 induces cell death through inactivation of Akt following traumatic brain injury. *Cell Death Dis*, 4, e754.
- FINFER, S. R. & COHEN, J. 2001. Severe traumatic brain injury. *Resuscitation*, 48, 77-90.
- FRANULIC, A., CARBONELL, C. G., PINTO, P. & SEPULVEDA, I. 2004. Psychosocial adjustment and employment outcome 2, 5 and 10 years after TBI. *Brain Inj*, 18, 119-29.
- FRICANO-KUGLER, C. J., WILLIAMS, M. R., SALINARO, J. R., LI, M. & LUIKART, B. 2016. Designing, Packaging, and Delivery of High Titer CRISPR Retro and Lentiviruses via Stereotaxic Injection. *J Vis Exp*.
- FRUHMESSER, A., BLAKE, J., HABERLANDT, E., BAYING, B., RAEDER, B., RUNZ, H., SPREIZ, A., FAUTH, C., BENES, V., UTERMANN, G., ZSCHOCKE, J. & KOTZOT, D. 2013. Disruption of EXOC6B in a patient with developmental delay, epilepsy, and a de novo balanced t(2;8) translocation. *Eur J Hum Genet*, 21, 1177-80.
- FUJIMOTO, B. A., YOUNG, M., CARTER, L., PANG, A. P. S., CORLEY, M. J., FOGELGREN, B. & POLGAR, N. 2019. The exocyst complex regulates insulin-stimulated glucose uptake of skeletal muscle cells. *Am J Physiol Endocrinol Metab*, 317, E957-E972.
- FUJITA, A., KOINUMA, S., YASUDA, S., NAGAI, H., KAMIGUCHI, H., WADA, N. & NAKAMURA, T. 2013. GTP hydrolysis of TC10 promotes neurite outgrowth through exocytic fusion of Rab11- and L1-containing vesicles by releasing exocyst component Exo70. *PLoS One*, 8, e79689.
- FUKAYA, M., KATO, A., LOVETT, C., TONEGAWA, S. & WATANABE, M. 2003. Retention of NMDA receptor NR2 subunits in the lumen of endoplasmic reticulum in targeted NR1 knockout mice. *Proc Natl Acad Sci U S A*, 100, 4855-60.
- FURUKAWA, H., SINGH, S. K., MANCUSSO, R. & GOUAUX, E. 2005. Subunit arrangement and function in NMDA receptors. *Nature*, 438, 185-92.
- GABRIELI, D., SCHUMM, S. N., VIGILANTE, N. F. & MEANEY, D. F. 2021. NMDA Receptor Alterations After Mild Traumatic Brain Injury Induce Deficits in Memory Acquisition and Recall. *Neural Comput*, 33, 67-95.
- GEORGES, A. & J, M. D. 2021. Traumatic Brain Injury. *StatPearls*. Treasure Island (FL).
- GERGES, N. Z., BACKOS, D. S., RUPASINGHE, C. N., SPALLER, M. R. & ESTEBAN, J. A. 2006. Dual role of the exocyst in AMPA receptor targeting and insertion into the postsynaptic membrane. *EMBO J*, 25, 1623-34.
- GIRGIS, F., PACE, J., SWEET, J. & MILLER, J. P. 2016. Hippocampal Neurophysiologic Changes after Mild Traumatic Brain Injury and Potential Neuromodulation Treatment Approaches. *Front Syst Neurosci*, 10, 8.
- GOEBEL-GOODY, S. M., DAVIES, K. D., ALVESTAD LINGER, R. M., FREUND, R. K. & BROWNING, M. D. 2009. Phospho-regulation of synaptic and extrasynaptic N-methyl-d-aspartate receptors in adult hippocampal slices. *Neuroscience*, 158, 1446-59.
- GOSSELIN, R. D. 2019. Guidelines on statistics for researchers using laboratory animals: the essentials. *Lab Anim*, 53, 28-42.
- GREENWALD, B. D., BURNETT, D. M. & MILLER, M. A. 2003. Congenital and acquired brain injury. 1. Brain injury: epidemiology and pathophysiology. *Arch Phys Med Rehabil*, 84, S3-7.
- GUO, W., GRANT, A. & NOVICK, P. 1999. Exo84p is an exocyst protein essential for secretion. *J Biol Chem*, 274, 23558-64.
- GUO, W., SACHER, M., BARROWMAN, J., FERRO-NOVICK, S. & NOVICK, P. 2000. Protein complexes in transport vesicle targeting. *Trends Cell Biol*, 10, 251-5.

- GUSKIEWICZ, K. M., MCCREA, M., MARSHALL, S. W., CANTU, R. C., RANDOLPH, C., BARR, W., ONATE, J. A. & KELLY, J. P. 2003. Cumulative effects associated with recurrent concussion in collegiate football players: the NCAA Concussion Study. *JAMA*, 290, 2549-55.
- GYLYS, K. H., FEIN, J. A. & COLE, G. M. 2000. Quantitative characterization of crude synaptosomal fraction (P-2) components by flow cytometry. *J Neurosci Res*, 61, 186-92.
- GYLYS, K. H., FEIN, J. A., YANG, F. & COLE, G. M. 2004a. Enrichment of presynaptic and postsynaptic markers by size-based gating analysis of synaptosome preparations from rat and human cortex. *Cytometry A*, 60, 90-6.
- GYLYS, K. H., FEIN, J. A., YANG, F., WILEY, D. J., MILLER, C. A. & COLE, G. M. 2004b. Synaptic changes in Alzheimer's disease: increased amyloid-beta and gliosis in surviving terminals is accompanied by decreased PSD-95 fluorescence. *Am J Pathol*, 165, 1809-17.
- HABERMACHER, C., ANGULO, M. C. & BENAMER, N. 2019. Glutamate versus GABA in neuron-oligodendroglia communication. *Glia*, 67, 2092-2106.
- HACKETT, J. T. & UEDA, T. 2015. Glutamate Release. *Neurochem Res*, 40, 2443-60.
- HAMBURGER, Z. A., HAMBURGER, A. E., WEST, A. P., JR. & WEIS, W. I. 2006. Crystal structure of the *S.cerevisiae* exocyst component Exo70p. *J Mol Biol*, 356, 9-21.
- HAN, R. Z., HU, J. J., WENG, Y. C., LI, D. F. & HUANG, Y. 2009. NMDA receptor antagonist MK-801 reduces neuronal damage and preserves learning and memory in a rat model of traumatic brain injury. *Neurosci Bull*, 25, 367-75.
- HANSEN, K. B., FURUKAWA, H. & TRAYNELIS, S. F. 2010. Control of assembly and function of glutamate receptors by the amino-terminal domain. *Mol Pharmacol*, 78, 535-49.
- HARDINGHAM, G. E., ARNOLD, F. J. & BADING, H. 2001. Nuclear calcium signaling controls CREB-mediated gene expression triggered by synaptic activity. *Nat Neurosci*, 4, 261-7.
- HARDINGHAM, G. E., FUKUNAGA, Y. & BADING, H. 2002. Extrasynaptic NMDARs oppose synaptic NMDARs by triggering CREB shut-off and cell death pathways. *Nat Neurosci*, 5, 405-14.
- HARRISON-FELIX, C., PRETZ, C., HAMMOND, F. M., CUTHBERT, J. P., BELL, J., CORRIGAN, J., MILLER, A. C. & HAARBAUER-KRUPA, J. 2015. Life Expectancy after Inpatient Rehabilitation for Traumatic Brain Injury in the United States. *J Neurotrauma*, 32, 1893-901.
- HARRISON-FELIX, C., WHITENECK, G., DEVIVO, M. J., HAMMOND, F. M. & JHA, A. 2006. Causes of death following 1 year postinjury among individuals with traumatic brain injury. *J Head Trauma Rehabil*, 21, 22-33.
- HAZUKA, C. D., FOLETTI, D. L., HSU, S. C., KEE, Y., HOPF, F. W. & SCHELLER, R. H. 1999. The sec6/8 complex is located at neurite outgrowth and axonal synapse-assembly domains. *J Neurosci*, 19, 1324-34.
- HEISE, C., PREUSS, J. M., SCHROEDER, J. C., BATTAGLIA, C. R., KOLIBIUS, J., SCHMID, R., KREUTZ, M. R., KAS, M. J. H., BURBACH, J. P. H. & BOECKERS, T. M. 2018. Heterogeneity of Cell Surface Glutamate and GABA Receptor Expression in Shank and CNTN4 Autism Mouse Models. *Front Mol Neurosci*, 11, 212.
- HERING, H. & SHENG, M. 2001. Dendritic spines: structure, dynamics and regulation. *Nat Rev Neurosci*, 2, 880-8.
- HERRING, B. E. & NICOLL, R. A. 2016. Long-Term Potentiation: From CaMKII to AMPA Receptor Trafficking. *Annu Rev Physiol*, 78, 351-65.
- HILL, C. S., COLEMAN, M. P. & MENON, D. K. 2016. Traumatic Axonal Injury: Mechanisms and Translational Opportunities. *Trends Neurosci*, 39, 311-324.
- HIROKAWA, N., NIWA, S. & TANAKA, Y. 2010. Molecular motors in neurons: transport mechanisms and roles in brain function, development, and disease. *Neuron*, 68, 610-38.

- HORAK, M., PETRALIA, R. S., KANIAKOVA, M. & SANS, N. 2014. ER to synapse trafficking of NMDA receptors. *Front Cell Neurosci*, 8, 394.
- HSU, S. C., TING, A. E., HAZUKA, C. D., DAVANGER, S., KENNY, J. W., KEE, Y. & SCHELLER, R. H. 1996. The mammalian brain rsec6/8 complex. *Neuron*, 17, 1209-19.
- IBRAHIM, S., HU, W., WANG, X., GAO, X., HE, C. & CHEN, J. 2016. Traumatic Brain Injury Causes Aberrant Migration of Adult-Born Neurons in the Hippocampus. *Sci Rep*, 6, 21793.
- INOUE, M., CHANG, L., HWANG, J., CHIANG, S. H. & SALTIEL, A. R. 2003. The exocyst complex is required for targeting of Glut4 to the plasma membrane by insulin. *Nature*, 422, 629-33.
- INOUE, M., CHIANG, S. H., CHANG, L., CHEN, X. W. & SALTIEL, A. R. 2006. Compartmentalization of the exocyst complex in lipid rafts controls Glut4 vesicle tethering. *Mol Biol Cell*, 17, 2303-11.
- IVANOV, A., PELLEGRINO, C., RAMA, S., DUMALSKA, I., SALYHA, Y., BEN-ARI, Y. & MEDINA, I. 2006. Opposing role of synaptic and extrasynaptic NMDA receptors in regulation of the extracellular signal-regulated kinases (ERK) activity in cultured rat hippocampal neurons. *J Physiol*, 572, 789-98.
- JAKOWEC, M. W., JACKSON-LEWIS, V., CHEN, X., LANGSTON, J. W. & PRZEDBORSKI, S. 1998. The postnatal development of AMPA receptor subunits in the basal ganglia of the rat. *Dev Neurosci*, 20, 19-33.
- JAMJOOM, A. A. B., RHODES, J., ANDREWS, P. J. D. & GRANT, S. G. N. 2021. The synapse in traumatic brain injury. *Brain*, 144, 18-31.
- JEON, S. G., KANG, M., KIM, Y. S., KIM, D. H., NAM, D. W., SONG, E. J., MOOK-JUNG, I. & MOON, M. 2018. Intrahippocampal injection of a lentiviral vector expressing neurogranin enhances cognitive function in 5XFAD mice. *Exp Mol Med*, 50, e461.
- JOHNSTONE, V. P., WRIGHT, D. K., WONG, K., O'BRIEN, T. J., RAJAN, R. & SHULTZ, S. R. 2015. Experimental Traumatic Brain Injury Results in Long-Term Recovery of Functional Responsiveness in Sensory Cortex but Persisting Structural Changes and Sensorimotor, Cognitive, and Emotional Deficits. *J Neurotrauma*, 32, 1333-46.
- KANDEL, M. B., YAMAMOTO, S., MIDORIKAWA, R., MORISE, J., WAKAZONO, Y., OKA, S. & TAKAMIYA, K. 2018. N-glycosylation of the AMPA-type glutamate receptor regulates cell surface expression and tetramer formation affecting channel function. *J Neurochem*, 147, 730-747.
- KANNINEN, K., HEIKKINEN, R., MALM, T., ROLOVA, T., KUHMENEN, S., LEINONEN, H., YLA-HERTTUALA, S., TANILA, H., LEVONEN, A. L., KOISTINAHO, M. & KOISTINAHO, J. 2009. Intrahippocampal injection of a lentiviral vector expressing Nrf2 improves spatial learning in a mouse model of Alzheimer's disease. *Proc Natl Acad Sci U S A*, 106, 16505-10.
- KAPLAN, G. B., LEITE-MORRIS, K. A., WANG, L., RUMBIKA, K. K., HEINRICH, S. C., ZENG, X., WU, L., ARENA, D. T. & TENG, Y. D. 2018. Pathophysiological Bases of Comorbidity: Traumatic Brain Injury and Post-Traumatic Stress Disorder. *J Neurotrauma*, 35, 210-225.
- KAZIM, S. F., SHAMIM, M. S., TAHIR, M. Z., ENAM, S. A. & WAHEED, S. 2011. Management of penetrating brain injury. *J Emerg Trauma Shock*, 4, 395-402.
- KILBOURNE, M., KUEHN, R., TOSUN, C., CARIDI, J., KELEDJIAN, K., BOCHICCHIO, G., SCALEA, T., GERZANICH, V. & SIMARD, J. M. 2009. Novel model of frontal impact closed head injury in the rat. *J Neurotrauma*, 26, 2233-43.
- KRISHNA, G., BEITCHMAN, J. A., BROMBERG, C. E. & CURRIER THOMAS, T. 2020. Approaches to Monitor Circuit Disruption after Traumatic Brain Injury: Frontiers in Preclinical Research. *Int J Mol Sci*, 21.
- KRISHNA, G., YING, Z. & GOMEZ-PINILLA, F. 2019. Blueberry Supplementation Mitigates Altered Brain Plasticity and Behavior after Traumatic Brain Injury in Rats. *Mol Nutr Food Res*, 63, e1801055.

- KRISTIANSEN, L. V., HUERTA, I., BENEYTO, M. & MEADOR-WOODRUFF, J. H. 2007. NMDA receptors and schizophrenia. *Curr Opin Pharmacol*, 7, 48-55.
- LEE, A. S., DUMAN, R. S. & PITTENGER, C. 2008. A double dissociation revealing bidirectional competition between striatum and hippocampus during learning. *Proc Natl Acad Sci U S A*, 105, 17163-8.
- LEE, S. L. T., LEW, D., WICKENHEISSER, V. & MARKUS, E. J. 2019. Interdependence between dorsal and ventral hippocampus during spatial navigation. *Brain Behav*, 9, e01410.
- LETINIC, K., SEBASTIAN, R., TOOMRE, D. & RAKIC, P. 2009. Exocyst is involved in polarized cell migration and cerebral cortical development. *Proc Natl Acad Sci U S A*, 106, 11342-7.
- LEWERENZ, J. & MAHER, P. 2015. Chronic Glutamate Toxicity in Neurodegenerative Diseases-What is the Evidence? *Front Neurosci*, 9, 469.
- LICHNEROVA, K., KANIAKOVA, M., PARK, S. P., SKRENKOVA, K., WANG, Y. X., PETRALIA, R. S., SUH, Y. H. & HORAK, M. 2015. Two N-glycosylation Sites in the GluN1 Subunit Are Essential for Releasing N-methyl-d-aspartate (NMDA) Receptors from the Endoplasmic Reticulum. *J Biol Chem*, 290, 18379-90.
- LIPSCHUTZ, J. H. & MOSTOV, K. E. 2002. Exocytosis: the many masters of the exocyst. *Curr Biol*, 12, R212-4.
- LIRA, M., ARANCIBIA, D., ORREGO, P. R., MONTENEGRO-VENEGAS, C., CRUZ, Y., GARCIA, J., LEAL-ORTIZ, S., GODOY, J. A., GUNDELFINGER, E. D., INESTROSA, N. C., GARNER, C. C., ZAMORANO, P. & TORRES, V. I. 2019. The Exocyst Component Exo70 Modulates Dendrite Arbor Formation, Synapse Density, and Spine Maturation in Primary Hippocampal Neurons. *Mol Neurobiol*, 56, 4620-4638.
- LIRA, M., MIRA, R. G., CARVAJAL, F. J., ZAMORANO, P., INESTROSA, N. C. & CERPA, W. 2020. Glutamatergic Receptor Trafficking and Delivery: Role of the Exocyst Complex. *Cells*, 9.
- LIRA, M., ZAMORANO, P. & CERPA, W. 2021. Exo70 intracellular redistribution after repeated mild traumatic brain injury. *Biol Res*, 54, 5.
- LIU, J., ZUO, X., YUE, P. & GUO, W. 2007. Phosphatidylinositol 4,5-bisphosphate mediates the targeting of the exocyst to the plasma membrane for exocytosis in mammalian cells. *Mol Biol Cell*, 18, 4483-92.
- LOIS, C., HONG, E. J., PEASE, S., BROWN, E. J. & BALTIMORE, D. 2002. Germline transmission and tissue-specific expression of transgenes delivered by lentiviral vectors. *Science*, 295, 868-72.
- LU, H., LIU, S., ZHANG, G., KWONG, L. N., ZHU, Y., MILLER, J. P., HU, Y., ZHONG, W., ZENG, J., WU, L., KREPLER, C., SPROESSER, K., XIAO, M., XU, W., KARAKOUSIS, G. C., SCHUCHTER, L. M., FIELD, J., ZHANG, P. J., HERLYN, M., XU, X. & GUO, W. 2016. Oncogenic BRAF-Mediated Melanoma Cell Invasion. *Cell Rep*, 15, 2012-24.
- LU, K. T., HUANG, T. C., TSAI, Y. H. & YANG, Y. L. 2017. Transient receptor potential vanilloid type 4 channels mediate Na-K-Cl-co-transporter-induced brain edema after traumatic brain injury. *J Neurochem*, 140, 718-727.
- LU, K. T., HUANG, T. C., WANG, J. Y., YOU, Y. S., CHOU, J. L., CHAN, M. W., WO, P. Y., AMSTISLAVSKAYA, T. G., TIKHONOVA, M. A. & YANG, Y. L. 2015. NKCC1 mediates traumatic brain injury-induced hippocampal neurogenesis through CREB phosphorylation and HIF-1alpha expression. *Pflugers Arch*, 467, 1651-61.
- LUCHKINA, N. V., HUUPPONEN, J., CLARKE, V. R., COLEMAN, S. K., KEINANEN, K., TAIRA, T. & LAURI, S. E. 2014. Developmental switch in the kinase dependency of long-term potentiation depends on expression of GluA4 subunit-containing AMPA receptors. *Proc Natl Acad Sci U S A*, 111, 4321-6.

- LUO, Y., ZOU, H., WU, Y., CAI, F., ZHANG, S. & SONG, W. 2017. Mild traumatic brain injury induces memory deficits with alteration of gene expression profile. *Sci Rep*, 7, 10846.
- LUSCHER, C. & MALENKA, R. C. 2012. NMDA receptor-dependent long-term potentiation and long-term depression (LTP/LTD). *Cold Spring Harb Perspect Biol*, 4.
- MAAS, A. I., STOCCHETTI, N. & BULLOCK, R. 2008. Moderate and severe traumatic brain injury in adults. *Lancet Neurol*, 7, 728-41.
- MAITI, P., MANNA, J., ILAVAZHAGAN, G., ROSSIGNOL, J. & DUNBAR, G. L. 2015. Molecular regulation of dendritic spine dynamics and their potential impact on synaptic plasticity and neurological diseases. *Neurosci Biobehav Rev*, 59, 208-37.
- MANEK, R., MOGHIEB, A., YANG, Z., KUMAR, D., KOBESSIY, F., SARKIS, G. A., RAGHAVAN, V. & WANG, K. K. W. 2018. Protein Biomarkers and Neuroproteomics Characterization of Microvesicles/Exosomes from Human Cerebrospinal Fluid Following Traumatic Brain Injury. *Mol Neurobiol*, 55, 6112-6128.
- MAO, L., ZHAN, Y. Y., WU, B., YU, Q., XU, L., HONG, X., ZHONG, L., MI, P., XIAO, L., WANG, X., CAO, H., ZHANG, W., CHEN, B., XIANG, J., MEI, K., RADHAKRISHNAN, R., GUO, W. & HU, T. 2020a. ULK1 phosphorylates Exo70 to suppress breast cancer metastasis. *Nat Commun*, 11, 117.
- MAO, X., TERPOLILLI, N. A., WEHN, A., CHENG, S., HELLAL, F., LIU, B., SEKER, B. & PLESNILA, N. 2020b. Progressive Histopathological Damage Occurring Up to One Year after Experimental Traumatic Brain Injury Is Associated with Cognitive Decline and Depression-Like Behavior. *J Neurotrauma*, 37, 1331-1341.
- MARSCHNER, L., SCHREURS, A., LECHAT, B., MOGENSEN, J., ROEBROEK, A., AHMED, T. & BALSCHUN, D. 2019. Single mild traumatic brain injury results in transiently impaired spatial long-term memory and altered search strategies. *Behav Brain Res*, 365, 222-230.
- MARTIN-URDIROZ, M., DEEKS, M. J., HORTON, C. G., DAWE, H. R. & JOURDAIN, I. 2016. The Exocyst Complex in Health and Disease. *Front Cell Dev Biol*, 4, 24.
- MATTISON, H. A., HAYASHI, T. & BARRIA, A. 2012. Palmitoylation at two cysteine clusters on the C-terminus of GluN2A and GluN2B differentially control synaptic targeting of NMDA receptors. *PLoS One*, 7, e49089.
- MCCRORY, P., MEEUWISSE, W., AUBRY, M., CANTU, B., DVORAK, J., ECHEMENDIA, R., ENGBRETSSEN, L., JOHNSTON, K., KUTCHER, J., RAFTERY, M., SILLS, A., BENSON, B., DAVIS, G., ELLENBOGEN, R., GUSKIEWICZ, K., HERRING, S. A., IVERSON, G., JORDAN, B., KISSICK, J., MCCREA, M., MCINTOSH, A., MADDOCKS, D., MAKDISSI, M., PURCELL, L., PUTUKIAN, M., SCHNEIDER, K., TATOR, C. & TURNER, M. 2013. Consensus statement on Concussion in Sport - The 4th International Conference on Concussion in Sport held in Zurich, November 2012. *Phys Ther Sport*, 14, e1-e13.
- MCINNES, K., FRIESEN, C. L., MACKENZIE, D. E., WESTWOOD, D. A. & BOE, S. G. 2017. Mild Traumatic Brain Injury (mTBI) and chronic cognitive impairment: A scoping review. *PLoS One*, 12, e0174847.
- MCKEE, A. C., CAIRNS, N. J., DICKSON, D. W., FOLKERTH, R. D., KEENE, C. D., LITVAN, I., PERL, D. P., STEIN, T. D., VONSATTEL, J. P., STEWART, W., TRIPODIS, Y., CRARY, J. F., BIENIEK, K. F., DAMS-O'CONNOR, K., ALVAREZ, V. E., GORDON, W. A. & GROUP, T. C. 2016. The first NINDS/NIBIB consensus meeting to define neuropathological criteria for the diagnosis of chronic traumatic encephalopathy. *Acta Neuropathol*, 131, 75-86.
- MEDDOWS, E., LE BOURDELLES, B., GRIMWOOD, S., WAFFORD, K., SANDHU, S., WHITING, P. & MCILHINNEY, R. A. 2001. Identification of molecular determinants that are important in the assembly of N-methyl-D-aspartate receptors. *J Biol Chem*, 276, 18795-803.
- MELDRUM, B. S. 2000. Glutamate as a neurotransmitter in the brain: review of physiology and pathology. *J Nutr*, 130, 1007S-15S.

- MELLONE, M. & GARDONI, F. 2013. Modulation of NMDA receptor at the synapse: promising therapeutic interventions in disorders of the nervous system. *Eur J Pharmacol*, 719, 75-83.
- MENON, D. K., SCHWAB, K., WRIGHT, D. W., MAAS, A. I., DEMOGRAPHICS, CLINICAL ASSESSMENT WORKING GROUP OF THE, I., INTERAGENCY INITIATIVE TOWARD COMMON DATA ELEMENTS FOR RESEARCH ON TRAUMATIC BRAIN, I. & PSYCHOLOGICAL, H. 2010. Position statement: definition of traumatic brain injury. *Arch Phys Med Rehabil*, 91, 1637-40.
- MILLER, J. E., SHIVAKUMAR, M. K., LEE, Y., HAN, S., HORGOSLUOGLU, E., RISACHER, S. L., SAYKIN, A. J., NHO, K., KIM, D. & ALZHEIMER'S DISEASE NEUROIMAGING, I. 2018. Rare variants in the splicing regulatory elements of EXOC3L4 are associated with brain glucose metabolism in Alzheimer's disease. *BMC Med Genomics*, 11, 76.
- MILLER, L. P., LYETH, B. G., JENKINS, L. W., OLENIK, L., PANCHISION, D., HAMM, R. J., PHILLIPS, L. L., DIXON, C. E., CLIFTON, G. L. & HAYES, R. L. 1990. Excitatory amino acid receptor subtype binding following traumatic brain injury. *Brain Res*, 526, 103-7.
- MINERBI, A., KAHANA, R., GOLDFELD, L., KAUFMAN, M., MAROM, S. & ZIV, N. E. 2009. Long-term relationships between synaptic tenacity, synaptic remodeling, and network activity. *PLoS Biol*, 7, e1000136.
- MIRA, R. G. & CERPA, W. 2021. Building a Bridge Between NMDAR-Mediated Excitotoxicity and Mitochondrial Dysfunction in Chronic and Acute Diseases. *Cell Mol Neurobiol*, 41, 1413-1430.
- MIRA, R. G., LIRA, M., QUINTANILLA, R. A. & CERPA, W. 2020. Alcohol consumption during adolescence alters the hippocampal response to traumatic brain injury. *Biochem Biophys Res Commun*, 528, 514-519.
- MOORE, B. A., ROBINSON, H. H. & XU, Z. 2007. The crystal structure of mouse Exo70 reveals unique features of the mammalian exocyst. *J Mol Biol*, 371, 410-21.
- MORRIS, R. G. 2013. NMDA receptors and memory encoding. *Neuropharmacology*, 74, 32-40.
- MURTHY, M., GARZA, D., SCHELLER, R. H. & SCHWARZ, T. L. 2003. Mutations in the exocyst component Sec5 disrupt neuronal membrane traffic, but neurotransmitter release persists. *Neuron*, 37, 433-47.
- NADA, S., SHIMA, T., YANAI, H., HUSI, H., GRANT, S. G., OKADA, M. & AKIYAMA, T. 2003. Identification of PSD-93 as a substrate for the Src family tyrosine kinase Fyn. *J Biol Chem*, 278, 47610-21.
- NEARY, J. T. 2005. Protein kinase signaling cascades in CNS trauma. *IUBMB Life*, 57, 711-8.
- NEARY, J. T. & KANG, Y. 2005. Signaling from P2 nucleotide receptors to protein kinase cascades induced by CNS injury: implications for reactive gliosis and neurodegeneration. *Mol Neurobiol*, 31, 95-103.
- NISHI, M., HINDS, H., LU, H. P., KAWATA, M. & HAYASHI, Y. 2001. Motoneuron-specific expression of NR3B, a novel NMDA-type glutamate receptor subunit that works in a dominant-negative manner. *J Neurosci*, 21, RC185.
- PAPADIA, S., SORIANO, F. X., LEVEILLE, F., MARTEL, M. A., DAKIN, K. A., HANSEN, H. H., KAINDL, A., SIFRINGER, M., FOWLER, J., STEFOVSKA, V., MCKENZIE, G., CRAIGON, M., CORRIVEAU, R., GHAZAL, P., HORSBURGH, K., YANKNER, B. A., WYLLIE, D. J., IKONOMIDOU, C. & HARDINGHAM, G. E. 2008. Synaptic NMDA receptor activity boosts intrinsic antioxidant defenses. *Nat Neurosci*, 11, 476-87.
- PAPADIA, S., STEVENSON, P., HARDINGHAM, N. R., BADING, H. & HARDINGHAM, G. E. 2005. Nuclear Ca²⁺ and the cAMP response element-binding protein family mediate a late phase of activity-dependent neuroprotection. *J Neurosci*, 25, 4279-87.
- PAPOUIN, T., LADEPECHE, L., RUEL, J., SACCHI, S., LABASQUE, M., HANINI, M., GROG, L., POLLEGIONI, L., MOTHET, J. P. & OLIET, S. H. 2012. Synaptic and extrasynaptic NMDA receptors are gated by different endogenous coagonists. *Cell*, 150, 633-46.

- PARK, Y., LUO, T., ZHANG, F., LIU, C., BRAMLETT, H. M., DIETRICH, W. D. & HU, B. 2013. Downregulation of Src-kinase and glutamate-receptor phosphorylation after traumatic brain injury. *J Cereb Blood Flow Metab*, 33, 1642-9.
- PENG, S., ZHANG, Y., ZHANG, J., WANG, H. & REN, B. 2011. Glutamate receptors and signal transduction in learning and memory. *Mol Biol Rep*, 38, 453-60.
- PENG, Y., LEE, J., ROWLAND, K., WEN, Y., HUA, H., CARLSON, N., LAVANIA, S., PARRISH, J. Z. & KIM, M. D. 2015. Regulation of dendrite growth and maintenance by exocytosis. *J Cell Sci*, 128, 4279-92.
- PETRALIA, R. S., AL-HALLAQ, R. A. & WENTHOLD, R. J. 2009. Trafficking and Targeting of NMDA Receptors. In: VAN DONGEN, A. M. (ed.) *Biology of the NMDA Receptor*. Boca Raton (FL).
- PFEFFER, S. R. 1999. Transport-vesicle targeting: tethers before SNAREs. *Nat Cell Biol*, 1, E17-22.
- PICCO, A., IRASTORZA-AZCARATE, I., SPECHT, T., BOKE, D., PAZOS, I., RIVIER-CORDEY, A. S., DEVOS, D. P., KAKSONEN, M. & GALLEGO, O. 2017. The In Vivo Architecture of the Exocyst Provides Structural Basis for Exocytosis. *Cell*, 168, 400-412 e18.
- PLATT, S. R. 2007. The role of glutamate in central nervous system health and disease--a review. *Vet J*, 173, 278-86.
- POMMEREIT, D. & WOUTERS, F. S. 2007. An NGF-induced Exo70-TC10 complex locally antagonises Cdc42-mediated activation of N-WASP to modulate neurite outgrowth. *J Cell Sci*, 120, 2694-705.
- RAI, S. N., DILNASHIN, H., BIRLA, H., SINGH, S. S., ZAHRA, W., RATHORE, A. S., SINGH, B. K. & SINGH, S. P. 2019. The Role of PI3K/Akt and ERK in Neurodegenerative Disorders. *Neurotox Res*, 35, 775-795.
- RANA, A., SINGH, S., SHARMA, R. & KUMAR, A. 2019. Traumatic Brain Injury Altered Normal Brain Signaling Pathways: Implications for Novel Therapeutics Approaches. *Curr Neuropharmacol*, 17, 614-629.
- REHMAN, S. U., AHMAD, A., YOON, G. H., KHAN, M., ABID, M. N. & KIM, M. O. 2018. Inhibition of c-Jun N-Terminal Kinase Protects Against Brain Damage and Improves Learning and Memory After Traumatic Brain Injury in Adult Mice. *Cereb Cortex*, 28, 2854-2872.
- REHMAN, S. U., IKRAM, M., ULLAH, N., ALAM, S. I., PARK, H. Y., BADSHAH, H., CHOE, K. & KIM, M. O. 2019. Neurological Enhancement Effects of Melatonin against Brain Injury-Induced Oxidative Stress, Neuroinflammation, and Neurodegeneration via AMPK/CREB Signaling. *Cells*, 8.
- REN, J. & GUO, W. 2012. ERK1/2 regulate exocytosis through direct phosphorylation of the exocyst component Exo70. *Dev Cell*, 22, 967-78.
- RENNER, M. C., ALBERS, E. H., GUTIERREZ-CASTELLANOS, N., REINDERS, N. R., VAN HUIJSTEE, A. N., XIONG, H., LODDER, T. R. & KESSELS, H. W. 2017. Synaptic plasticity through activation of GluA3-containing AMPA-receptors. *Elife*, 6.
- RIEDEL, G., PLATT, B. & MICHEAU, J. 2003. Glutamate receptor function in learning and memory. *Behav Brain Res*, 140, 1-47.
- RISLING, T. E., CAULKETT, N. A. & FLORENCE, D. 2012. Open-drop anesthesia for small laboratory animals. *Can Vet J*, 53, 299-302.
- ROOZENBEEK, B., MAAS, A. I. & MENON, D. K. 2013. Changing patterns in the epidemiology of traumatic brain injury. *Nat Rev Neurol*, 9, 231-6.
- ROSSI, G., LEPORE, D., KENNER, L., CZUCHRA, A. B., PLOOSTER, M., FROST, A., MUNSON, M. & BRENNWALD, P. 2020. Exocyst structural changes associated with activation of tethering downstream of Rho/Cdc42 GTPases. *J Cell Biol*, 219.

- RUIZ, C., MIMICA, X., LISBONA, M. L., DONOSO, J., ARRIAGADA, P., ROA, M., BRAVO, S. & GODOY, J. 2013. [Characteristics of trauma patients admitted to the intensive care unit of a general hospital in Chile]. *Rev Med Chil*, 141, 1389-94.
- SANDOVAL, M., LUARTE, A., HERRERA-MOLINA, R., VARAS-GODOY, M., SANTIBANEZ, M., RUBIO, F. J., SMIT, A. B., GUNDELFINGER, E. D., LI, K. W., SMALLA, K. H. & WYNEKEN, U. 2013. The glycolytic enzyme aldolase C is up-regulated in rat forebrain microsomes and in the cerebrospinal fluid after repetitive fluoxetine treatment. *Brain Res*, 1520, 1-14.
- SANS, N., PRYBYLOWSKI, K., PETRALIA, R. S., CHANG, K., WANG, Y. X., RACCA, C., VICINI, S. & WENTHOLD, R. J. 2003. NMDA receptor trafficking through an interaction between PDZ proteins and the exocyst complex. *Nat Cell Biol*, 5, 520-30.
- SANS, N., RACCA, C., PETRALIA, R. S., WANG, Y. X., MCCALLUM, J. & WENTHOLD, R. J. 2001. Synapse-associated protein 97 selectively associates with a subset of AMPA receptors early in their biosynthetic pathway. *J Neurosci*, 21, 7506-16.
- SANS, N., WANG, P. Y., DU, Q., PETRALIA, R. S., WANG, Y. X., NAKKA, S., BLUMER, J. B., MACARA, I. G. & WENTHOLD, R. J. 2005. mPins modulates PSD-95 and SAP102 trafficking and influences NMDA receptor surface expression. *Nat Cell Biol*, 7, 1179-90.
- SCHUMM, S. N., GABRIELI, D. & MEANEY, D. F. 2020. Neuronal Degeneration Impairs Rhythms Between Connected Microcircuits. *Front Comput Neurosci*, 14, 18.
- SCHWABE, L. 2013. Stress and the engagement of multiple memory systems: integration of animal and human studies. *Hippocampus*, 23, 1035-43.
- SCHWARZBACH, E., BONISLAWSKI, D. P., XIONG, G. & COHEN, A. S. 2006. Mechanisms underlying the inability to induce area CA1 LTP in the mouse after traumatic brain injury. *Hippocampus*, 16, 541-50.
- SHAHEEN, R., FAQEIH, E., ALSHAMMARI, M. J., SWAID, A., AL-GAZALI, L., MARDAWI, E., ANSARI, S., SOGATY, S., SEIDAHMED, M. Z., ALMOTAIRI, M. I., FARRA, C., KURDI, W., AL-RASHEED, S. & ALKURAYA, F. S. 2013. Genomic analysis of Meckel-Gruber syndrome in Arabs reveals marked genetic heterogeneity and novel candidate genes. *Eur J Hum Genet*, 21, 762-8.
- SHALATA, A., LAUHASURAYOTIN, S., LEIBOVITZ, Z., LI, H., HEBERT, D., DHANRAJ, S., HADID, Y., MAHROUM, M., BAJAR, J., EGENBURG, S., ARAD, A., SHOHAT, M., HADDAD, S., BAKRY, H., MOSHIRI, H., SCHERER, S. W., TZUR, S. & DROR, Y. 2019. Biallelic mutations in EXOC3L2 cause a novel syndrome that affects the brain, kidney and blood. *J Med Genet*, 56, 340-346.
- SHIMSHEK, D. R., BUS, T., SCHUPP, B., JENSEN, V., MARX, V., LAYER, L. E., KOHR, G. & SPRENGEL, R. 2017. Different Forms of AMPA Receptor Mediated LTP and Their Correlation to the Spatial Working Memory Formation. *Front Mol Neurosci*, 10, 214.
- SHIPTON, O. A. & PAULSEN, O. 2014. GluN2A and GluN2B subunit-containing NMDA receptors in hippocampal plasticity. *Philos Trans R Soc Lond B Biol Sci*, 369, 20130163.
- SIEDLER, D. G., CHUAH, M. I., KIRKCALDIE, M. T., VICKERS, J. C. & KING, A. E. 2014. Diffuse axonal injury in brain trauma: insights from alterations in neurofilaments. *Front Cell Neurosci*, 8, 429.
- SILLEVIS SMITT, P., KINOSHITA, A., DE LEEUW, B., MOLL, W., COESMANS, M., JAARSMA, D., HENZEN-LOGMANS, S., VECHT, C., DE ZEEUW, C., SEKIYAMA, N., NAKANISHI, S. & SHIGEMOTO, R. 2000. Paraneoplastic cerebellar ataxia due to autoantibodies against a glutamate receptor. *N Engl J Med*, 342, 21-7.
- SILVERBERG, N. D. & IVERSON, G. L. 2011. Etiology of the post-concussion syndrome: Physiogenesis and Psychogenesis revisited. *NeuroRehabilitation*, 29, 317-29.
- SKRENKOVA, K., LEE, S., LICHNEROVA, K., KANIAKOVA, M., HANSIKOVA, H., ZAPOTOCKY, M., SUH, Y. H. & HORAK, M. 2018. N-Glycosylation Regulates the Trafficking and Surface Mobility of GluN3A-Containing NMDA Receptors. *Front Mol Neurosci*, 11, 188.

- SLOBOUNOV, S., SLOBOUNOV, E., SEBASTIANELLI, W., CAO, C. & NEWELL, K. 2007. Differential rate of recovery in athletes after first and second concussion episodes. *Neurosurgery*, 61, 338-44; discussion 344.
- SMALLA, K.-H., KLEMMER, P. & WYNEKEN, U. 2013. Isolation of the Postsynaptic Density: A Specialization of the Subsynaptic Cytoskeleton. *In: DERMIETZEL, R. (ed.) The Cytoskeleton: Imaging, Isolation, and Interaction*. Totowa, NJ: Humana Press.
- SMOLDERS, K., LOMBAERT, N., VALKENBORG, D., BAGGERMAN, G. & ARCKENS, L. 2015. An effective plasma membrane proteomics approach for small tissue samples. *Sci Rep*, 5, 10917.
- SOHN, H. & PARK, M. 2019. Palmitoylation-mediated synaptic regulation of AMPA receptor trafficking and function. *Arch Pharm Res*, 42, 426-435.
- SONMEZ, A., SAYIN, O., GURGEN, S. G. & CALISIR, M. 2015. Neuroprotective effects of MK-801 against traumatic brain injury in immature rats. *Neurosci Lett*, 597, 137-42.
- SOTO, D., ALTAFAJ, X., SINDREU, C. & BAYES, A. 2014. Glutamate receptor mutations in psychiatric and neurodevelopmental disorders. *Commun Integr Biol*, 7, e27887.
- SOWERS, J. L., WU, P., ZHANG, K., DEWITT, D. S. & PROUGH, D. S. 2018. Proteomic changes in traumatic brain injury: experimental approaches. *Curr Opin Neurol*, 31, 709-717.
- STUICHLIK, A. 2014. Dynamic learning and memory, synaptic plasticity and neurogenesis: an update. *Front Behav Neurosci*, 8, 106.
- SU, E. & BELL, M. 2016. Diffuse Axonal Injury. *In: LASKOWITZ, D. & GRANT, G. (eds.) Translational Research in Traumatic Brain Injury*. Boca Raton (FL).
- SUNG, Y. K. & KIM, S. W. 2019. Recent advances in the development of gene delivery systems. *Biomater Res*, 23, 8.
- TAKEUCHI, T., DUSZKIEWICZ, A. J. & MORRIS, R. G. 2014. The synaptic plasticity and memory hypothesis: encoding, storage and persistence. *Philos Trans R Soc Lond B Biol Sci*, 369, 20130288.
- TEODORO, R. O., PEKKURNAZ, G., NASSER, A., HIGASHI-KOVTUN, M. E., BALAKIREVA, M., MCLACHLAN, I. G., CAMONIS, J. & SCHWARZ, T. L. 2013. Ral mediates activity-dependent growth of postsynaptic membranes via recruitment of the exocyst. *EMBO J*, 32, 2039-55.
- TERASHIMA, A., SUH, Y. H. & ISAAC, J. T. R. 2019. The AMPA Receptor Subunit GluA1 is Required for CA1 Hippocampal Long-Term Potentiation but is not Essential for Synaptic Transmission. *Neurochem Res*, 44, 549-561.
- TERBUSH, D. R., MAURICE, T., ROTH, D. & NOVICK, P. 1996. The Exocyst is a multiprotein complex required for exocytosis in *Saccharomyces cerevisiae*. *EMBO J*, 15, 6483-94.
- TESTA, C. M., FRIBERG, I. K., WEISS, S. W. & STANDAERT, D. G. 1998. Immunohistochemical localization of metabotropic glutamate receptors mGluR1a and mGluR2/3 in the rat basal ganglia. *J Comp Neurol*, 390, 5-19.
- TEZUKA, T., UMEMORI, H., AKIYAMA, T., NAKANISHI, S. & YAMAMOTO, T. 1999. PSD-95 promotes Fyn-mediated tyrosine phosphorylation of the N-methyl-D-aspartate receptor subunit NR2A. *Proc Natl Acad Sci U S A*, 96, 435-40.
- TITUS, D. J., WILSON, N. M., FREUND, J. E., CARBALLOSA, M. M., SIKAH, K. E., FURONES, C., DIETRICH, W. D., GURNEY, M. E. & ATKINS, C. M. 2016. Chronic Cognitive Dysfunction after Traumatic Brain Injury Is Improved with a Phosphodiesterase 4B Inhibitor. *J Neurosci*, 36, 7095-108.
- TORRES, V., BARRA, L., GARCES, F., ORDENES, K., LEAL-ORTIZ, S., GARNER, C. C., FERNANDEZ, F. & ZAMORANO, P. 2010. A bicistronic lentiviral vector based on the 1D/2A sequence of foot-and-mouth disease virus expresses proteins stoichiometrically. *J Biotechnol*, 146, 138-42.

- TRAYNELIS, S. F., WOLLMUTH, L. P., MCBAIN, C. J., MENNITI, F. S., VANCE, K. M., OGDEN, K. K., HANSEN, K. B., YUAN, H., MYERS, S. J. & DINGLEDINE, R. 2010. Glutamate receptor ion channels: structure, regulation, and function. *Pharmacol Rev*, 62, 405-96.
- TSIEN, J. Z., HUERTA, P. T. & TONEGAWA, S. 1996. The essential role of hippocampal CA1 NMDA receptor-dependent synaptic plasticity in spatial memory. *Cell*, 87, 1327-38.
- VAN BERGEN, N. J., AHMED, S. M., COLLINS, F., COWLEY, M., VETRO, A., DALE, R. C., HOCK, D. H., DE CAESTECKER, C., MENEZES, M., MASSEY, S., HO, G., PISANO, T., GLOVER, S., GUSMAN, J., STROUD, D. A., DINGER, M., GUERRINI, R., MACARA, I. G. & CHRISTODOULOU, J. 2020. Mutations in the exocyst component EXOC2 cause severe defects in human brain development. *J Exp Med*, 217.
- VEGA, I. E. & HSU, S. C. 2001. The exocyst complex associates with microtubules to mediate vesicle targeting and neurite outgrowth. *J Neurosci*, 21, 3839-48.
- VORHEES, C. V. & WILLIAMS, M. T. 2006. Morris water maze: procedures for assessing spatial and related forms of learning and memory. *Nat Protoc*, 1, 848-58.
- WALKER, C. L., LIU, N. K. & XU, X. M. 2013. PTEN/PI3K and MAPK signaling in protection and pathology following CNS injuries. *Front Biol (Beijing)*, 8.
- WANG, I. F., WANG, Y., YANG, Y. H., HUANG, G. J., TSAI, K. J. & SHEN, C. J. 2021. Activation of a hippocampal CREB-pCREB-miRNA-MEF2 axis modulates individual variation of spatial learning and memory capability. *Cell Rep*, 36, 109477.
- WANG, R. & REDDY, P. H. 2017. Role of Glutamate and NMDA Receptors in Alzheimer's Disease. *J Alzheimers Dis*, 57, 1041-1048.
- WANG, S., CRISMAN, L., MILLER, J., DATTA, I., GULBRANSON, D. R., TIAN, Y., YIN, Q., YU, H. & SHEN, J. 2019. Inducible Exoc7/Exo70 knockout reveals a critical role of the exocyst in insulin-regulated GLUT4 exocytosis. *J Biol Chem*, 294, 19988-19996.
- WEN, J., LOPES, F., SOARES, G., FARRELL, S. A., NELSON, C., QIAO, Y., MARTELL, S., BADUKKE, C., BESSA, C., YLSTRA, B., LEWIS, S., ISOHERRANEN, N., MACIEL, P. & RAJCAN-SEPAROVIC, E. 2013. Phenotypic and functional consequences of haploinsufficiency of genes from exocyst and retinoic acid pathway due to a recurrent microdeletion of 2p13.2. *Orphanet J Rare Dis*, 8, 100.
- WENTHOLD, R. J., PRYBYLOWSKI, K., STANDLEY, S., SANS, N. & PETRALIA, R. S. 2003. Trafficking of NMDA receptors. *Annu Rev Pharmacol Toxicol*, 43, 335-58.
- WHITLOCK, J. R., HEYNEN, A. J., SHULER, M. G. & BEAR, M. F. 2006. Learning induces long-term potentiation in the hippocampus. *Science*, 313, 1093-7.
- WHYTE, J. R. & MUNRO, S. 2002. Vesicle tethering complexes in membrane traffic. *J Cell Sci*, 115, 2627-37.
- WILLIAMS, M. T., MORFORD, L. L., WOOD, S. L., WALLACE, T. L., FUKUMURA, M., BROENING, H. W. & VORHEES, C. V. 2003. Developmental D-methamphetamine treatment selectively induces spatial navigation impairments in reference memory in the Morris water maze while sparing working memory. *Synapse*, 48, 138-48.
- WINSTON, C. N., CHELLAPPA, D., WILKINS, T., BARTON, D. J., WASHINGTON, P. M., LOANE, D. J., ZAPPLE, D. N. & BURNS, M. P. 2013. Controlled cortical impact results in an extensive loss of dendritic spines that is not mediated by injury-induced amyloid-beta accumulation. *J Neurotrauma*, 30, 1966-72.
- WU, B. & GUO, W. 2015. The Exocyst at a Glance. *J Cell Sci*, 128, 2957-64.
- WU, P. K., BECKER, A. & PARK, J. I. 2020. Growth Inhibitory Signaling of the Raf/MEK/ERK Pathway. *Int J Mol Sci*, 21.
- XIONG, Y., MAHMOOD, A. & CHOPP, M. 2019. Remodeling dendritic spines for treatment of traumatic brain injury. *Neural Regen Res*, 14, 1477-1480.

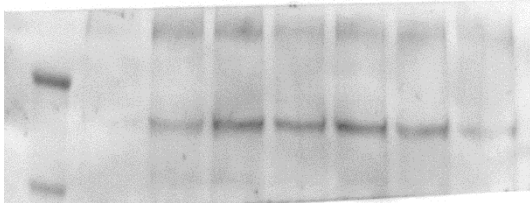
- XU, F., PLUMMER, M. R., LEN, G. W., NAKAZAWA, T., YAMAMOTO, T., BLACK, I. B. & WU, K. 2006. Brain-derived neurotrophic factor rapidly increases NMDA receptor channel activity through Fyn-mediated phosphorylation. *Brain Res*, 1121, 22-34.
- XU, S. Y., LIU, M., GAO, Y., CAO, Y., BAO, J. G., LIN, Y. Y., WANG, Y., LUO, Q. Z., JIANG, J. Y. & ZHONG, C. L. 2019. Acute histopathological responses and long-term behavioral outcomes in mice with graded controlled cortical impact injury. *Neural Regen Res*, 14, 997-1003.
- XU, X., COWAN, M., BERALDO, F., SCHRANZ, A., MCCUNN, P., GEREMIA, N., BROWN, Z., PATEL, M., NYGARD, K. L., KHAZAEI, R., LU, L., LIU, X., STRONG, M. J., DEKABAN, G. A., MENON, R., BARTHA, R., DALEY, M., MAO, H., PRADO, V., PRADO, M. A. M., SAKSIDA, L., BUSSEY, T. & BROWN, A. 2021. Repetitive mild traumatic brain injury in mice triggers a slowly developing cascade of long-term and persistent behavioral deficits and pathological changes. *Acta Neuropathol Commun*, 9, 60.
- ZHANG, B., BAI, M., XU, X., YANG, M., NIU, F., GAO, F. & LIU, B. 2020. Corticosteroid receptor rebalancing alleviates critical illness-related corticosteroid insufficiency after traumatic brain injury by promoting paraventricular nuclear cell survival via Akt/CREB/BDNF signaling. *J Neuroinflammation*, 17, 318.
- ZHANG, B., CHEN, X., LIN, Y., TAN, T., YANG, Z., DAYAO, C., LIU, L., JIANG, R. & ZHANG, J. 2011. Impairment of synaptic plasticity in hippocampus is exacerbated by methylprednisolone in a rat model of traumatic brain injury. *Brain Res*, 1382, 165-72.
- ZHANG, C., BROWN, M. Q., VAN DE VEN, W., ZHANG, Z. M., WU, B., YOUNG, M. C., SYNEK, L., BORCHARDT, D., HARRISON, R., PAN, S., LUO, N., HUANG, Y. M., GHANG, Y. J., UNG, N., LI, R., ISLEY, J., MORIKIS, D., SONG, J., GUO, W., HOOLEY, R. J., CHANG, C. E., YANG, Z., ZARSKY, V., MUDAY, G. K., HICKS, G. R. & RAIKHEL, N. V. 2016. Endosidin2 targets conserved exocyst complex subunit EXO70 to inhibit exocytosis. *Proc Natl Acad Sci U S A*, 113, E41-50.
- ZHAO, Y., LIU, J., YANG, C., CAPRARO, B. R., BAUMGART, T., BRADLEY, R. P., RAMAKRISHNAN, N., XU, X., RADHAKRISHNAN, R., SVITKINA, T. & GUO, W. 2013. Exo70 generates membrane curvature for morphogenesis and cell migration. *Dev Cell*, 26, 266-78.
- ZOU, H., BAO, W. X. & LUO, B. Y. 2018. Applications of Proteomics in Traumatic Brain Injury: Current Status and Potential Prospects. *Chin Med J (Engl)*, 131, 2143-2145.

8.- APPENDICES

Appendix A

1.- PSD Exo70 immunoprecipitation

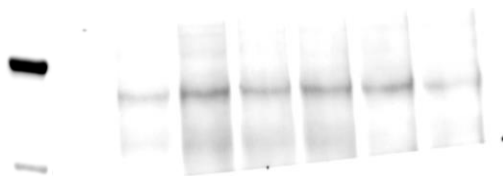
GluN2A



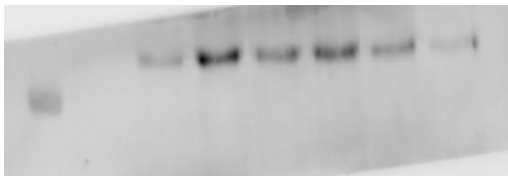
Stripping



GluN2B



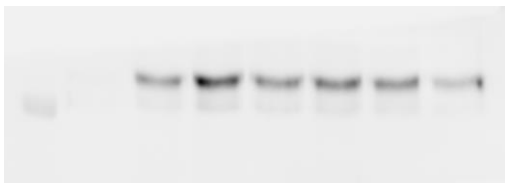
GluR1



Stripping



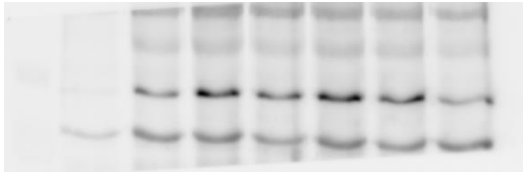
GluR2



Stripping



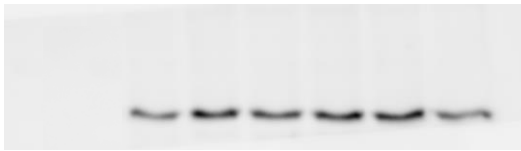
Sec6



Stripping



Sec10



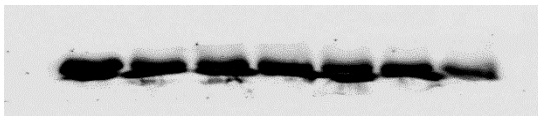
Stripping



Exo70

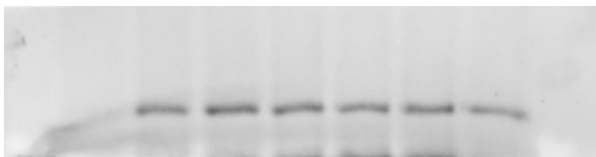


IgG

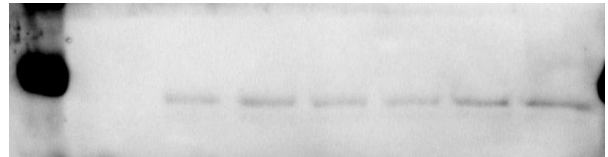


2.- nonPSD Exo70 immunoprecipitation

Sec10



Exo70



IgG

